GEOMEDICAL RISK ASSESSMENT BY GEOCHEMISTRY FOR IZMIR CITY CENTER, TÜRKİYE

A THESIS SUBMITTED TO
THE GRADUATE SCHOOL OF NATURAL AND APPLIED SCIENCES
OF
MIDDLE EAST TECHNICAL UNIVERSITY

BY

ATİLLA KILIÇ

IN PARTIAL FULFILLMENT OF THE REQUIREMENTS
FOR
THE DEGREE OF MASTER OF SCIENCE
IN
GEOLOGICAL ENGINEERING

SEPTEMBER 2023

Approval of the thesis:

GEOMEDICAL RISK ASSESSMENT BY GEOCHEMISTRY FOR İZMİR CITY CENTER, TÜRKİYE

submitted by **ATİLLA KILIÇ** in partial fulfillment of the requirements for the degree of **Master of Science** i**n Geological Engineering, Middle East Technical University** by,

Prof. Dr. Halil Kalıpçılar
Dean, Graduate School of **Natural and Applied Sciences** _____

Prof. Dr. Erdin Bozkurt
Head of the Department, **Geological Engineering** _____

Assoc. Prof. Dr. Fatma Toksoy Köksal
Supervisor, **Geological Engineering, METU** _____

Examining Committee Members:

Prof. Dr. Kaan Sayıt
Geological Engineering, METU _____

Assoc. Prof. Dr. Fatma Toksoy Köksal
Geological Engineering, METU _____

Assoc. Prof. Dr. Hüseyin Evren Çubukçu
Geological Engineering, Hacettepe University _____

Assoc. Prof. Dr. Şebnem Arslan
Geological Engineering, Ankara University _____

Assist. Prof. Dr Ali İmer
Geological Engineering, METU _____

Date: 07.09.2023

I hereby declare that all information in this document has been obtained and presented in accordance with academic rules and ethical conduct. I also declare that, as required by these rules and conduct, I have fully cited and referenced all material and results that are not original to this work.

Name Last Name: Atilla Kılıç

Signature:

ABSTRACT

GEOMEDICAL RISK ASSESSMENT BY GEOCHEMISTRY FOR İZMİR CITY CENTER, TÜRKİYE

Kılıç, Atilla
Master of Science, Geological Engineering
Supervisor: Assoc. Prof. Dr. Fatma TOKSOY KÖKSAL

September 2023, 118 pages

Geogenic materials, such as minerals and elements, have a significant impact on all living beings. Humans are exposed to them through various means, including ingestion, skin absorption and inhalation, which may have either positive or negative effects on health. Hence, geomedical studies have been conducted in many advanced countries to identify the distribution and potential risks associated with elements found in geogenic materials. However, in Türkiye, the importance of such studies is still being recognized, and research in this field has only recently begun. In this thesis, a pilot study has been undertaken in the context of risk assessment, focusing on the İzmir city center. The selection of sample locations was based on geological maps, satellite images, and settlements. The study area was divided into grids, and samples were collected from rocks, soils, and sediments considering the geological characteristics of these grids. Geochemical investigations with a geomedical approach revealed the presence and distribution of toxic elements. In the case of Izmir city center, soil contamination by elements poses carcinogenic and non-carcinogenic risks to individual groups. Therefore, soil rehabilitation in areas with potential risk and city planning considering the risks are highly recommended. In conclusion, the results of this study highlight the need for more extensive research in this field and the importance of conducting such studies to identify the potential

risks associated with geogenic materials. The findings of this study provide a strong scientific basis for future research and policy decisions regarding risk assessments and the management of geogenic materials.

Keywords: Geochemical survey, geomedical risk, medical geology, toxic elements, arsenic enrichment, Western Anatolia.

ÖZ

İZMİR ŞEHİR MERKEZİ İÇİN JEOKİMYA İLE JEOMEDİKAL RİSK DEĞERLENDİRMESİ, TÜRKİYE

Kılıç, Atilla
Yüksek Lisans, Jeoloji Mühendisliği
Tez Yöneticisi: Doç. Dr. Fatma TOKSOY KÖKSAL

Eylül 2023, 118 sayfa

Mineraller ve elementler gibi jeojenik malzemeler tüm canlılar üzerinde önemli bir etkiye sahiptir. Özellikle insanlar, insan sağlığı üzerinde olumlu ya da olumsuz etkileri olabilecek olan jeojenik malzemelere yutma, deri emilimi ve soluma gibi çeşitli yollarla maruz kalmaktadır. Bu nedenle, birçok gelişmiş ülkede kaya, toprak ve sedimanda bulunan elementlerin dağılımını ve potansiyel risklerini belirlemek için risk hesaplamaları ve jeokimyasal çalışmalar yapılmıştır. Ancak Türkiye'de bu tür çalışmaların önemi yeni yeni anlaşılmaya başlanmış ve bu alandaki araştırmalar yeni başlamıştır. Bu tez içerisinde risk değerlendirmesi bağlamında İzmir şehir merkezine odaklanan bir pilot çalışma gerçekleştirilmiştir. Örnek yerlerinin seçiminde jeoloji haritaları, uydu görüntüleri ve yerleşim yerleri esas alınarak çalışma alanı karelajlanmış ve birimlerin jeolojik özellikleri dikkate alınarak her karelajdan kaya, toprak ve sediman örnekleri toplanmaya çalışılmıştır. Jeomedikal bir yaklaşımla yapılan jeokimyasal incelemeler toksik elementlerin mevcudiyetini ve dağılımını ortaya koymuştur. İzmir şehir merkezi örneğinde, toprağın elementlerle kirlenmesi farklı birey grupları için kanserojen ve kanserojen olmayan sağlık riski oluşturmaktadır. Bu nedenle, potansiyel risk taşıyan alanlarda toprak rehabilitasyonu ve riskleri dikkate alan şehir planlaması şiddetle tavsiye

edilmektedir. Sonuç olarak, bu çalışmanın sonuçları, bu alanda daha kapsamlı araştırmalara duyulan ihtiyacı ve jeojenik malzemelerle ilişkili potansiyel riskleri belirlemek için benzer çalışmaların yapılmasının önemini vurgulamaktadır. Bu çalışmanın bulguları, risk değerlendirmeleri ve jeojenik malzemelerin yönetimine ilişkin gelecekteki araştırma ve kararlar için güçlü bir bilimsel temel sağlamaktadır.

Anahtar Kelimeler: Jeokimyasal araştırma, jeomedikal risk, tıbbi jeoloji, toksik elementler, arsenik zenginleşmesi, Batı Anadolu.

For those who know it was the best of times, it was the worst of times

ACKNOWLEDGMENTS

I wish to express my gratitude to my supervisor Assoc. Prof. Dr. Fatma Toksoy Köksal for her dedicated mentoring, invaluable guidance and impactful advice on life and geology.

I want to thank İzmir Metropolitan Municipality for financial support of this research as a part of the project entitled “Izmir Province Seismicity Survey and Bayraklı, Bornova, and Konak District Boundaries Soil Structure and Soil Behaviour of Approximately 10802 Hectare Area Modelling of Characteristics” and the project coordinator Prof. Dr. Erdin Bozkurt.

I'm desiring to express my thanks to Assoc. Prof. Dr. Serhat Köksal for his advice and comments during the fieldwork of this study and making me pursue on research.

I want to thank my colleagues Devin Aykasım and person next door Taner Tekin who were there for support, help and critical discussions.

I wish to express my gratitude towards examining committee members, Prof. Dr. Kaan Sayıt, Assoc. Prof. Dr. Hüseyin Evren Çubukçu, Assoc. Prof. Dr. Şebnem Arslan, Assist. Prof. Dr. Ali İmer for their valuable comments and corrections on my thesis, without their valuable comments, this thesis wouldn’t be complete.

I would like to thank Cem Sinan and Sarp Onat Yücel, my brothers not related by blood for being there for me over a decade and always will be there.

I wish to thank my family Mine Olcay Kılıç, Ömer Faruk Kılıç and my brother Fevzi Kılıç for being there for me all the time in my life and supporting me.

TABLE OF CONTENTS

ABSTRACT v

ÖZ vii

ACKNOWLEDGMENTS x

TABLE OF CONTENTS xi

LIST OF TABLES xv

LIST OF FIGURES xvii

LIST OF ABBREVIATIONS xxiii

CHAPTERS

1 INTRODUCTION 1

1.1 Purpose and Scope 1

1.2 Geographic Setting 3

2 GEOLOGY OF İZMİR CITY CENTER 5

2.1 Regional Geology 5

2.1.1 Paleozoic Units 6

2.1.2 Mesozoic Units 7

2.1.3 Neogene Sedimentary Units 7

2.1.4 Neogene Volcanics 8

2.1.5 Quaternary Deposits 8

2.2 Local Geology 8

2.2.1 Bornova Mélange 9

2.2.2 Kızıldere formation 10
2.2.3 Sabuncubeli formation 10
2.2.4 Yamanlar Volcanics 11
2.2.5 Kızılca formation 12
2.2.6 Yaka formation 13
2.2.7 Görece formation 13
2.2.8 Quaternary deposits 13
3 MATERIALS AND METHODS 15
3.1 Sampling and Analysis 15
3.1.1 Sampling Methodology 16
3.1.2 Sample Locations 17
3.1.3 Sample Procedures 18
3.1.4 Laboratory Analyses 25
3.2 Quality Assurance and Quality Control 25
3.3 Soil Contamination Indices 29
3.3.1 Contamination Factor 29
3.3.2 Geo-accumulation Index 29
3.3.3 Pollution Load Index (PLI) 30
3.4 Geomedical Risk Assessment Indices 30
3.4.1 Total Noncarcinogenic Risk 31
3.4.2 Total Carcinogenic Risk 35
3.5 Distribution Mapping 36
4 GEOCHEMISTRY 41
4.1 Potentially Toxic Elements 41

4.1.1 Arsenic 43
4.1.2 Barium 43
4.1.3 Beryllium 44
4.1.4 Cadmium 44
4.1.5 Chromium 44
4.1.6 Cobalt 45
4.1.7 Molybdenum 45
4.1.8 Nickel 46
4.1.9 Antimony 46
4.1.10 Selenium 46
4.1.11 Tin 47
4.1.12 Lead 47
4.1.13 Zinc 47
4.2 Descriptive Statistics of İzmir City Center Samples 48
4.3 Soil Contamination Indices of İzmir City Center 52
4.4 Geochemical Distribution Maps 61
4.4.1 Arsenic Distribution Maps 61
4.4.2 Cobalt Distribution Maps 64
4.4.3 Chromium Distribution Maps 66
4.4.4 Nickel Distribution Maps 68
4.4.5 Lead Distribution Maps 70
4.4.6 Antimony Distribution Maps 72
5 GEOMEDICAL RISK ASSESSMENT OF İZMİR CİTY CENTER 75
5.1 Geomedical Risk Assessment of İzmir City Center 76

5.1.1 Noncarcinogenic Risk Assessment for İzmir City Center 76
5.1.2 Carcinogenic Risk Assessment for İzmir City Center 84
6 DISCUSSION 95
6.1 Sources of Toxic Elements 95
6.1.1 Volcanism and Tectonism 95
6.1.2 İzmir Bay Studies 99
6.2 Risk Assessment of İzmir City Center 102
7 CONCLUSION AND RECOMMENDATIONS 103
REFERENCES 107

LIST OF TABLES

TABLES

Table 3.1 Sampling density and classification of the geochemical surveys, modified from Demetriades et al. (2018). 16
Table 3.2 Factors used in calculation of CDI..... 32
Table 3.3 RfD Values of Elements (mgkg × day) (IC = IRIS (Integrated Risk Information System); AF = ATSDR Final (Agency for Toxic Substances and Disease Registry); C = CALEPA (California Environmental Protection Agency)) 34
Table 3.4 Carcinogenic Slope Factors 35
Table 3.5 Geostatistical interpolation methods used for elemental distribution maps and ranked accuracy of these methods (produced for intermediate layer elemental (Co, Pb, As) distribution maps for children)..... 38
Table 3.6 Geostatistical interpolation methods that are used for distribution map calculation and ranked accuracy of the methods (produced for upper layer hazard index distribution maps for children)..... 38
Table 3.7 Geostatistical interpolation methods that are used for distribution map calculation and ranked accuracy of the methods (produced for intermediate layer carcinogenic risk distribution maps for children) 39
Table 4.1 Crustal and soil averages of elements and trigger action values for these elements (Kabata-Pendias, 2011), World soil averages (Kabata-Pendias, 2011), European upper layer soil averages (FOREGS, 2005), Izmir city center's soil and sediment averages, Izmir city center's rock averages in ppm (this study). 42
Table 4.2 Descriptive statistics of potentially toxic elements in İzmir city center's rock samples..... 50
Table 4.3 Descriptive statistics of potentially toxic elements in Upper Layer (0-10 cm). 51
Table 4.4 Descriptive statistics of potentially toxic elements in Intermediate Layer (10-30 cm)..... 51

Table 4.5 Descriptive statistics of potentially toxic elements (ppm) in Bottom Layer (30-50 cm) 52

LIST OF FIGURES

FIGURES

Figure 1.1 Location map of the study area. 4
Figure 2.1 Regional geology map of İzmir. Retrieved and modified from MTA 1/500000 and Uzel et al., 2012. 5
Figure 2.2 Local geological map of the study area, modified from 1/25000 MTA maps. 9
Figure 3.1 Sample locations (Squares are rock samples, red spheres are soil and sediment samples, and green spheres sample locations are without data). 18
Figure 3.2 Soil sampling with a portable drilling machine. 19
Figure 3.3 Exposed soil horizons (before digging), 113-Humus, 114- Topsoil, 115-Subsoil. 20
Figure 3.4 Outline of sampling pit (modified from Salminen et al., 1998). 20
Figure 3.5 Soil sampling locations. 21
Figure 3.6 Sediment sampling locations. 22
Figure 3.7 Sediment sampling locations. 23
Figure 3.8 Rock sampling. 24
Figure 3.9 Rock sampling locations. 24
Figure 3.10 Duplicate and original sample result comparison for As (blue line represents 45° slope and red lines represent 20% error limits). 26
Figure 3.11 Duplicate and original sample result comparison for Ba (blue line represent 45° slope and red lines represent 20% error limits). 27
Figure 3.12 Duplicate and original sample result comparison for Co (blue line represent 45° slope and red lines represent 20% error limits). 27
Figure 3.13 Duplicate and original sample result comparison for Pb (blue line represent 45° slope and red lines represent 20% error limits). 28
Figure 3.14 Duplicate and original sample result comparison for Sn (blue line represent 45° slope and red lines represent 20% error limits). 28

Figure 3.15 Noncarcinogenic distribution map bounded by Bayraklı, Bornova and Konak districts' borders 37
Figure 3.16 Noncarcinogenic distribution map bounded by Bayraklı, Bornova and Konak districts' borders and unsampled areas 37
Figure 4.1 Contamination Factor (CF) of As, Ba, Be, Cd, Co, Cr of the soil and sediments from 54 sites of İzmir city center, regarding soil and sediment depths; upper layer (0-10 cm), intermediate layer (10-30 cm), bottom layer (30-50 cm). The added line indicates CF levels (Green=1, Orange=3, Red=6), below 1 low contamination, between 1 and 3 moderate contamination and above 6 high grade contamination is indicated. 54
Figure 4.2 Contamination Factor (CF) of Mo, Ni, Pb, Sb, Se, Sn of the soil and sediments from 54 sites of İzmir city center, regarding soil and sediment depths; upper layer (0-10 cm), intermediate layer (10-30 cm), bottom layer (30-50 cm). The added lines indicate CF levels (Green=1, Orange=3, Red=6), below 1 low contamination, between 1 and 3 moderate contamination and above 6 high grade contamination is indicated. 55
Figure 4.3 Contamination Factor (CF) of Zn of the soil and sediments from 54 sites of İzmir city center, regarding soil and sediment depths; upper layer (0-10 cm), intermediate layer (10-30 cm), bottom layer (30-50 cm). The added lines indicate CF levels (Green=1, Orange=3, Red=6), below 1 low contamination, between 1 and 3 moderate contamination and above 6 high grade contamination is indicated. 56
Figure 4.4 Geo-accumulation Index (I_{geo}) of As, Ba, Be, Cd, Co, Cr of the soil and sediments from 54 sites of İzmir city center, regarding soil and sediment depths; upper layer (0-10 cm), intermediate layer (10-30 cm), bottom layer (30-50 cm). The added lines indicate I_{geo} levels (Green=1, Orange=3, Dark Orange=4, Red=5), below 1 low pollution, between 1 and 3 moderate pollution, between 4 and 5 high pollution, and 5 very high pollution is indicated. 58
Figure 4.5 Geo-accumulation Index (I_{geo}) of Mo, Ni, Pb, Sb, Se, Sn of the soil and sediments from 54 sites of İzmir city center, regarding soil and sediment depths; upper layer (0-10 cm), intermediate layer (10-30 cm), bottom layer (30-50 cm). The

added lines indicate I_{geo} levels (Green=1, Orange=3, Dark Orange=4, Red=5), below 1 low pollution, between 1 and 3 moderate pollution, between 4 and 5 high pollution, and 5 very high pollution is indicated. 59
Figure 4.6 Geo-accumulation Index (I_{geo}) of Zn of the soil and sediments from 54 sites of İzmir city center, regarding soil and sediment depths; upper layer (0-10 cm), intermediate layer (10-30 cm), bottom layer (30-50 cm). The added lines indicate I_{geo} levels (Green=1, Orange=3, Dark Orange=4, Red=5), below 1 low pollution, between 1 and 3 moderate pollution, between 4 and 5 high pollution, and 5 very high pollution is indicated. 60
Figure 4.7 PLI Distribution of Samples in İzmir city center. 61
Figure 4.8 Geochemical distribution of arsenic in upper layer in İzmir city center. 62
Figure 4.9 Geochemical distribution of arsenic in intermediate layer in İzmir city center. 63
Figure 4.10 Geochemical distribution of arsenic in bottom layer in İzmir city center. 63
Figure 4.11 Geochemical distribution of cobalt in upper layer in İzmir city center. 64
Figure 4.12 Geochemical distribution of cobalt in intermediate layer in İzmir city center. 65
Figure 4.13 Geochemical distribution of cobalt in bottom layer in İzmir city center. 65
Figure 4.14 Geochemical distribution of chromium in upper layer in İzmir city center. 66
Figure 4.15 Geochemical distribution of chromium in intermediate layer in İzmir city center. 67
Figure 4.16 Geochemical distribution of chromium in bottom layer in İzmir city center. 67
Figure 4.17 Geochemical distribution of nickel in upper layer in İzmir city center. 68

Figure 4.18 Geochemical distribution of nickel in intermediate layer in İzmir city center. 69
Figure 4.19 Geochemical distribution of nickel in bottom layer in İzmir city center. 69
Figure 4.20 Geochemical distribution of lead in intermediate layer in İzmir city center. 70
Figure 4.21 Geochemical distribution of lead in intermediate layer in İzmir city center. 71
Figure 4.22 Geochemical distribution of lead in bottom layer in İzmir city center. 71
Figure 4.23 Geochemical distribution of antimony in upper layer in İzmir city center. 72
Figure 4.24 Geochemical distribution of antimony in intermediate layer in İzmir city center. 73
Figure 4.25 Geochemical distribution of antimony in bottom layer in İzmir city center. 73
Figure 5.1 Hazard index box plots of the soil and sediments from İzmir city center's upper layer (0-10 cm), (a) dermal hazard index, (b) inhalation hazard index, (c) inhalation hazard index, (d) sum of hazard indexes, above 1 (red line) indicates noncarcinogenic health risk. 77
Figure 5.2 Hazard index box plots of the soil and sediments from İzmir city center's intermediate layer (10-30 cm), (a) dermal hazard index, (b) inhalation hazard index, (c) inhalation hazard index, (d) sum of hazard indexes, above 1 (red line) indicates noncarcinogenic health risk. 78
Figure 5.3 Hazard index box plots of the soil and sediments from center's bottom layer (30-50 cm), (a) dermal hazard index, (b) inhalation hazard index, (c) inhalation hazard index, (d) sum of hazard indexes, above 1 (red line) indicates noncarcinogenic health risk. 79
Figure 5.4 Elemental contributions for hazard quotients for different soil/sediment levels. 80

Figure 5.5 Hazard Index Distribution map of upper layer for women in soil and sediments of İzmir City Center. 81
Figure 5.6 Hazard Index Distribution map of intermediate layer for women in soil and sediments of İzmir City Center. 82
Figure 5.7 Hazard Index Distribution map of bottom layer for women in soil and sediments of İzmir City Center. 82
Figure 5.8 Hazard Index Distribution map of upper layer of soil and sediments in İzmir City Center. 83
Figure 5.9 Hazard Index Distribution map of intermediate layer (10-30 cm) of soil and sediments in İzmir City Center..... 83
Figure 5.10 Hazard Index Distribution map of bottom layer (30-50 cm) of soil and sediments in İzmir City Center. 84
Figure 5.11 Total carcinogenic risk for individual box plots of the soil and sediments of İzmir city center's upper layer (0-10 cm), (a) dermal carcinogenic risk, (b) inhalation carcinogenic risk, (c) inhalation carcinogenic risk, (d) sum of carcinogenic risks, above 0.0001 (black line) indicates carcinogenic health risk..... 85
Figure 5.12 Total carcinogenic risk for individual box plots of the soil and sediments of İzmir city center's intermediate layer (10-30 cm), (a) dermal carcinogenic risk, (b) inhalation carcinogenic risk, (c) inhalation carcinogenic risk, (d) sum of carcinogenic risks, above 0.0001 (black line) indicates carcinogenic health risk. . 86
Figure 5.13 Total carcinogenic risk for individual box plots of the soil and sediments of İzmir city center's bottom layer (30-50 cm), (a) dermal carcinogenic risk, (b) inhalation carcinogenic risk, (c) inhalation carcinogenic risk, (d) sum of carcinogenic risks, above 0.0001 (black line) indicates carcinogenic health risk..... 87
Figure 5.14 Elemental contributions for carcinogenic risk for different soil/sediment levels. 87
Figure 5.15 Carcinogenic risk distribution for men at upper layer..... 89
Figure 5.16 Carcinogenic risk distribution for men at intermediate layer..... 89
Figure 5.17 Carcinogenic risk distribution for men at bottom layer..... 90
Figure 5.18 Carcinogenic risk distribution for women at upper layer..... 90

Figure 5.19 Carcinogenic risk distribution for women at intermediate layer.....91
Figure 5.20 Carcinogenic risk distribution for women at bottom layer. 91
Figure 5.21 Carcinogenic risk distribution for children at upper layer. 92
Figure 5.22 Carcinogenic risk distribution for children at intermediate layer. 92
Figure 5.23 Carcinogenic risk distribution for men at bottom layer. 93
Figure 6.2 Noncarcinogenic distribution map of children at upper layer, Altıntepe and Çilektepe gold provinces marked as black star.....96
Figure 6.3 Limestone quarry located at eastern part of İzmir and Bornova (38.46291674759309, 27.31025118444313). 97
Figure 6.4 Recrystalized aragonite mineralization in limestone blocks from the quarry located in easter part of İzmir and Bornova (38.4629167, 27.3102511) with values of As=79.5, Cd=0.14, Co=2.18, Ni=8.06, Sb=2.08, Zn=29.5 ppm. 98
Figure 6.5 Soil sample from fault zone (38.448830, 27.286847) around the eastern part of İzmir and Bornova which shows elemental values of As=121, Cd=0.548, Co=19.1, Cr=68, Ni=60 Pb=64.9, Sb=2.75, Zn=12.75 ppm.....98
Figure 6.6 Sediment core sampling location in İzmir Bay. Retrieved from Atalar et al. (2013).....100
Figure 6.7 Depth profiles of the concentration of As, Cr, Co, Ni, Pb, Zn (C1: Black square, C2: Black triangle, C3: circle) of Izmir Bay's sediment cores. The black line represents the distribution of the elements at sedimentary rocks (Turekian and Wedepohl 1961), and green line is average soil content (Kabata-Pendias, 2011). Retrieved and modified from Atalar et al. (2013), red line represents rock averages from İzmir city center, orange line represents soil and sediment averages from İzmir city center. 101

LIST OF ABBREVIATIONS

ABBREVIATIONS

Ag – Silver

Al – Aluminium

As – Arsenic

Au – Gold

Ba – Barium

Be – Beryllium

Bi – Bismuth

Cd – Cadmium

Co – Cobalt

Cr – Chromium

Cu – Copper

Fe – Iron

Ga – Gallium

Ge – Germanium

Hg – Mercury

In – Indium

Li - Lithium

Mg – Magnesium

Mn – Manganese

Mo – Molybdenum

Ni – Nickel

Pb – Lead

Pt – Platinum

Se – Selenium

Sb – Antimony

Sr – Strontium

Sn – Tin

Te – Tellurium

Ti – Titanium

Tl – Thallium

U – Uranium

V – Vanadium

Zn - Zinc

CHAPTER 1

INTRODUCTION

1.1 Purpose and Scope

Every day humans are interacted with different minerals or trace elements by either eating, drinking, or inhaling. This exposure may impact human health beneficially or devastatingly, and this interaction is the subject of medical geology. *"Medical geology is the study of the effects of geologic materials and processes on human, animal and plant health, with both good and possibly hazardous results."* (Finkelman et al., 2001), which makes medical geology an interdisciplinary scientific field.

Even in ancient times, some health problems were associated with the environment; Chinese medical texts show that around 1000 BC, mining workers crushing rocks had lung problems and noted symptoms related to lead poisoning (Davies et al., 2013). Moreover, Hippocrates (460-377 BC) stated, *"Whoever wishes to investigate medicine properly should proceed thus...We must also consider the qualities of the waters, for as they differ from one another in taste and weight, so also do they differ much in their quality*" he also noted in his treatise *On Airs, Waters, and Places* that, under certain circumstances, water *"comes from soil which produces thermal waters, such as those having iron, copper, silver, gold, sulphur, alum, bitumen, or nitre"* and such water is *"bad for every purpose."*

According to Latham (1958), famous traveller Marco Polo, during his travel in China, stated that *"Travelers passing this way do not venture to go among these mountains with any beast except those of the country because a poisonous herb grows here, which makes beasts that feed on it lose their hoofs; but beasts born in the country recognise this herb and avoid it."* This observation is similar to the

consumption of selenium-accumulated plants and can be the earliest report of selenium toxicity.

Several descriptions of the usage of toxic elements in historical times were documented, for instance, lead, which was used extensively by Romans to preserve food, in plumbing and architecture (Nriagu, 1998). Mercury was used for easing tooth pain in Roman Empire and syphilis treatment between 16th and 18th centuries (Fergusson, 1990). The ancient Greeks, Romans, Arabs, and Peruvians believed that administering small amounts of arsenic could improve complexion, making it a part of their therapeutic practices, and it was also used as a poison (Fergusson, 1990).

Apart from the toxic effects of elements, the lack of some elements in soil may result in problems for farming and livestock farming. Geologist J. H. L. Vogt became aware that adding crushed bones to the diets of farm animals was common in some regions of Norway to prevent osteomalacia, which is known as softening of the bones in the body. When bedrocks of the area were examined, small amounts of apatite in the rock were found and it is found that phosphorus deficiency caused osteomalacia in animals (Lag, 1990). In order to prevent the damage adding fertilisers rich in phosphorous to the soil was the solution.

Although this branch of geology has numerous studies around the world (Underwood & Filmer, 1935; Prasad, 1978; Kabata-Pendias, 2001, and so on), in Türkiye, there are limited studies about the subject.

This thesis aims to be one of the first city center scaled medical geology study in Türkiye by implementing geochemical analyses in medical geology in İzmir city center, as a result possible harmful element concentrations in soils and sediments of the city center and possible risk posed by these elements would be found. In order to understand the role of geology on different element distributions around three districts of İzmir province: Bayraklı, Bornova and Konak, key elements are sampling and evaluating the data of different types of samples (rock, sediment, and soil) by constructing a statistical model and geochemical and risk dispersion maps. Accurate geochemical surveys are critical to assess potential health issues caused by exposure

to high levels of potentially toxic compounds or regions where deficiency of essential elements in soil may impact animals' and humans' health, according to Finkelman et al. (2018). Therefore, this study is necessary for a metropolis like İzmir (3rd largest city of Türkiye). Moreover, each toxicant is subjected to different distribution patterns and amounts, compatibility with other elements, and reaction to the human body, so the amount of exposure from a particular environment should be investigated. A total number of 190 samples were used for chemical analyses, and eight samples were duplicates for quality assurance and control. Analysis of these samples was conducted at ALS Laboratories (geochemical analyses). However, data results cannot be shared since this research is a part of a project supported by İzmir Metropolitan Municipality.

1.2 Geographic Setting

The study area covers an area of 140 km^2 area at the city center of İzmir (Figure 1.1) and comprises Bornova, Bayraklı and Konak districts which are in K18-d3, K18-c4, L18-a1, L18-a2, L18-b1 quadrangles. The study area was chosen by İzmir Metropolitan Municipality as a part of “Izmir Province Seismicity Survey and Bayraklı, Bornova, and Konak District Boundaries Soil Structure and Soil Behaviour of Approximately 10802 Hectare Area Modelling of Characteristics” project because

these districts are one of the most populated areas in İzmir and approximately includes 25% population of İzmir.

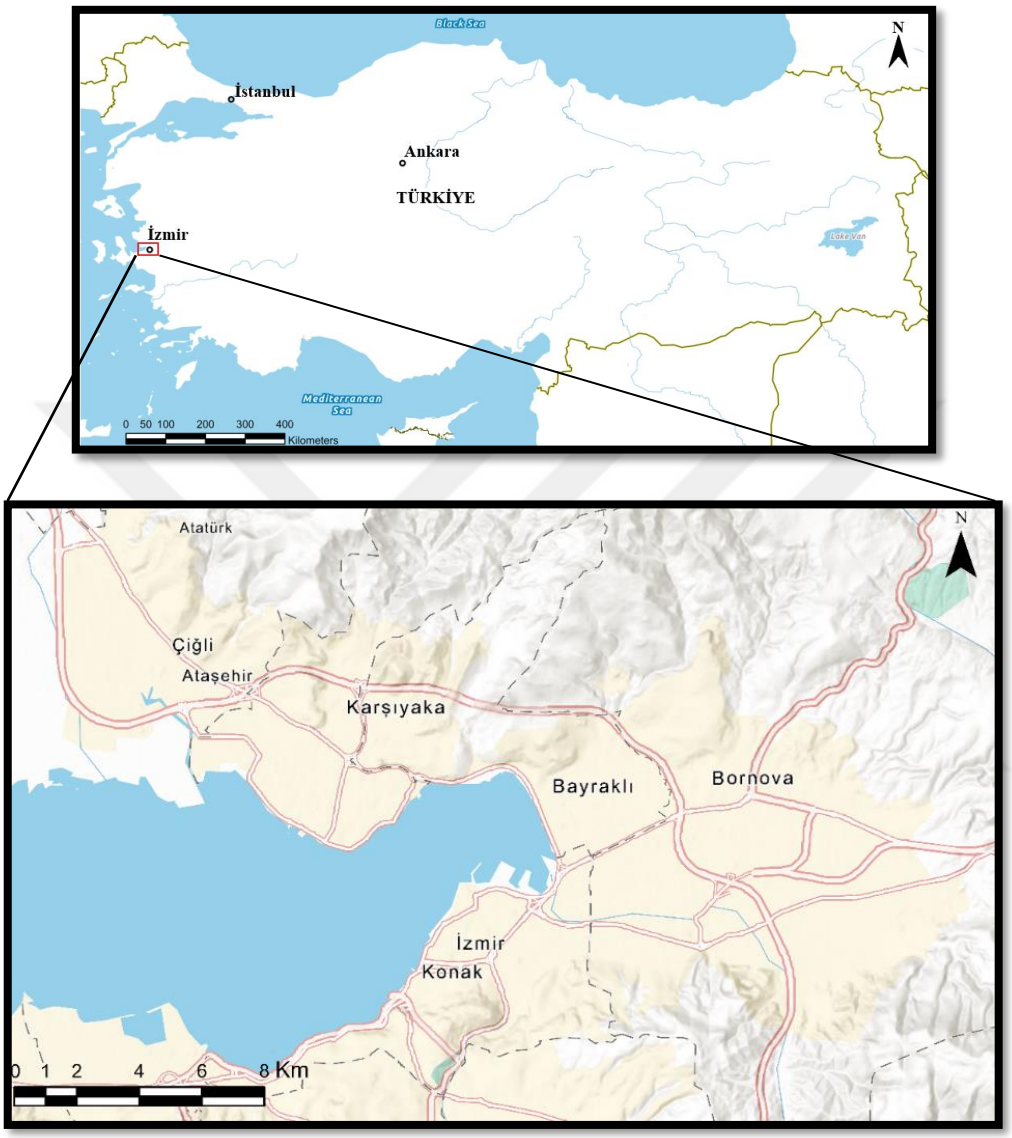

Figure 1.1 Location map of the study area.

CHAPTER 2

GEOLOGY OF İZMİR CITY CENTER

2.1 Regional Geology

Paleozoic units (Karaburun belt, Cycladic core complex and Menderes Massif) and Mesozoic units (Bornova Mélange) are the basement rock units of the İzmir region. These basement units are overlain by Neogene sedimentary, Neogene volcanics and Quaternary deposits around the basins of İzmir (Uzel et al., 2012). Therefore, the regional geology of İzmir can be analysed in four groups (Figure 2.1).

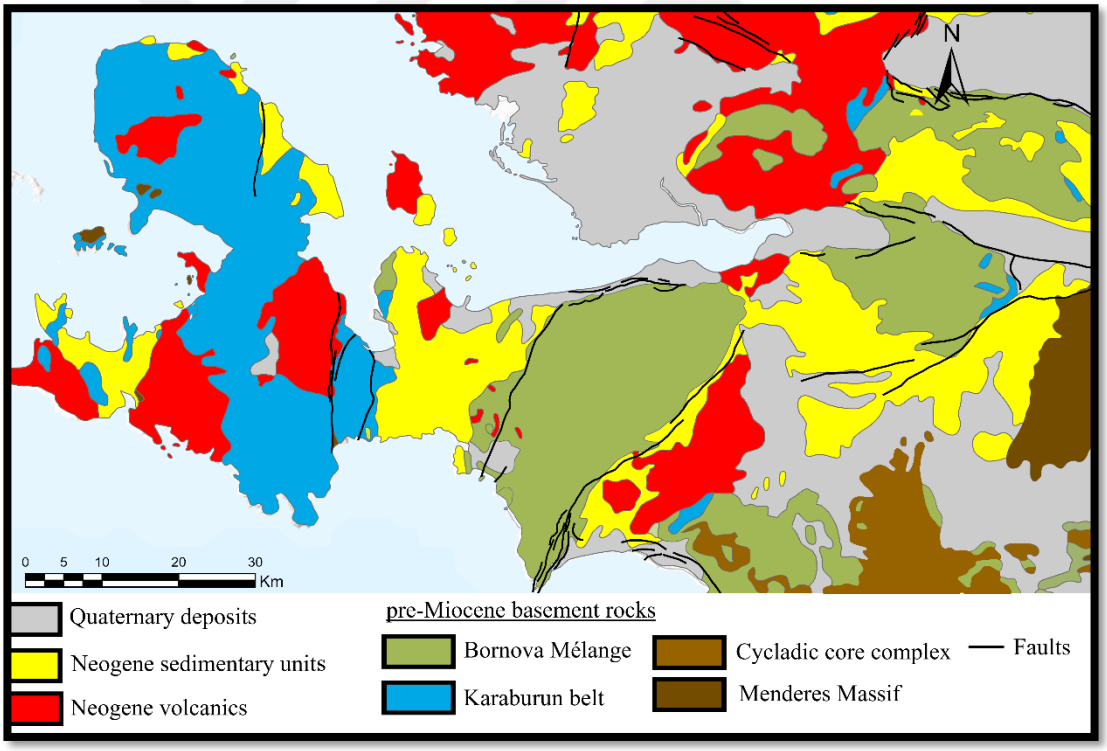

Figure 2.1 Regional geology map of İzmir. Retrieved and modified from MTA 1/500000 and Uzel et al., 2012.

2.1.1 Paleozoic Units

Paleozoic units in the İzmir region are consists of Menderes massif, Cycladic core complex and Karaburun belt.

Menderes massif, defined as the Menderes core complex, is one of the areas with a crystalline basement in the Aegean region. The massif is bounded to the north by the Izmir-Ankara-Erzincan zone and by the Lycian nappes to the south. The massif consists of crystalline rocks, mainly gneisses, and stratigraphy of the massif starts with Precambrian gneisses and ends with lower Eocene recrystallized limestones (Çağlayan et al.,1980; Şengör et al.,1984). Core rocks are composed of gneiss and high-grade metamorphic rocks.

Different interpretations have been made about the protolith of these gneisses. Schuiling (1962) stated that they were of sedimentary origin based on zircon morphology, while Graciansky (1965) implied that they were of magmatic origin. Moreover, the geochemical characteristics of these rocks indicated that they are of magmatic origin according to Bozkurt et al. (1993). Tectonic events in the Paleozoic and Mesozoic Eras caused a broad dome-shaped exposure of the Menderes core complex in Western Anatolia.

Cycladic Metamorphic Core Complex comprises pelagic volcano-sedimentary sequences and ophiolites (Makris et al., 2022). Main rock units are mica-schist, calc-schist, marble, meta-chert, serpentinite, and meta-volcanic rocks in western Anatolia (Okay, 2001; Uzel et al., 2013).

Karaburun Belt comprising rock unit from the Paleozoic to late Cretaceous (Uzel et al., 2013). Main rock units are neritic limestone, granite, turbiditic sequences with olistoliths and tectonic blocks of Paleozoic to Cretaceous aged rock units (Erdoğan, 1990).

2.1.2 Mesozoic Units

Mesozoic units around the region are part of the İzmir-Ankara-Erzincan suture zone defined for the first time by Brinkman (1966). Mesozoic units are exposed mainly over the southern part of İzmir. During the Mesozoic, Menderes Massif and Sakarya Continent were surrounded by an arm of the Tethys Ocean (Şengör and Yılmaz, 1981). The continental collision in the Palaeocene resulted in the overthrust of ocean floor deposits such as submarine volcanics and ocean floor sediments onto Paleozoic units (Menderes core complex), which caused the formation of Bornova Mélange, composed of sandstone, mudstone, shale intercalation and different-sized blocks of recrystallized limestone, chert, serpentinite, and mafic rock units inside of a micritic limestone matrix (Erdoğan, 1990).

2.1.3 Neogene Sedimentary Units

Neogene sedimentary units around the region can be divided into lower and upper volcano-sedimentary sequences (Uzel et al., 2012). Lower volcano-sedimentary sequence units consist of conglomerate at the base, limestone, mudstone, and sandstone alternations upwards and overlain by Yamanlar volcanics. Lower sequence, named as Kızıldere formation around Menemen, Çatalca formation in the southern part of İzmir (Genç et al., 2001; Uzel et al., 2012) and Sabuncubeli formation around the northern part of İzmir.

The upper volcano-sedimentary sequence overlies Yamanlar volcanics and consists of terrestrial deposits which are intercalated with carbonate levels; the sequence starts with conglomerate with clasts of Bornova Mélange and Yamanlar volcanics at the base and is overlain by sandstone and mudstone levels with intercalation of grey limestone at top. Upper sequence named as Yaka formation around northern part of İzmir (Uzel and Sözbilir, 2008), Ürkmez formation at the southwest of İzmir city center (Eşder & Şimşek 1975; Genç et al. 2001; Uzel et al., 2012). The upper sequence is intercalated and overlain by Cumaovası volcanics.

2.1.4 Neogene Volcanics

Neogene volcanics consist of Yamanlar Volcanics its age estimated as ~17.48–14.94 Ma (Seghedi et al., 2015) and Cumaovası volcanics its age estimated as ~11.5-9 Ma (Borsi et al., 1972). Yamanlar volcanics consist of rhyolitic, andesitic and dacitic rocks in composition (Dora, 1964; Borsi et al., 1972; Akdeniz et al., 1986; Seghedi et al., 2015). Cumaovası volcanics consist of felsic pyroclastic rocks, lava flows and tuff and are overlain by rhyolitic lavas, obsidian, and perlite fragments (Özgenç, 1978).

2.1.5 Quaternary Deposits

Around the İzmir center principal flat planes are covered by alluvial deposits, the northern part of the center is encased Gediz River's alluvial deposits, which has loose sand and soft clay material, and andesitic gravels, the eastern part of the center has Bornova, Manda, Kocasu, Arap rivers' alluvial deposits which have different sized blocks, gravels, sand, silt, and clay material.

2.2 Local Geology

The local geology of the study area is composed of Jurassic sedimentary units (Neritic limestone), Bornova Mélange, Kızıldere formation, Sabuncubeli formation, Yamanlar volcanics, Kızılca formation, Yaka Formation, Görece formation and Quarternary deposits (Figure 2.2).

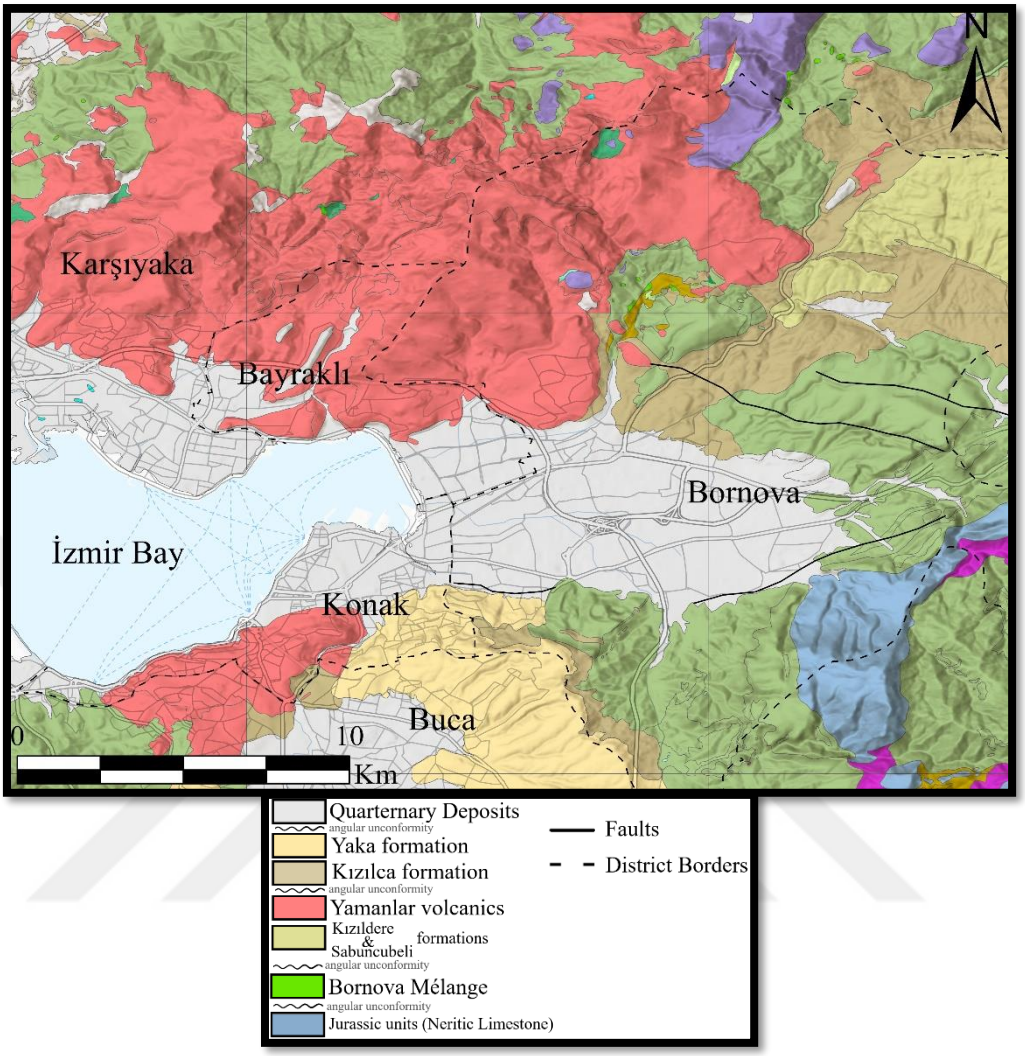

Figure 2.2 Local geological map of the study area, modified from 1/25000 MTA maps.

2.2.1 Bornova Mélange

Bornova Mélange is largely exposed over the southern part of İzmir Bay and Bornova district. These rock units are first defined around the İzmir region (Parejas, 1940) and known as Bornova flysch (Konuk, 1977). The unit is also named as Bornova Flysch zone by Okay and Siyako (1991). However, the unit's name is widely accepted as Bornova Mélange, named by Erdoğan (1990).

Around the region, Bornova Mélange is composed of sandstone, mudstone, shale intercalation and different-sized blocks of recrystallized limestone, chert,

serpentinite, and mafic rock inside of a micritic limestone matrix (Erdoğan, 1990), which is an Upper Cretaceous flysch matrix according to Okay and Siyako (1991).

The stratigraphic base of Bornova Mélange cannot be observed around the İzmir region without tectonic relations between the Mélange and the Menderes Massif. Moreover, carbonate sections that are observable around the area embedded in the micritic calcite matrix in the age of Campanian-Danian. Shallow marine carbonate blocks (Triassic-Upper Cretaceous) were incorporated into the micritic calcite matrix (flysch basin) during the deposition (Maestrichtian-Danian), thus below these limestone blocks, soft sediment deformations are typical, according to Erdoğan (1990).

2.2.2 Kızıldere formation

The formation is exposed over the western part of İzmir; the unit is defined by Uzel et al. (2012). The Kızıldere formation is characterized by a predominant brownish-red lithology, consisting of thick to massive beds of poorly to moderately sorted conglomerate. The clasts, mainly derived from the Bornova mélange, are of pebble size. The conglomerate is alternated with grey-reddish-brown sandstone, siltstone, marl, and shale. The formation culminates in yellowish-brown lacustrine limestone, indicating an alluvial to fluvial depositional sequence conformably overlain by the Sabuncubeli formation (lacustrine carbonates), according to Uzel et al. (2012).

2.2.3 Sabuncubeli formation

The formation is exposed around the northern part of Bornova, and the unit is defined by Uzel et al. (2012). Sabuncubeli formation comprises thick-bedded conglomerate, sandstone, marl, and mudstone alternations with limestone towards the top. The lateral equivalent of the Sabuncubeli formation in the southern part of İzmir is Çatalca formation, composed of yellow shale, grey siltstones, yellow sandstones with red mudstone interbeds and thick lignite beds (10-75 cm), fossiliferous

limestone lenses and conglomerate lenses. It is faulted above to Bornova Mélange in the western part of İzmir (Genç et al. 2001). The formation is dated as lower-middle Miocene (Akartuna 1962; Lüttig and Steffens 1976; Kaya 1981; Genç et al. 2001; Uzel et al. 2012). The formation is overlain by Yamanlar volcanics.

2.2.4 Yamanlar Volcanics

Yamanlar Volcanics can be observed around the northern and southern parts of İzmir city center. These volcanic have been studied by various authors (Dora, 1964; Borsi et al., 1972; Akdeniz et al., 1986; Ercan et al., 1996; Dönmez et al., 1998; Sayılı and Şener 1999; Seghedi et al., 2015). Dora (1964) concluded two types of volcanic rock units exist: dacites and andesites. Akdeniz et al. (1986) named these volcanics as Yamanlar volcanics and they concluded that Yamanlar volcanics have a calc-alkaline composition in general and comprized of dacitic and andesitic lava flows, pyroclastic rocks, dykes, domes with dacitic, andesitic, and rhyolitic compositions, tuffs, and agglomerates.

Phenocrysts of plagioclase, potassium feldspar, amphibole, biotite, clinopyroxene, orthopyroxene minerals and accessory minerals sphene, apatite and opaque minerals can be found in Yamanlar volcanics (Seghedi et al., 2015).

Yamanlar volcanics overlies pre-Miocene units in some areas, and thin layers of conglomerate and tuff alternations are present on the base of the volcanic rocks. On top of these alternations, agglomerates and lava covers after thick tuff layers are present. According to Akdeniz et al. (1986) and references therein, lavas associated with the Yamanlar volcanism generally show flow texture, at the lavas and tuffs are alternated with lake sediments in some locations. These features indicate that the volcanism developed on land and that the lavas and tuffs were periodically transported to a water environment.

These volcanic rocks are dated as ~17.48–14.94 Ma by K/Ar method (Seghedi et al., 2015) indicating an early to middle Miocene age for the Yamanlar volcanics.

In Yamanlar volcanics, ore provinces named as Altıntepe (Arapdağ), Çilektepe (Pilavtepe) (Dora, 1970; Sönmez and Gonca, 1999) are found and antimony mineralization can be found on the surface of Çilektepe area, and these veins are in 5cm-2m thicknesses. Minerals like stibnite (Sb_2S_3), pyrite (FeS_2), cinnabar (HgS), senarmontite (Sb_2O_3) occurring with quartz and baryte can be observed in Çilektepe. Drillholes at Çilektepe show gold levels varying between 40 ppb to 4.37 ppm, and along with gold, 700 ppm Pb (lead), 70 ppm to 1% Sb (antimony) levels are also found (Sönmez and Gonca, 1999).

At the Altıntepe area, rutile-anatase (TiO_2), pyrite (FeS_2), arsenopyrite (FeAsS), marcasite (FeS_2), hematite (Fe_2O_3), sphalerite (ZnS), galena (PbS), chalcopyrite ($CuFeS_2$), fahlore, bournonite ($PbCuSbS_3$), boulangerite ($Pb_5Sb_4S_{11}$), zinkenite ($Pb_9Sb_{22}S_{42}$), and electrum observed in ore microscopy (Sönmez and Gonca, 1999).

Dora (1970) observed a sample containing 39.3% sphalerite (ZnS), 36.7% pyrite (FeS_2), 18.3% galena (PbS), 3.6% chalcopyrite ($CuFeS_2$), 0.8% marcasite (FeS_2), 0.6% arsenopyrite (FeAsS), and 0.4% fahlore [$(Cu_6(Cu_4(Fe,Zn)_2^{2+})(As_4,Sb_4)S_{12}S]$.

2.2.5 Kızılca formation

The formation is exposed over the northern part of Bornova and defined by Sözbilir et al. (2010). The Kızılca formation is characterized by a basal unit of poorly sorted brown alluvial conglomerates that grade upward into greyish to brown sandstone and mudstone, ending with light grey and yellowish-white marl intercalations; these carbonate-rich strata signify shallow lacustrine depositional environments according to Sözbilir et al. (2010). They suggested that Kızılca and Yeniköy formations can be stratigraphically correlated. Thus, the age of Kızılca formation is determined as middle to late Miocene since Yeniköy formation's age is found by spores and pollens in coal seams as middle to late Miocene (Ercan et al. 1978). Kızılca formation is conformably overlain by the Yaka formation.

2.2.6 Yaka formation

The formation is exposed over the northern parts of Bornova and named by Uzel et al. (2012). At the bottom of the formation, intercalations of limestone, sandstone, shale, and serpentinite can be observed; at the middle part, reddish conglomerate, reddish sandstone with limestone lenses are observed. The top dominant rock unit is massive yellowish white limestone with intercalations of greyish-brown mudstone and green claystone (Akdeniz et al., 1986; Uzel et al., 2012). The geological age of the formation is middle to late Miocene (Kaya, 1981; Uzel et al., 2012), and it is overlain by Görece formation.

2.2.7 Görece formation

Uzel and Sözbilir (2008) reported that the Görece Formation is exposed around northern parts of Bornova region and Cumaovası basin. The formation comprises semi-consolidated red continental clastics, which are poorly bedded, moderately sorted yellowish-brown sandstone and poorly bedded, poorly to moderately sorted reddish-brown conglomerate alternations and formation age is Plio–Pleistocene. Based on its geological characteristics, the Görece Formation is interpreted as an alluvial fan deposit (Uzel & Sözbilir 2008).

2.2.8 Quaternary deposits

The area surrounding İzmir city center is predominantly characterized by alluvial deposits. In particular, the northern part of the center is encased by the alluvial deposits of the Gediz River, consisting of loose sand and soft clay material, as well as andesitic gravels. Meanwhile, the eastern part of the center is marked by the alluvial deposits of several rivers including Meles, Bornova, Manda, Kocasu, and Arap rivers. These deposits are comprised of a mixture of different sized blocks, gravels, sand, silt, and clay material.

CHAPTER 3

MATERIALS AND METHODS

3.1 Sampling and Analysis

Mapping of the spatial distribution of elements with a systematic geochemical method provides regional to global scaled (Table 3.1) level changes of chemical elements in materials occurring at or below the Earth's surface such as rock, soil, floodplain or overbank sediments, regolith, water, and vegetation. Thus, careful geochemical sampling is the key to geochemical mapping practices, and to do so, different survey protocols have been prepared (Salminen et al., 1998, 2004, 2005; Johnson, 2005; EuroGeoSurveys Geochemistry Working Group, 2008; Smith et al., 2005; Lech et al., 2007).

Additionally, geochemical atlases have been prepared by various authors (e.g., IGS, 1978; Bølviken et al., 1986, 2000; Lahermo et al., 1990, 1996; BGS, 1992, 2000; Reimann et al., 2005; Tarvainen et al., 2006; Smith et al., 2014). Most of these protocols and atlases are mainly focused on the environmental impact of elements in soil resulting from anthropogenic or geogenic effects. Thus, the geochemical survey is one of the most essential parts in the aspect of medical geology.

In every geochemical survey from continental to local scale, it can be stated that eight different steps (Demetriades et al., 2018) should be followed and done carefully.

- Planning
- Sampling
- Sample preparation
- Laboratory analysis
- Quality control/Quality assessment (QA/QC)

- Interpretations
- Report writing

Table 3.1 Sampling density and classification of the geochemical surveys, modified from Demetriades et al. (2018).

Normal sampling density	Sampling grid dimension	Map scale	Geochemical mapping phase
1 sample/10,000 km^2	100 x 100 km	1/10,000,000	Continental
1 sample/6400 km^2	80 x 80 km		
1 sample/2500 km^2	50 x 50 km	1/5,000,000	
1 sample/1600 km^2	40 x 40 km		
1 sample/100 km^2	10 x 10 km	1/1,000,000	Regional
1 sample/1 km^2	1 x 1 km	1/100,000	
1 sample/250,000 m^2	500 x 500 m	1/50,000	
1 sample/62,500 m^2	250 x 250 m	1/25,000	Regional (or Follow-up phase in mineral exploration)
1 sample/10,000 m^2	100 x 100 m	1/10,000	
1 sample/2500 m^2	50 x 50 m	1/5,000	Local / Detailed
1 sample/625 m^2	25 x 25 m	1/2,500	Ultra detailed in mineral exploration
1 sample/100 m^2	10 x 10 m	1/1,000	
1 sample/25 m^2	5 x 5 m	1/500	

3.1.1 Sampling Methodology

Sample locations and sample taking must represent the surrounding area for medical geology studies for better interpolation results and should not be affected by anthropogenic effects. Thus, the sampling methodology of this research is coherent with IGCP 259 (1995) and IGCP 360 (1996) (IGCP-International Geoscience Programme is a joint project of UNESCO and the International Union of Geological Sciences (IUGS)). These projects (Reimann et al., 2005; Tarvainen et al., 2006; Salminen et al., 1998, 2004, 2005) are done by coordinated government institutions of European countries, and their goal was to have standardized sampling methods, geochemical analyses, and management of data to create a geochemical baseline of

Europe since most countries' environmental authorities define limits for contaminants in soils for different land use purposes.

Different sampling media and its properties are chosen, and these are residual soil, upper horizon (topsoil) 0 - 25 cm without the top organic layer, lower (C) horizon (subsoil); a 25 cm layer within a depth range of 25 cm-100 cm and humus where present. Overbank sediment, upper horizon 0-25 cm, bottom layer. Floodplain sediment, upper horizon 0 - 25 cm, according to Salminen et al. (1998). Hence, for this study, these sampling media types are chosen; soil, sediment (geochemical mapping) and rock (geogenic source) samples, for soil and sediment layers are divided as an upper layer (0-10 cm), intermediate layer (10-30 cm) and bottom layer (30-50 cm) according to depths (Salminen et al., 1998).

3.1.2 Sample Locations

Sample locations are selected by considering geological map of İzmir, satellite images, military bases, drainage basins, private properties, roads, parks (artificial soil movements), forests, archaeological sites and field observations.

The study area has been segmented into 4 km^2 grid squares, thereby enabling the geochemical mapping phase to be conducted at a regional level. The study area's scale has been established at 1/200,000, despite the fact that the scale of the study area itself is 1/120,000. This methodology was selected due to its feasibility of incorporating additional districts of İzmir city center in future studies.

The total number of 62 different sample locations (Figure 3.1) are chosen in these grids. However, around the Konak district, which has a lower area with higher property density than Bornova and Bayraklı resulted in fewer sample locations. Moreover, in Bayraklı and Bornova, some forest roads were closed due to wildfire danger in 2021, which caused no access to some grids in the city center. From these locations, a total number of 182 samples (139 soil/sediment and 43 rock samples) and 8 field duplicate samples are taken in 2021. Moreover, 78 more samples (62

soil/sediment, 16 rock samples) were taken in 2023, because concerning elemental concentrations are found from some sample results and accessibility to certain grids are possible.

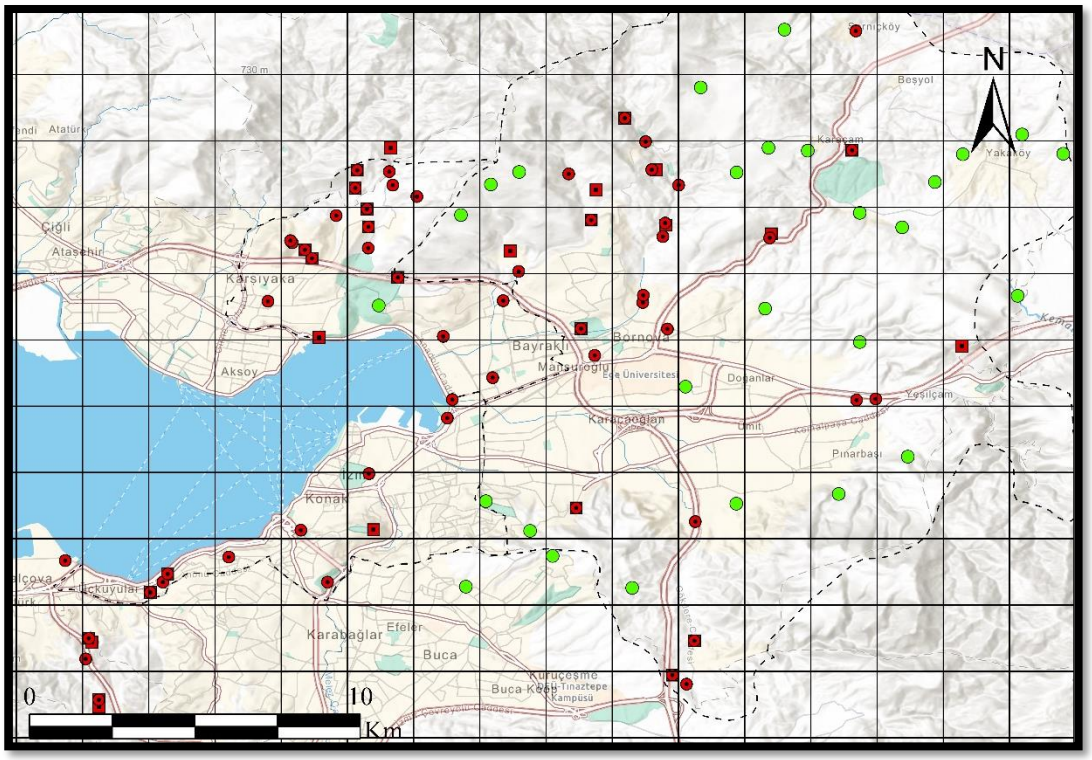

Figure 3.1 Sample locations (Squares are rock samples, red spheres are soil and sediment samples, and green spheres sample locations are without data).

3.1.3 Sample Procedures

To obtain accurate and reliable data a variety of tools, portable drilling machine (Figure 3.2) for collection of samples alongside with metal shovels, pickaxes, geological hammers, and sledgehammers for sample procedures were used in the study area. To ensure that there was no cross-contamination between the samples, the equipments were carefully cleaned before taking each new sample. Efforts were made to visit each sample grid in the study area to take a rock, sediment, and soil

samples. This approach allows a comprehensive understanding of the geology and compositions of the area.

Figure 3.2 Soil sampling with a portable drilling machine.

3.1.3.1 Soil Sampling

When conducting soil sampling in the İzmir province, it was determined that the first 5 cm of soil (from the top) should not be included in the samples due to the anthropogenic effect on the soil in this area. Instead, samples of humus/upper layer (5-10 cm), topsoil/intermediate layer (10-30 cm), and subsoil/bottom layer (30-50 cm) were collected (Figure 3.3). These intervals were specifically chosen based on the territory properties around İzmir.

Humus and topsoil samples were collected at the same depth as the FOREGS guideline (Salminen, 1998) (Figure 3.4), while subsoil samples were not accessible after 50 cm due to the presence of bedrock fragments or bedrock itself in all sample locations except for one. The sampling area was selected to be as flat as possible,

and the composite total amount of humus material was taken while removing any roots from the soil samples (Figure 3.5).

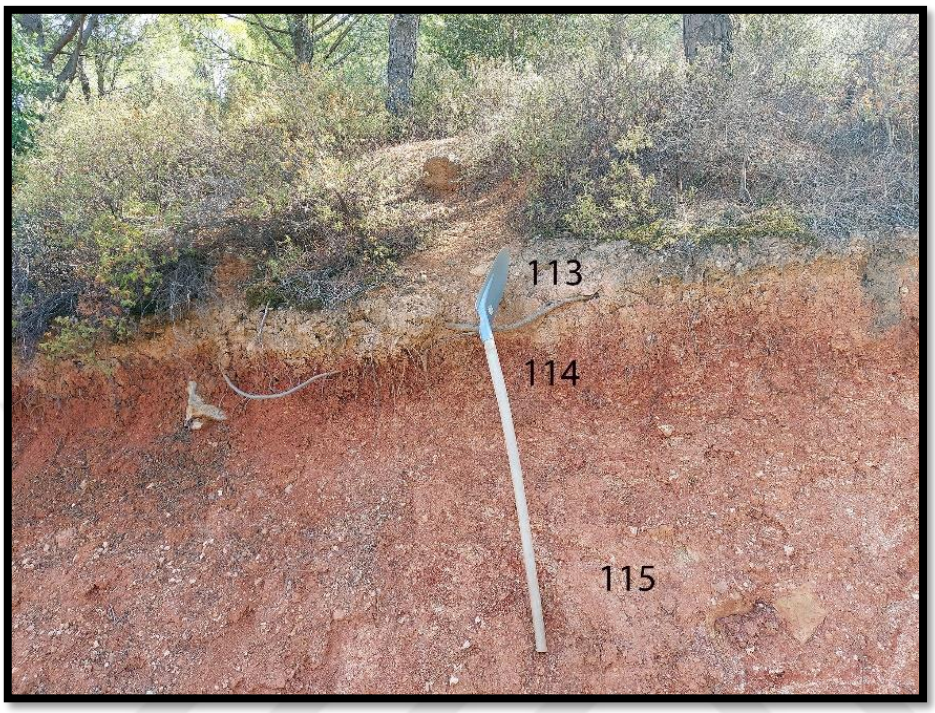

Figure 3.3 Exposed soil horizons (before digging), 113-Humus, 114- Topsoil, 115-Subsoil.

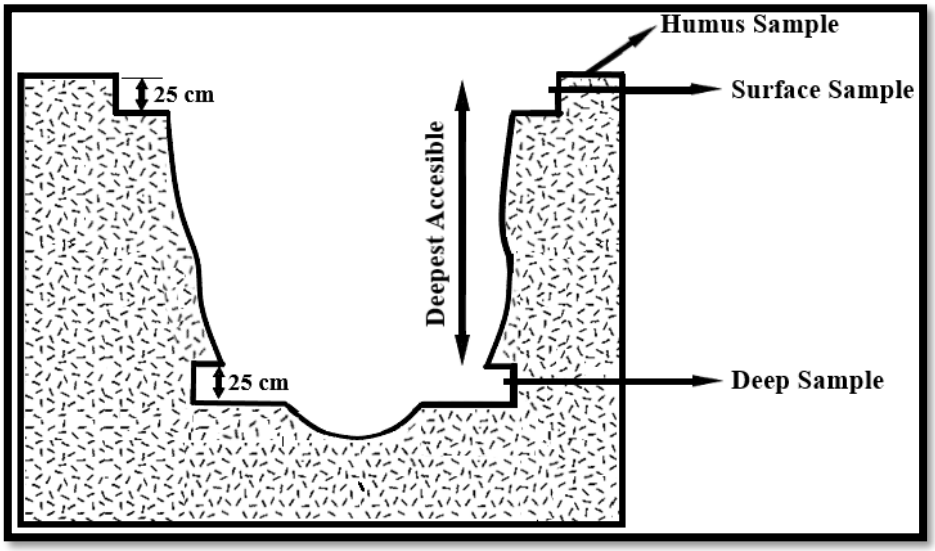

Figure 3.4 Outline of sampling pit (modified from Salminen et al., 1998).

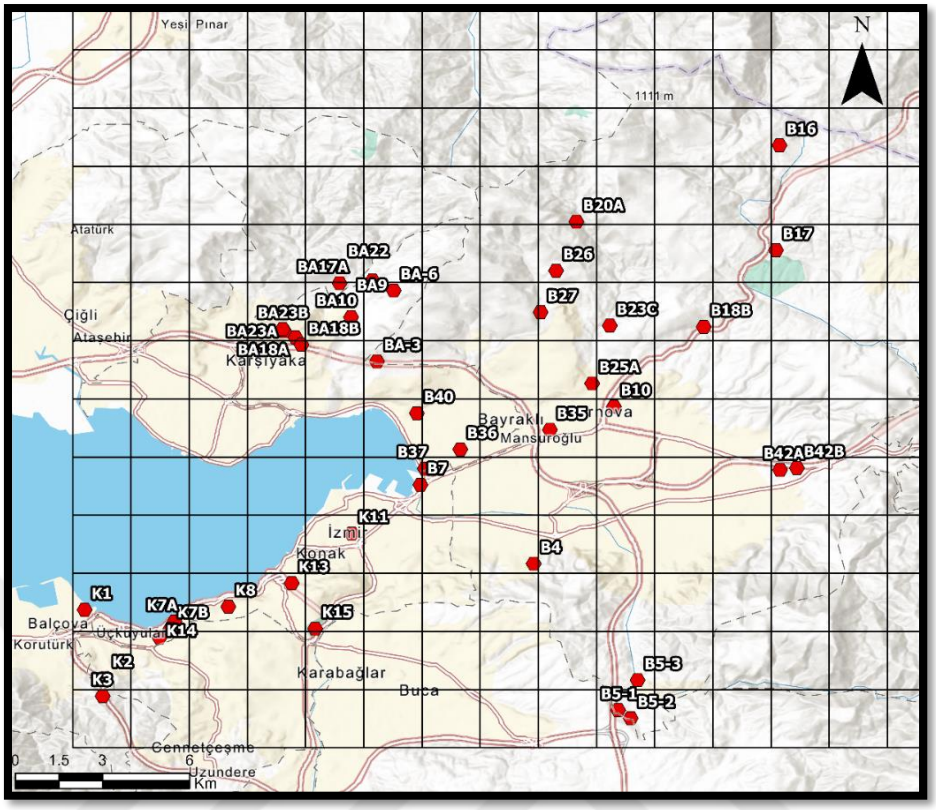

Figure 3.5 Soil sampling locations.

3.1.3.2 Sediment Sampling

Sediment sampling was done similarly to soil sampling using the equipment; samples were derived from dry stream sediment sampling (Figures 3.6). In each sample location (Figure 3.7), samples were taken by considering the change in the particle size of sediments, from clay size to gravel size. Hence, from 0-10 cm (upper layer), from 10-30 cm (intermediate layer), and from 30-50 cm (bottom layer), samples were taken by digging with a metal shovel or by using an auger bit of a portable drilling machine.

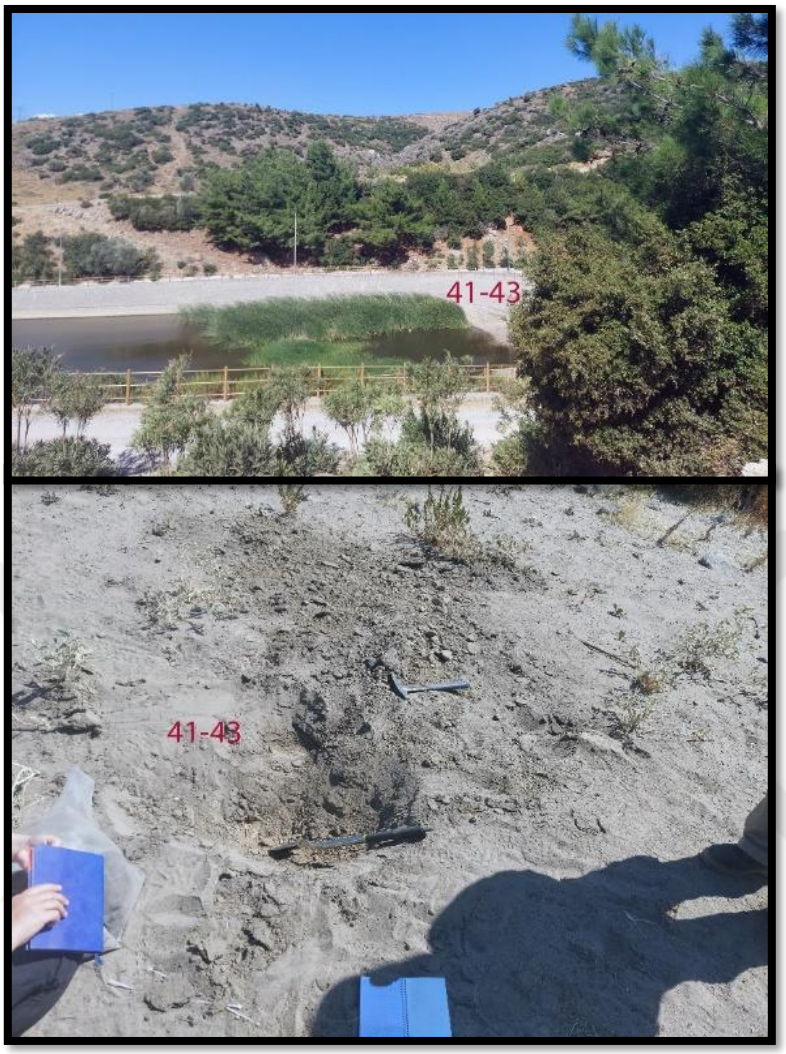

Figure 3.6 Sediment sampling locations.

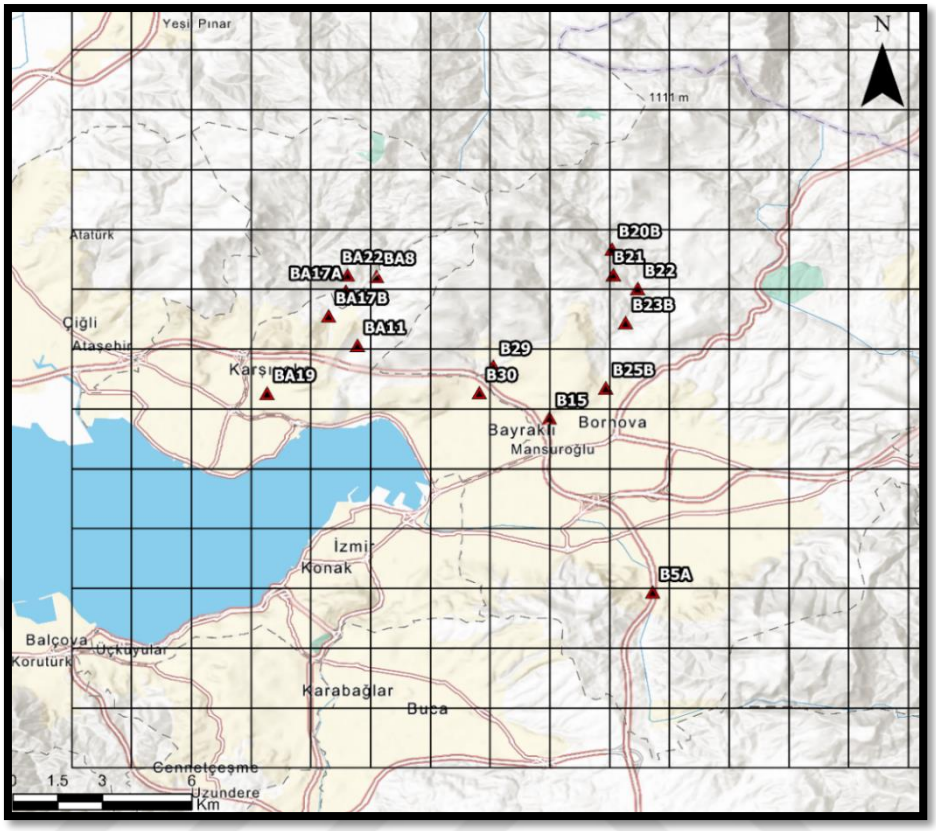

Figure 3.7 Sediment sampling locations.

3.1.3.3 Rock Sampling

Identifying the origin of soil and sediment samples is an essential part of a geochemical study, and having bedrock samples from an area is necessary to have a general opinion on the geological properties of the region. Thus, from every geological unit and possible grid with rock outcrops in the area, the freshest samples

are taken using a geological hammer, a sledgehammer and a portable drilling machine (Figures 3.8 and 3.9).

Figure 3.8 Rock sampling.

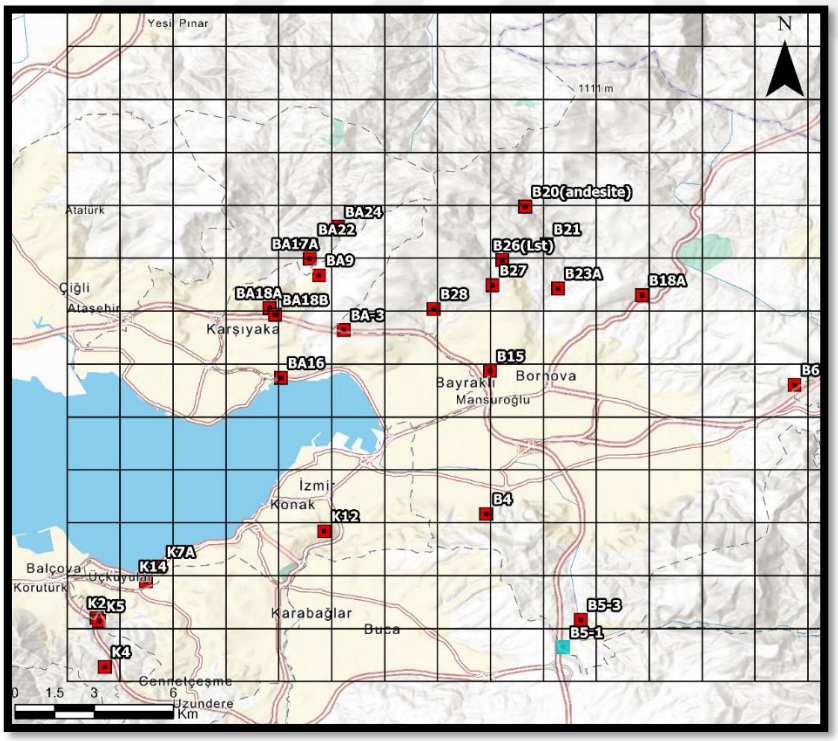

Figure 3.9 Rock sampling locations.

3.1.4 Laboratory Analyses

Samples prepared for geochemical analyses and analyses were done for whole rock, trace element, rare earth element, halogen, and loss on ignition (LOI) analyses. For geochemical laboratory analyses, ALS Global is chosen because the company have accreditations from International Accreditation Forum (IAF) in accordance with International Standard ISO/IEC 17025:2017– general requirements for the competence of testing and calibration laboratories and from the Turkish Accreditation Agency (TÜRKAK).

Samples were prepared at ALS İzmir, and analyses were done at ALS Vancouver. Whole rock major and minor oxide analyses were performed by inductively coupled plasma atomic emission spectroscopy (ICP-AES) and trace elements and rare earth elements (REE) analyses were done with inductively coupled plasma mass spectrometry (ICP-MS) with aqua regia digestion. Halogens were analysed by ionic leach. Loss on ignition analyses (LOI) were done at 1000ºC

3.2 Quality Assurance and Quality Control

Quality assurance and quality control (QA/QC) are critical components of a geochemical study, and its main objective is to identify the quality of the reported data while ensuring the data is adequate for end use, according to Barth and Mason (1984).

Soil and rock samples are relatively inhomogeneous mediums. Thus, there might be errors in data due to sampling procedure USEPA (2000), for instance, mixing soil levels, mislabelling samples, or using contaminated equipment in the field.

During laboratory analysis, samples might get mixed by technicians or inefficient laboratory conditions, such as calibration of instruments, might result in wrong data results, so accredited laboratories should be chosen.

QA/QC procedures ensure the accuracy and precision of the data; as a result, in this study, 8 duplicate samples (6 soil and 2 rock samples) are used. Duplicate samples provide precision and reproducibility of the analysis results. The reliability and consistency of sampling methodology and laboratory analysis were checked with duplicate sample results. For QA/QC procedures of field duplicates, a precision less than ±20 % is unrealistic according to Barth and Mason (1984); to check this precision, potentially toxic elements As, Ba, Co, Pb and Sn results (Figure 3.10-3.14) are compared with error limit of 20% and all of the results are within the error limits.

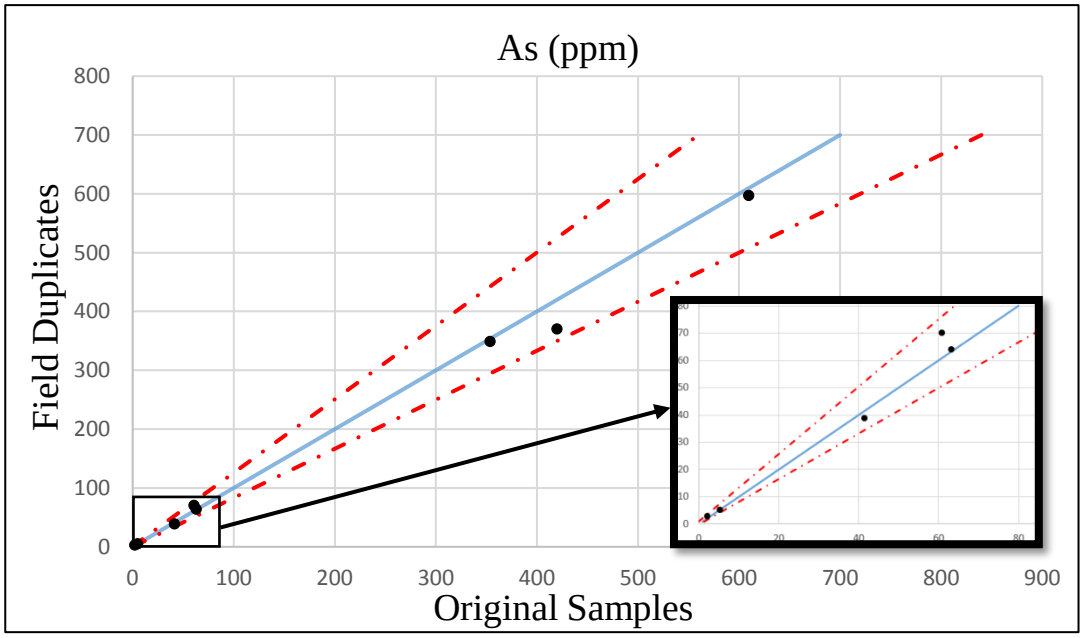

Figure 3.10 Duplicate and original sample result comparison for As (blue line represents 45° slope and red lines represent 20% error limits).

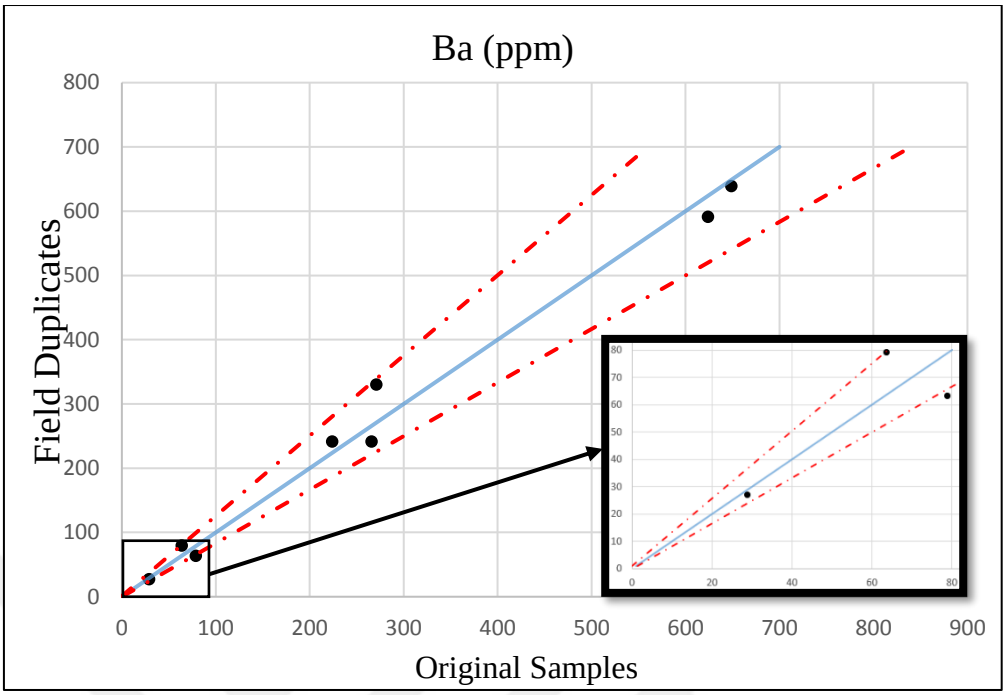

Figure 3.11 Duplicate and original sample result comparison for Ba (blue line represent 45° slope and red lines represent 20% error limits).

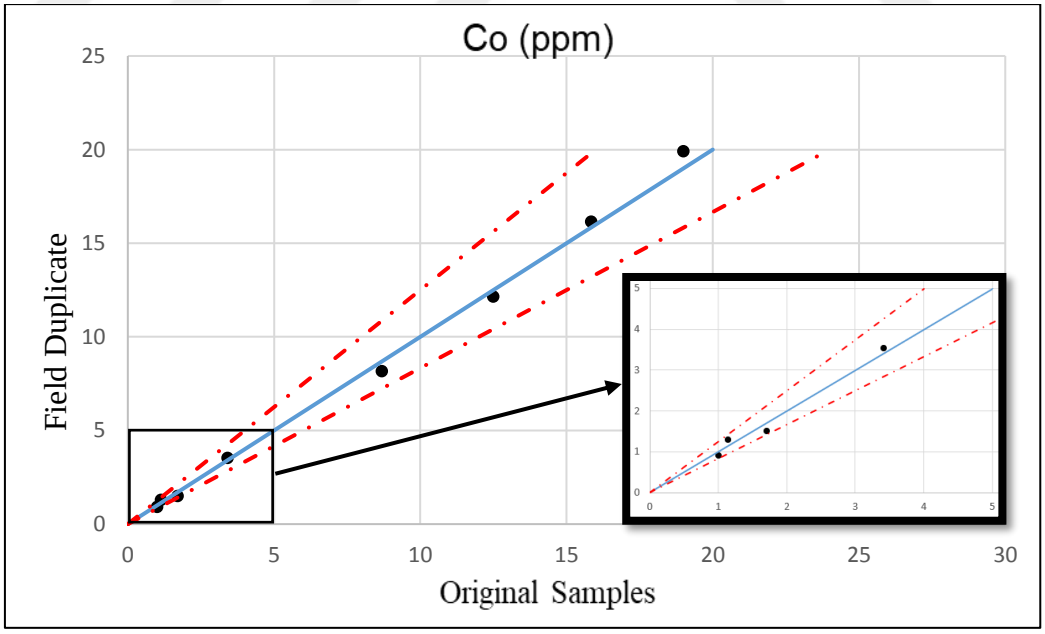

Figure 3.12 Duplicate and original sample result comparison for Co (blue line represent 45° slope and red lines represent 20% error limits).

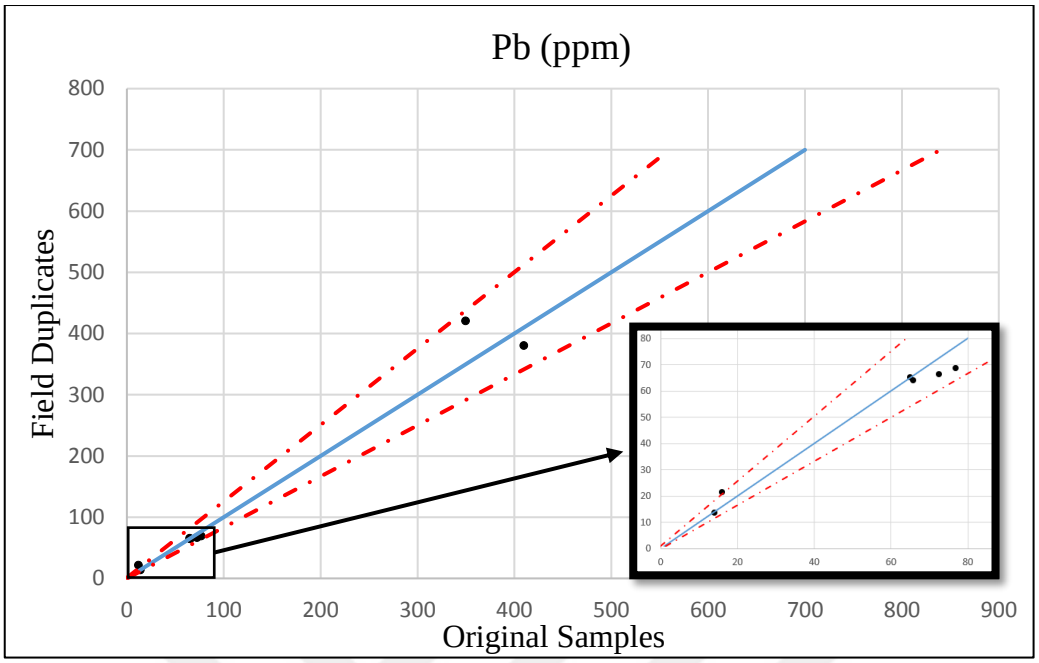

Figure 3.13 Duplicate and original sample result comparison for Pb (blue line represent 45° slope and red lines represent 20% error limits).

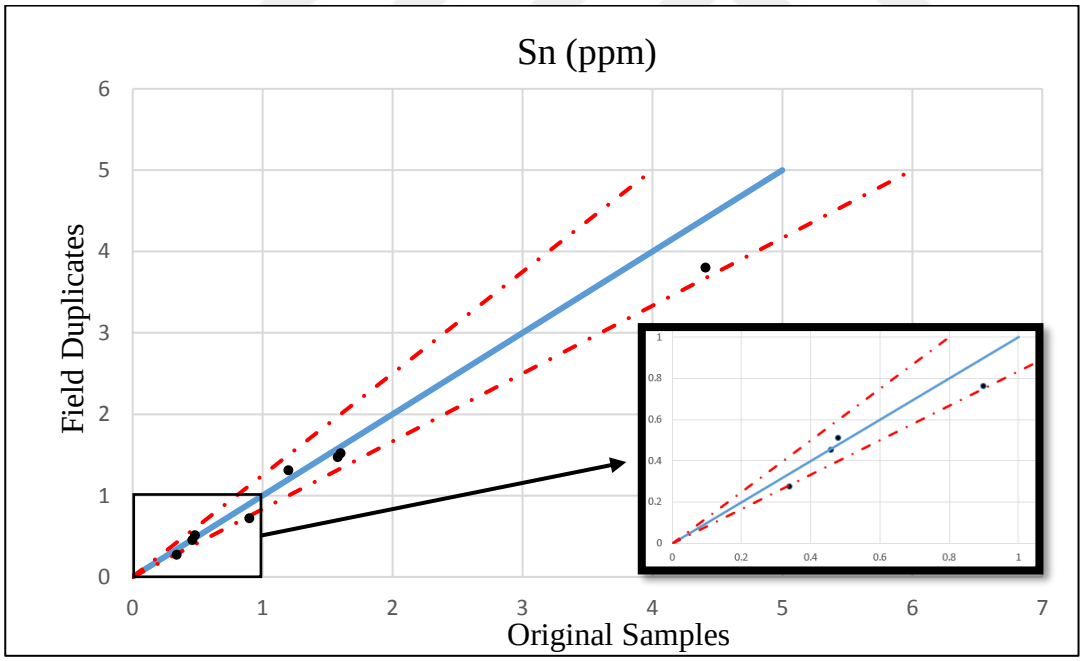

Figure 3.14 Duplicate and original sample result comparison for Sn (blue line represent 45° slope and red lines represent 20% error limits).

3.3 Soil Contamination Indices

Contamination factor (CF), geo accumulation index (Igeo), and pollution load index (PLI) indices have been used as a means of comprehensive and accurate soil and sediment pollution evaluation tools (Teppo, 1998; Sutherland, 2000; Ferreira-Baptista & Miguel, 2005; Reimann & de Caritat, 2005; Yongming et al., 2006; Wei & Yang, 2010; Tchounwou et al., 2012; Wang et al., 2015; Zheng et al., 2015; Delgado-Iniesta et al., 2022; Tian et al., 2022).

3.3.1 Contamination Factor

Contamination factor (CF) is a measure of the degree of contamination of a particular element in a sample relative to either the average crustal composition of that element for rock samples or the measured background values from geologically similar media such as average soil content in Europe or World (Hakanson, 1980). The contamination factor can be calculated by comparing the elemental concentration of the analysed result with a reference value; $CF=C_t/C_{reft}$ (C_t; analysis result of sample C_{reft}; reference value). Contamination classifications can be made according to value ranges in environmental risk assessments (Hakanson, 1980).

- Low grade: $CF < 1$.
- Moderate grade: $1 \leq CF < 3$.
- Significant grade: $3 \leq CF < 6$.
- High grade: $CF \geq 6$.

3.3.2 Geo-accumulation Index

Geo-accumulation is the process of accumulation of chemical substances over time, especially in geological materials such as soil and sediment. This accumulation can occur naturally or because of human activities such as industrial pollution, mining, and agriculture (Muller, 1969). Geo-accumulation index (I_{geo}) = $\log_2(C_t/1.5C_{ref})$

(C_t; analysis result of sample and C_{reft}; reference value). I_{geo} consists of five different classes.

- Unpolluted: $I_{geo} < l$.
- Very low and low polluted: $1 < I_{geo} < 3$.
- Moderately polluted: $3 < I_{geo} < 4$.
- Highly polluted: $4 < I_{geo} < 5$.
- Very highly polluted: $5 < I_{geo} < 6$.

3.3.3 Pollution Load Index (PLI)

The pollution load index (PLI) is used for quantifying the impact of different pollutants present in each area using contamination factors (Tomlinson et al., 1980). These contaminants can include organic and inorganic chemicals, heavy metals and pesticides.

Pollution load index can be calculated with the formula of; $PLI = (CF_{As} \times CF_{Ba} \times CF_{Be} \times .... \times CF_{Zn})^{1/n}$ where contamination factor of different toxic elements in the sample is multiplied and power of 1 divided by the total number of elements. If the PLI value is greater than 1, there is high contamination in that sample (Tomlinson et al., 1980). In this study, contamination factors of contaminants in soil and sediment were used for PLI calculation of each sample.

3.4 Geomedical Risk Assessment Indices

Risk assessments for human health can be used to evaluate the effects of exposure to a particular hazard or toxin on human health (USEPA, 1989). This process can be used to determine risk levels by considering many factors, such as the source of the toxin, the level of human exposure, the toxicity of the toxic element and its potential effects (Tomatis, 1976; Cornfield, 1977; Carter, 1980; Fritz, 1983; Choi et al., 2006; Ferreira-Baptista and Miguel, 2005; Yalcin et al., 2019; Saleh et al., 2019;

Balamurugan et al., 2020; Yousefi et al., 2021; Masri et al., 2021; Aendo et al., 2022). Regarding human health, the risk levels posed by elements found in soil can be divided into two categories: non-carcinogenic and carcinogenic.

3.4.1 Total Noncarcinogenic Risk

Total noncarcinogenic risk index (sum of hazard quotients: Hazard Index (HI)) is a measure used to estimate the potential health risks to human health from exposure to certain toxic elements over a certain time in an area. The non-carcinogenic risk index is calculated by summing the hazard coefficients (HQ) calculated for each element depending on the different routes of exposure such as dermatological, ingestion and inhalation.

$$\text{Total noncarcinogenic risk index} = \text{HI} = \sum_{n=1}^{13} \text{HQ}_{\text{dermatological,ingestion,inhalation}}$$

Where, hazard quotients can be calculated from this formula for each element.

$$\text{HQ}_{\text{dermatological,ingestion,inhalation}} = \frac{\text{CDI}_{\text{dermatological,ingestion,inhalation}}}{\text{RfD}_{\text{dermatological,ingestion,inhalation}}}$$

The CDI (chronic daily intake) in this formula can be calculated differently according to age, gender, exposure area, exposure time, and exposure type, such as dermatological, inhalation and ingestion (USEPA, 2002). The factors used in the formulae (USEPA, 2002) are shown in Table 3.2.

$$\text{CDI}_{\text{ingestion}} = \frac{\text{C}_\text{t} \times \text{CF} \times \text{IR}_\text{s} \times \text{EF} \times \text{ED}}{\text{BW} \times \text{AT}}$$

$$\text{CDI}_{\text{dermal}} = \frac{\text{C}_\text{t} \times \text{CF} \times \text{SA} \times \text{AF} \times \text{ABS} \times \text{EF} \times \text{ED}}{\text{BW} \times \text{AT}}$$

$$\text{CDI}_{\text{inhalation}} = \frac{\text{C}_\text{t} \times \frac{1}{\text{PEF}} \times \text{IR}_\text{a} \times \text{ET} \times \text{EF} \times \text{ED}}{\text{BW} \times \text{AT}}$$

Table 3.2 Factors used in calculation of CDI.

Factor	Explanation	Unit	Children	Man/Woman
C_t	Element amount	$\frac{mg}{kg}$	-	-
IR_s	Ingestion rate of soil	$\frac{mg}{day}$	200	100
SA	Skin surface area	$\frac{cm^2}{day}$	2373	6032
AF	Adherence factor	$\frac{mg}{cm^2}$	0.2	07
IR_a	Inhalation rate of soil	$\frac{m^3}{hour}$	0.53	0.83
ED	Exposure duration	Year	6	20
BW	Bodyweight	Kg	18	77/67
AT	Average time	Day	365xED	365xED
PEF	Particle emission factor	$\frac{m^3}{kg}$	1.36×10^9	
CF	Conversion multiplier	$\frac{kg}{mg}$	$1x10^{-6}$	
ET	Exposure time	$\frac{hour}{day}$	24	
EF	Exposure frequency	$\frac{day}{year}$	350	
ABS	Absorption	-	Arsenic 0.3 Other 0.1	

RfD ($\frac{mg}{kg \times day}$) means the chronic daily intake threshold calculated by various health organisations that may lead to chronic disorders (Table 3.3). However, for chronic daily intake of inhalation RfC ($\frac{mg}{m^3}$) is given in a different unit where in terms of soil and rock analysis results are usually given in ppm a conversion is needed to use soil analysis results.

$$\frac{[\text{RfC (mg/m3) x 20 m3/day (Daily inhalation rate)}]}{\text{70 kg (bodyweight)}} = \text{RfD } (\frac{\text{mg}}{\text{kg} \times \text{day}})$$

For children (average weight of 18 kg and daily inhaled air volume of 10 m3/day), the value would be higher in a calculation using this formula. However, since this conversion may have overestimation, adult results which give lower values were used in the risk calculation for children. Furthermore, dermatological RfD values can be found by multiplying the absorption coefficient of inorganic substances (0.2) by RfD ingestion values (USEPA, 1992).

Exposure for elements is considered safe if HI value < 1, if the value of HI>1, exposure poses a potential health risk (USEPA, 2002). As this number increases, it can be stated that the amount of risk increases.

Table 3.3 RfD Values of Elements ($\frac{mg}{kg \times day}$) (IC = IRIS (Integrated Risk Information System); AF = ATSDR Final (Agency for Toxic Substances and Disease Registry); C = CALEPA (California Environmental Protection Agency))

Element	RfD Ingestion (mg/kg-day)	RfD Ingestion/ Dermal reference	RfC Inhalation (mg/m3)	RfC Inhalation Reference	RfD Dermal	Health problem
Antimony	4.00E-04	IC	3.00E-04	AF	8.00E-05	Metabolic
Arsenic	3.00E-04	IC	1.50E-05	C	6.00E-05	Cardiovascular
Barium	2.00E-01	IC	5.00E-04	AF	4.00E-02	Renal
Beryllium	2.00E-03	IC	2.00E-05	IC	4.00E-04	Respitory
Cadmium	1.00E-04	AF	1.00E-05	AF	2.00E-05	Muscular
Cobalt	3.00E-04	AF	6.00E-06	AF	6.00E-05	Hematologic
Lead and compounds	3.50E-03	C	-		7.00E-04	Neurologic
Molybdenum	5.00E-03	IC	2.00E-03	AF	1.00E-03	Renal
Nickel and compounds	1.10E-02	C	1.40E-05	C	2.20E-03	Respitory
Selenium	5.00E-03	IC	2.00E-02	C	1.00E-03	Renal
Tin	6.00E-01	AF	-	-	1.20E-01	Hematologic
Zinc and compounds	3.00E-01	IC	-	-	6.00E-02	Hematologic

3.4.2 Total Carcinogenic Risk

A carcinogenic risk assessment is a calculation used to assess the potential health risks when a person is exposed to substances that increase the likelihood of developing cancer, and one cancer per ten thousand population (10^{-4}) is high risk value (USEPA, 2002). In this process, calculations can be made by considering factors such as the type of substances that may cause cancer, route of exposure, duration, and amount of exposure.

Elements such as arsenic, beryllium, cadmium, nickel, and lead are classified as carcinogenic substances (USEPA, 2002). However, beryllium and cadmium can only cause this effect when inhaled (USEPA, 2002), so the factors of exposure routes for elements found in soil are different from each other.

During the risk calculation, the total risk can be calculated using the CDI values and the CSF (cancer slope factor) values of the exposure pathway. CSF values changes for different elements in soil (Table 3.4).

$$Risk = CDI \times CSF_{\text{dermal,ingestion,inhalation}}$$

$$Total\ Carcinogenic\ Risk = \sum_{n=1}^{5} Risk$$

- High risk value: Risk > 10^{-4}
- Acceptable risk value: 10^{-4} < Risk < 10^{-6}

Table 3.4 Carcinogenic Slope Factors

Element	$CSF_{Ingestion}$	CSF_{Dermal}	$CSF_{Inhalation}$	Reference Agencies
Arsenic	1.5	7.5	15.1	USEPA
Beryllium	-	-	8.4	USEPA
Cadmium	-	-	6.3	USEPA
Nickel	0.91	4.55	0.91	CALEPA
Lead	0.85	0.425	0.42	CALEPA

3.5 Distribution Mapping

Distribution maps are used for representation of data on an area for better understanding of results by using interpolation methods. Thus, soil and sediments of İzmir city center's geochemical results and noncarcinogenic/carcinogenic risk calculations are created by using maximum 5 neighbours and minimum 2 neighbours with circular radius of 2 kilometers in different interpolation methods.

Statistically, the empirical Bayesian kriging regression interpolation method (EBK regression) shows most realistic results with lower RMSE values than other interpolation methods such as, inverse distance weighting, radial basis function, global polynomial interpolation methods for elemental (Table 3.5) and risk (Table 3.6 and 3.7) interpolations.

Moreover, in EBK regression interpolations topographical elevations (digital elevation model) can be used in ArcGIS Pro, which is useful for interpolation since drainage basins are also considered in distribution maps.

Distribution maps are firstly, bounded in district borders (Figure 3.15) and during sampling procedures, some areas in the city center were not accessible such as, buildings, military bases, archaeological sites these areas are extracted from the maps to have statistically more accurate visualization. Extracted areas of the İzmir city center are chosen by using topographical features and unsampled areas. The selection process involved considering samples that had no neighbours within a radius of 2 kilometers since nearest neighbours used in the interpolation radius is 2 km (Figure 3.16). This approach allowed for a more comprehensive and detailed analysis of geochemical and risk distribution maps, as it ensured that all areas of the city center were adequately represented in the data. By incorporating topographical features, the method was able to identify areas with unique characteristics that may have an impact on the risk distribution. Therefore, for all the distribution maps same areas are extracted.

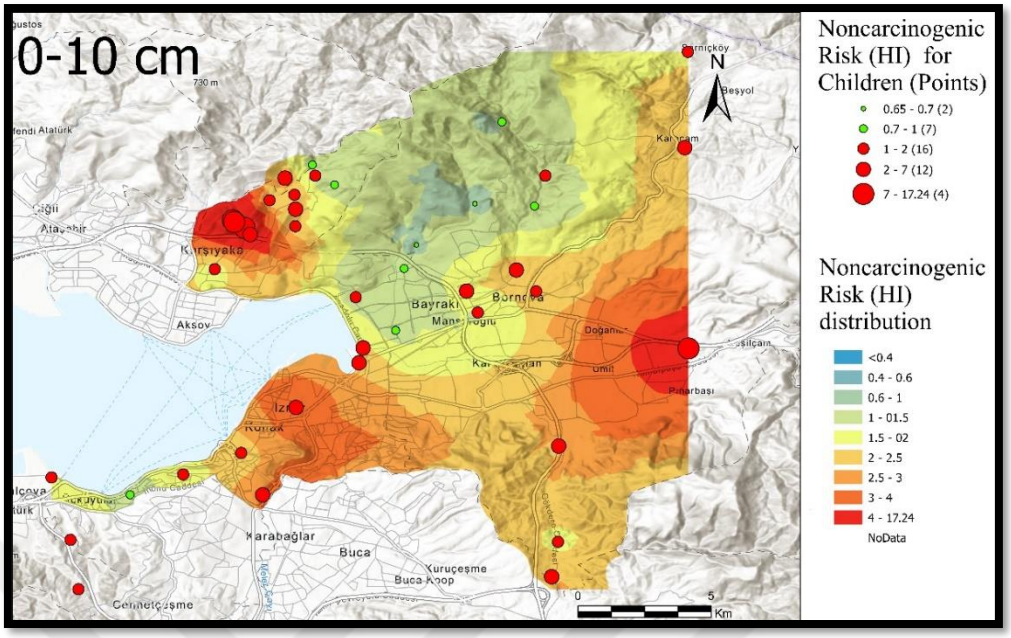

Figure 3.15 Noncarcinogenic distribution map bounded by Bayraklı, Bornova and Konak districts' borders

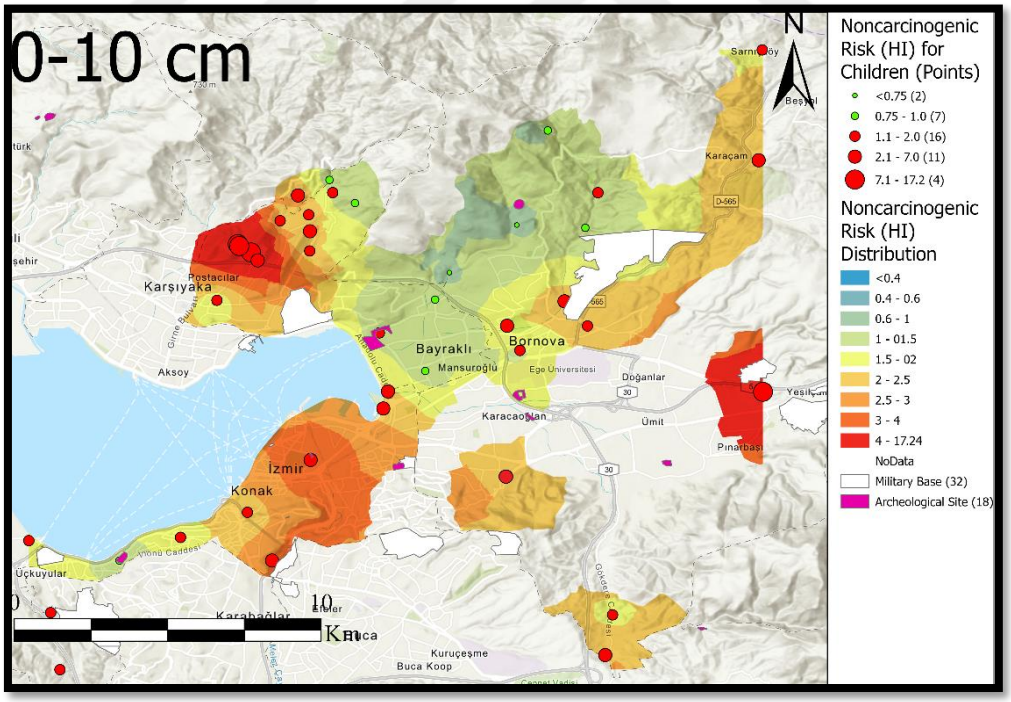

Figure 3.16 Noncarcinogenic distribution map bounded by Bayraklı, Bornova and Konak districts' borders and unsampled areas

Table 3.5 Geostatistical interpolation methods used for elemental distribution maps and ranked accuracy of these methods (produced for intermediate layer elemental (Co, Pb, As) distribution maps for children)

Geostatistical Layer	Rank	Root Mean Square Error	Mean Error	Mean Standardized Error	Root Mean Square Standardized Error	Average Standard Error	Maximum Absolute Error
EBK Reg. Co	1	7.12	0.13	0.018	0.97	7.32	27.16
Global Poly. Co	2	7.41	-0.18	n.d.	n.d.	n.d.	28.73
Inv. Dist. Co	3	8.41	-0.56	n.d.	n.d.	n.d.	30.98
EBK Reg. Pb	4	48.46	0.61	0.006	0.96	51.27	168.35
RBF Pb	5	50.13	0.17	n.d.	n.d.	n.d.	168.42
Kriging Pb	6	50.57	-2.99	-0.052	0.92	56.92	169.24
EBK Reg. As	7	56.74	-2.59	n.d.	n.d.	n.d.	235.00
RBF As	8	80.72	29.12	n.d.	n.d.	n.d.	342.49
Inv. Dist. As	9	81.76	-21.48	-0.017	0.85	104.03	417.38

Inv dist.: Inverse distance weighting, Global poly: Global polynomial interpolation method., RBF: radial basis function, EBK Reg.: Empirical Bayesian kriging regression method.

Table 3.6 Geostatistical interpolation methods that are used for distribution map calculation and ranked accuracy of the methods (produced for upper layer hazard index distribution maps for children)

Geostatistical Layer	Rank	Root Mean Square Error	Mean Error	Mean Standardized Error	Root Mean Square Standardized Error	Average Standard Error	Maximum Absolute Error
EBK Reg.	1	2.725	0.044	0.007	0.61	5.21	10.47
Kernel	2	2.952	0.132	0.07	0.79	3.06	10.96
Kriging	3	3.002	0.300	0.12	0.67	3.76	11.86
RBF	4	3.079	0.120	n.d.	n.d.	n.d.	11.45
Inv. Dist.	5	3.092	0.297	n.d.	n.d.	n.d.	11.5
Diffusion	6	3.767	0.181	n.d.	n.d.	n.d.	13.64

EBK Reg.: Empirical Bayesian kriging regression method, RBF: radial basis function, Inv dist.: Inverse distance weighting

Table 3.7 Geostatistical interpolation methods that are used for distribution map calculation and ranked accuracy of the methods (produced for intermediate layer carcinogenic risk distribution maps for children)

Geostatistical Layer	Rank	Root Mean Square Error	Mean Error	Mean Standardized Error	Root Mean Square Standardized Error	Average Standard Error	Maximum Absolute Error
EBK Reg.	1	0.00118	0.000067	0.107	0.586	0.0016	0.0059
Kriging	2	0.00119	0.000014	0.047	0.877	0.0010	0.0058
Local Polynomial	3	0.00130	0.000050	0.042	0.985	0.0013	0.0065
RBF	4	0.00132	0.000008	n.d.	n.d.	n.d.	0.0059
Inv. Dist.	5	22.23	0.193846	n.d.	n.d.	n.d.	8.17

EBK Reg.: Empirical Bayesian kriging regression method, Inv. dist.: Inverse distance weighting, RBF: radial basis function

CHAPTER 4

GEOCHEMISTRY

4.1 Potentially Toxic Elements

Geogenic materials can be toxic or essential for the human body and can be an element, a molecule compound, or a mineral. It has been reported that some elements such as Co, Cu, Cr, Fe, Mg, Mn, Mo, Ni, Se, and Zn are essential nutrients that are required for various biochemical and physiological functions in the human body; other elements, such as Ag, Al, As, Au, Ba, Be, Bi, Cd, Ga, Ge, Hg, In, Li, Ni, Pb, Pt, Sb, Sr, Sn, Te, Ti, Tl, U, V have no established biological functions and are considered as non-essential elements according to WHO (1996).

Potentially toxic elements can pose hazardous effects on human health and the environment. They can reduce plant growth, affect food quality, and enter the food chain, ultimately posing hazardous effects for all living, including human health.

Some of the most common potentially toxic elements are Cd, Pb, Zn, Cu, Ni, V, As, Hg, and Sb (Pan et al., 2018). The studied potentially toxic elements in the area indicate some areas are polluted, and some are pristine when average values to average soil values around the world and crustal average values for rocks are compared (Table 4.1).

When elemental averages of As, Hg, Pb, and Sb are compared to soil/sediment and rock averages, these 3 elements show enrichment for both media. In the case of elements, Cd, Co, Mo, Ni, Sn, and Zn show enrichment in soil/sediment averages, but in terms of rock averages, these elements show depletion. Oppose to other elements, Se shows depletion in soil/sediment but enrichment in rocks. Ba, Br, Cl, Li, Mn V show depletion for both media.

In this study, potentially toxic elements As, Ba, Be, Cd, Co, Pb, Mo, Ni, Sb, Se, Sn, and Zn are studied, which are above crustal and world soil averages, trigger action values (Table 4.1) or near averages or pose carcinogenic effects (USEPA, 2002).

Table 4.1 Crustal and soil averages of elements and trigger action values for these elements (Kabata-Pendias, 2011), World soil averages (Kabata-Pendias, 2011), European upper layer soil averages (FOREGS, 2005), Izmir city center's soil and sediment averages, Izmir city center's rock averages in ppm (this study).

Element	Crust Average (ppm)	World Soil Average (ppm)	FOREGS Europe (ppm)	İzmir Soil and Sediment Average (ppm)	İzmir Rock Average (ppm)	Trigger Action Value (ppm)
Arsenic, As	1.8	6.83	11.6	45.51	39.83	65
Barium, Ba	400	460	400	232.11	145.29	400
Beryllium, Be	3	1.34	2	1.19	0.72	10
Bromine, Br	2	10	-	4.22	0.69	-
Cadmium, Cd	0.1	0.41	0.28	0.29	0.08	20
Cobalt, Co	10	11.3	10.4	13.72	8.42	2
Chromium, Cr	100	59.5	94.8	33.13	16.58	50
Chlorine, Cl	640	300	380	104.54	12.55	-
Copper, Cu	55	38.9	17.3	28.55	37.04	60
Fluorine, F	625	321	264	16.29	21.98	-
Mercury, Hg	0.07	0.07	0.061	0.16	0.08	1.5
Iodine, I	0.5	2.8	2.4	0.16	0.08	-
Lithium, Li	20	21	-	15.53	15.03	-
Manganese, Mn	900	488	524	686.77	480.82	-
Molybdenum, Mo	1.5	1.1	0.94	1.75	0.99	5
Nickel, Ni	20	29	37	35.18	20.27	75
Lead, Pb	15	27	32	56.66	54.68	50
Antimony, Sb	0.2	0.67	1.04	2.55	0.88	10
Selenium, Se	0.05	0.44	-	0.4	0.17	3
Tin, Sn	2.5	2.5	4.5	2.61	0.99	35
Vanadium, V	135	129	60	54.03	48.35	100
Zinc, Zn	70	70	68.1	94.87	39.46	200

4.1.1 Arsenic

Arsenic is a metalloid distributed widely in the earth's crust; it is generally not found in its elemental form. It is commonly seen as bonds with other elements like oxygen, sulphur, and chlorine to form arsenic compounds.

Its most toxic compounds are water-soluble trivalent (arsenic trioxide, sodium arsenite and arsenic trichloride) and pentavalent (arsenic pentoxide, arsenic acid, and arsenates, e.g., lead arsenate and calcium arsenate) (WHO, 2000).

Arsenic can also be found in different minerals like arsenopyrite (FeAsS), orpiment (As_2S_3), realgar (As_4S_4) enargite (Cu_3AsS_4); additionally, it can be found in coal.

Arsenic exposure can affect nearly all organ systems, including the cardiovascular, dermatologic, nervous, hepatobiliary, renal, gastrointestinal, and respiratory systems (Tchounwou et al., 2013). Severe adverse health effects of arsenic depend on the chemical form of arsenic with time and dose dependence (Yedjou et al., 2006) if arsenic consumption exceeds three µg/kg.BW/day (bodyweight/day) (lung cancer); 5.2 µg/kg.BW/day (bladder cancer); 5.4 µg/kg.BW/day (skin lesions) may occur (WHO, 1989). Thus, it can be stated that a high amount of arsenic in soil may be dangerous for those who live around arsenic-enriched areas.

4.1.2 Barium

Barium can be found in low quantities but widely distributed in igneous and sedimentary rocks such as sandstone, shale, and coal (Miner, 1969; Kunesh, 1978). As a result of weathering of minerals, most commonly found ones baryte ($BaSO_4$) and witherite ($BaCO_3$), barium can be found in soil or sediments.

Ingestion of 0.2 mg/kg/day of barium element can cause renal(kidney) problems, and larger amounts of eating or drinking barium, can cause heart rhythm change or paralysis, also after consuming excess quantities of barium, people can die by not seeking medical treatment (ATSDR, 2007).

4.1.3 Beryllium

Beryllium occurs naturally in rocks, and common minerals that contain the element are Beryl ($Be_3Al_2Si_6O_{18}$) and Bertrandite ($Be_4Si_2O_7(OH)_2$). Limited data are available regarding health problems due to beryllium absorption via inhalation in humans; however, one ng/m^3 inhalation can cause respiratory issues for humans other than inhalation, ingestion, and dermal contact has no known effect (ATSDR, 2022). Beryllium is mainly found as particulate matter in the atmosphere, and accumulation in the lungs depends on particle size, form, and solubility (IRSST 2012).

4.1.4 Cadmium

Cadmium is a heavy metal that can rarely be found in mineral forms, such as greenockite, hawleyite (CdS), otavite ($CdCO_3$). Health problems associated with cadmium are respiratory and renal (kidney) problems.

Respitory problems can occur if cadmium is inhaled above the rate of 0.00003 mg/m^3/day. If cadmium is ingested above the rate 0.0001 mg/kg/day or 0.0005 mg/kg/day, renal (kidney) or muscular problems can be observed in human body (ATSDR, 2012). In that case, symptoms such as abdominal pain, burning sensation, nausea, vomiting, salivation, muscle cramps, vertigo, shock, loss of consciousness and convulsions can be observed (Baselt & Cravey, 1995).

4.1.5 Chromium

Chromium is a naturally occurring heavy metal present in the crust. Chromium can enter soil, sediment, or water media due to weathering, and chromium enrichment is mainly linked with ultramafic, mafic rocks. Some common chromium minerals are chromite ($FeCr_2O_4$) and magnesiochromite ($MgCr_2O_4$) and crocoite ($PbCrO_4$).

Ingestion of high doses of Cr^{6+} compounds can result in severe respiratory, cardiovascular, hematological, renal (kidney), and neurological problems for humans, according to Goyer (2001). Cr^{3+} compounds are also problematic; inhaling 0.005 μg/m3 Cr^{3+} can cause respiratory problems. However, it is also an essential nutrient, so ingestion of 20-45 μg/day of it is adequate for humans (ATSDR, 2012), which means exposure type to certain elements is essential for health problems.

4.1.6 Cobalt

Cobalt can be beneficial since it is part of vitamin B12 or harmful to human health. Cobalt can be found in minerals; glaucodot ((Co,Fe)AsS), cobaltite (CoAsS), linnaeite ($CoCo_2S_4$), skutterudite ($CoAs_3$).

Non-radioactive cobalt has not been shown to cause carcinogenic risk for humans or animals by ingestion. However, the carcinogenic risk was observed in animals which breathe cobalt or injected cobalt into the muscle or under the skin.

Ingestion of 0.01 mg Co/kg/day can cause hematological problems, and inhalation of 0.1 $\mu g/m^3$ can cause respiratory problems; additionally, lung, heart, and skin problems can be caused by high levels of cobalt exposure (Davis & Fields, 1958; ATSDR, 2004).

4.1.7 Molybdenum

Molybdenum is a trace element found in minerals such as wulfenite ($PbMoO_4$) and powellite ($CaMoO_4$), and most commonly as molybdenite (MoS_2). It cannot be found in pure elemental form easily in nature but principally as oxide or sulfide compounds (Barceloux, 1999). Inhalation of 2 $\mu g/m^3$ molybdenum causes respiratory problems and ingestion of 0.06 mg/kg/day causes renal (kidney) problems, and exposure to higher amounts can cause a decrease in sperm count and anaemia following oral exposure (ATSDR, 2020).

4.1.8 Nickel

Nickel is a naturally occurring heavy metal that may be found extensively in nature. In minerals nickel is found in pentlandite ($(Fe,Ni)_9S_8$), nickeline (NiAs) or as millerite (NiS).

Nickel exposure can lead to various health effects, including allergic contact dermatitis, respiratory carcinogenicity, reproductive and developmental toxicity, and non-cancer lung effects (Buxton et al., 2019), and inhalation of 0.2 $\mu g/m^3$ can cause respiratory problems (ATSDR, 2004). Nickel can cause allergic skin reactions, particularly in individuals sensitive to nickel (Das et al., 2019).

4.1.9 Antimony

Antimony is a naturally occurring heavy metal that can be found in the earth's crust as stibnite (Sb_2S_3), valentinite (Sb_2O_3) (rare) and kermesite (Sb_2S_2O) (rare) minerals Antimony ingestion 0.0006 mg/kg/day can cause metabolic problems in humans over time, but ingestion of 1 mg/kg/day can cause acute (1-14 days) hepatic problems. Moreover, inhalation of 0.0003 mg/m^3 can cause long-term respiratory problems, and inhalation of 0.001 mg/m^3 will cause acute (1-14 days) respiratory problems (ATSDR, 2019).

4.1.10 Selenium

Selenium is an essential element, necessary for body processes, and 55 µg/day is the threshold recommended dietary value for people (NAS, 2000). At the same time, above-normal intake values can lead to adverse health effects; for example, ingestion of 0.005 mg/kg/day can cause dermal problems (ATSDR, 2003).

4.1.11 Tin

Tin is generally considered to be non-toxic, and there are no known health effects associated with exposure to tin in food or water. Tin is generally sourced from minerals such as cassiterite (SnO_2) and stannite (Cu_2FeSnS_4). However, some tin compounds, such as tin tetrachloride 0.01 mg/m3 (respiratory) and tin oxide 0.0003 mg/kg/day (immunological), can be harmful if inhaled or ingested in large amounts (ATSDR, 2005), also, if tin ingestion (inorganic compounds) exceeds 0.3 mg/kg/day hematological problems can occur in long exposure.

4.1.12 Lead

Lead is a heavy metal present in the crust; some of its mineral forms are galena (PbS), anglesite ($PbSO_4$) and boulangerite, cerussite ($PbCO_3$). Anthropogenic emissions mainly cause Pb enrichment in the environment because until the end of the 1990s, leaded gasoline was used as a fuel, and it is still used in piston-driven aeroplanes.

Lead can cause adverse health effects, such as neurological, renal, cardiovascular, hematological, immunological, carcinogenic, and so on (ATSDR, 2020). Ingestion of above 0.003 mg/day can cause loss of memory and dullness at the start then the central nervous system would be damaged (ATSDR, 2020).

4.1.13 Zinc

Zinc is a transition metal that can be found in crust as mineral forms such as, sphalerite (ZnS), smithsonite ($ZnCO_3$), and hemimorphite ($Zn_4Si_2O_7(OH_2)H_2O$). Zinc is an essential nutrient and has many functions as enzymes which work in alcohol dehydrogenase and carbonic anhydrase in the body, and deficiency of it can cause dermatitis, poor wound healing and anorexia (WHO, 1996). However, overexposure can be harmful; ingestion of 0.3 mg/kg/day can cause hematological problems in a year (ATSDR, 2005).

4.2 Descriptive Statistics of İzmir City Center Samples

In order to differentiate the source of enrichment in soil/sediment, statistics of different layers of soil and sediments should be evaluated (Table 4.2, 4.3, 4.4 and 4.5).

Median As values (in ppm) are 39.1 for rock, 17.1 in the upper layer (UL), 14.6 in the intermediate layer (IL), bottom layer (BL), and 16, which is over the average value of 6.8 (soil average in world; Cref) in soil. As values ranged from 0.9-74.4 for rock, 5.1-84.5 for UL, 5.2-71.8 IL, and 3.5-127.9 BL (10th-90th percentile, respectively).

Co median values are 8.3 in rock, 12.9 in UL, 26.1 in IL, and 12.9 in BL, over the average value of 11.3 (Cref) in soil. Co values ranged from 0.5-16.2 for rock, 8.4-20.8 for UL, 13.4-61.6 IL, and 4.9-25.6 BL (10th-90th percentile, respectively).

Pb median values are 52 in rock, 29.8 in UL, 27.8 in IL, and 29.8 in BL., higher than the average in soil 27 (Cref). Pb values ranged from 1.0-90.2 for rock, 15.6 to 84.9 for UL, 13.5 to 223.0 for IL, and 14.4 to 146.0 for BL (10th-90th percentile, respectively).

Sb median values are 0.9 in rock, 0.7 in UL, 0.7 in IL, and 0.8 in BL, higher than the average in soil 0.67 (Cref). Sb values ranged from 0.1-2 for rock 0.3-4.4 for UL, 0.4-7.2 for IL, and 0.3- 9.2 for BL (10th-90th percentile, respectively).

Sn median values are 1 in rock, 1.4 in UL, 1.5 in IL, and 1.3 in BL, higher than the average in soil 0.67 (Cref). Sn values ranged from 0.1-1.8 for rock 0.7-6.3 for UL, 0.5-4.9 for IL, and 0.5-5.3 for BL (10th-90th percentile, respectively).

In terms of median values and 90th percentiles, As, Co, Pb, Sb, and Sn elements are way higher than average values of soil/sediment, and the 10th percentile values are close to average values. This distribution shows pollution of these elements (Rinklebe et al., 2019) in the soil and sediments of İzmir.

Ba median values are 145.3 for rock, UL 209, IL 211.5, and BL 211.5, which are lower than the average value of 460 (Cref) in soil, meaning soil/sediment layers are not contaminated with Ba.

Be median values are 0.7 for rock and 1 for all layers, and the 10th-90th percentiles are lower than the average soil value of 1.34 (Cref), so, in terms of Be, there seems to be no contamination in layers of soil and sediments.

Cd median values are 0.1 for rock 0.1 in UL, 0.1 in IL, and 0.1 in BL, and the 10th-90th percentiles are lower than the average value of 0.41 soil (Cref).

Cr median values are 13.0 in rock 26.3 in UL, 13.3 in IL, and 22.4 in BL, and the 10th-90th percentiles are lower than the average value of 59.5 of soil (Cref). Cr values ranged from 2.7-39.7 for rock, 12.0-107.8 for UL, 0-0.6 for IL, and 11.2-66.5 for BL (10th-90th percentile, respectively).

Mo median values are 0.6 in rock, 0.6 in UL, 0.1 in IL, and 0.6 in BL, which are lower than the average value in soil 1.1 (Cref). Mo values ranged from 0.1-1.8 for rock 0.3-2.4 for UL, 0.2- 2.2 for IL, and 0.1-2.8 for BL (10th-90th percentile, respectively).

Ni median values are 19.9 in rock, 27.2 in UL, 20.4 in IL, and 20.7 in BL, lower than the average in soil 29 (Cref). Ni values ranged from 1.5-57.3 for rock, 8.1-86.8 for UL, 8.7-81.6 for IL, and 6.4-78.6 for BL (10th-90th percentile, respectively).

Se median values are 0.1 in rock, 0.1 in UL, 0.1 in IL, and 0.1 in BL, lower than the average in soil 0.44 (Cref). Se values ranged from 0-0.4 for rock, 0.1 to 1.3 for UL, 0 to 0.7 for IL, and 0 to 0.8 for BL (10th-90th percentile, respectively).

Zn median values are 33.3 in rock, 64.9 in UL, 67.9 in IL, and 64.2 in BL, lower than the average value in soil 70 (Cref). Zn values ranged from 3.8-80.4 for rock, 37.1-208.0 for UL 34.0-134.3 for IL, and 29.4-125.3 for BL (10th-90th percentile, respectively).

Hence, in terms of contamination, Ba, Be, Cd, Cr, Mo, Se, and Zn elements are not contaminating the soil and sediments of İzmir when median values are considered. However, the 90th percentiles of Cr, Mo, Ni, Se, and Zn elements show above-average soil values, so other geostatistical methods should also be considered to determine which can cause pollution. Furthermore, it can be noted that median values of elements show relatively similar results for all layers of İzmir city center and rock averages, which might mean that the source of these elements is geogenic.

Table 4.2 Descriptive statistics of potentially toxic elements in İzmir city center's rock samples.

	As (ppm)	Ba (ppm)	Be (ppm)	Cd (ppm)	Co (ppm)	Cr (ppm)	Mo (ppm)	Ni (ppm)	Pb (ppm)	Sb (ppm)	Se (ppm)	Sn (ppm)	Zn (ppm)
Detection Limit	0.01	0.5	0.01	0.001	0.001	0.01	0.01	0.04	0.005	0.005	0.003	0.01	0.1
Mean	39.1	142.5	0.7	0.1	8.3	16.3	1	19.9	52.0	0.9	0.2	1	38.7
Median	39.8	145.3	0.7	0.1	7.9	13	0.6	8.3	8.24	0.3	0.1	0.6	33.3
Std. Deviation	104.8	145.4	0.6	0.1	6.5	15	1.4	27.7	24.0	2.3	0.4	1.5	30.8
Range	626	675.5	3	0.6	31.4	70	8.3	137	53.6	16.1	2.9	10.2	138.9
Minimum	0.54	3.5	0.05	0.006	0.14	1.51	0.05	1.22	150.7	0.26	0.04	0.01	1.6
Maximum	626	676	3	0.6	31.4	70	8.3	137	804.0	16.2	2.9	10.2	139
MAC[a]	20	n.d.	10	5	50	200	10	60	300	10	n.d.	n.d.	300
TAV[b]	30	600	300	20	100	450	20	20	300	50	10	50	1500
Average Crust[b]	1.8	400	3	0.1	10	100	1.5	20	15	0.2	0.5	2.5	70
Percentiles													
10	0.9	14.2	0.1	0.05	0.5	2.7	0.1	1.5	1.0	0.1	0.01	0.1	3.8
50	5.2	99.6	0.5	0.1	7.9	13	0.6	8.3	8.2	0.3	0.01	0.6	33.3
90	74.4	326.7	1.6	0.2	16.2	39.7	1.8	57.3	90.2	2	0.4	1.8	80.4

(a) Maximum allowable concentration (MAC) values can be found commonly in the literature, compiled from Kabata-Pendias and Sadurski (2004). (b) Trigger action values (TAV) proposed in some European countries and average soil content Kabata-Pendias (2011).

Table 4.3 Descriptive statistics of potentially toxic elements in Upper Layer (0-10 cm).

	As (ppm)	Ba (ppm)	Be (ppm)	Cd (ppm)	Co (ppm)	Cr (ppm)	Mo (ppm)	Ni (ppm)	Pb (ppm)	Sb (ppm)	Se (ppm)	Sn (ppm)	Zn (ppm)
Detection Limit	0.01	0.5	0.01	0.001	0.001	0.01	0.01	0.04	0.005	0.005	0.003	0.01	0.1
Mean	41	201.1	1.2	0.3	13.6	39.4	2.2	39.9	52.6	2.4	0.3	2.5	103.2
Median	17.1	209	1	0.1	12.9	26.3	0.6	27.2	29.8	0.7	0.1	1.4	64.9
Std. Deviation	73.9	78.1	0.6	0.6	4.8	36.1	9	35.6	83.2	5.2	0.5	3.8	106.1
Range	324.6	393	2.7	3	21.9	155.9	58.1	148.6	474.3	26.4	2.2	21.9	572.4
Minimum	1.4	47	0.3	0.3	2.4	8.1	0.2	2.4	11.7	0.2	0.02	0.3	17.6
Maximum	326	440	2.9	3	24.3	164	58.3	151	486	26.6	2.2	22.2	590
MAC[a]	20	n.d.	10	5	50	200	10	60	300	10	n.d.	n.d.	300
TAV[b]	30	600	300	20	100	450	20	20	300	50	10	50	1500
Average Soil[b]	6.83	460	1.34	0.41	11.3	59.5	1.1	29	27	0.67	0.44	2.5	70
Percentiles													
10th	5.1	96.6	0.7	0.05	8.4	12	0.3	8.1	15.6	0.3	0.04	0.7	37.1
50th	17.1	209	1	0.1	12.9	26.3	0.6	27.2	29.8	0.7	0.1	1.4	64.9
90th	84.5	309	2	0.6	20.8	107	2.4	86.8	84.9	4.4	1.3	6.3	208

(a) Maximum allowable concentration (MAC) values can be found commonly in the literature, compiled from Kabata-Pendias and Sadurski (2004). (b) Trigger action values (TAV) proposed in some European countries and average soil content Kabata-Pendias (2011).

Table 4.4 Descriptive statistics of potentially toxic elements in Intermediate Layer (10-30 cm).

	As (ppm)	Ba (ppm)	Be (ppm)	Cd (ppm)	Co (ppm)	Cr (ppm)	Mo (ppm)	Ni (ppm)	Pb (ppm)	Sb (ppm)	Se (ppm)	Sn (ppm)	Zn (ppm)
Detection Limit	0.01	0.5	0.01	0.001	0.001	0.01	0.01	0.04	0.005	0.005	0.003	0.01	0.1
Mean	33.8	269.2	1.2	0.3	30.2	13.6	1.4	33.7	57.0	2.1	0.3	3.0	94.3
Median	14.6	211.5	1.0	0.1	26.1	13.3	0.5	20.4	27.8	0.7	0.1	1.5	67.9
Std. Deviation	60.4	227.2	0.4	0.5	20.3	5.2	3.4	31.2	80.7	4.0	0.5	6.0	121.3
Range	350.7	1381	1.9	2.5	99.4	30.5	17.5	150.7	330.9	22.8	2.5	29.9	765
Minimum	3.4	44.0	0.6	0.01	6.6	1.7	0.1	5.3	9.1	0.2	0.02	0.3	16.4
Maximum	354.0	1425	2.5	2.6	106.0	32.2	17.6	156.0	340	23.0	2.5	30.2	782
MAC[a]	20	n.d.	10	5	50	200	10	60	300	10	n.d.	n.d.	300
TAV[b]	30	600	300	20	100	450	20	20	300	50	10	50	1500
Average Soil[b]	6.83	460	1.34	0.41	11.3	59.5	1.1	29	27	0.67	0.44	2.5	70
Percentiles													
10th	5.2	86.2	0.8	0.04	13.4	0.04	0.2	8.7	13.5	0.4	0.02	0.5	34.0
50th	14.6	211.5	1.0	0.1	26.1	0.1	0.5	20.4	27.8	0.7	0.1	1.5	67.9
90th	71.8	548.5	1.9	0.54	61.6	0.6	2.2	81.6	223.0	7.2	0.7	4.9	134.3

(a) Maximum allowable concentration (MAC) values can be found commonly in the literature, compiled from Kabata-Pendias and Sadurski (2004). (b) Trigger action values (TAV) proposed in some European countries and average soil content Kabata-Pendias (2011).

Table 4.5 Descriptive statistics of potentially toxic elements (ppm) in Bottom Layer (30-50 cm)

	As (ppm)	Ba (ppm)	Be (ppm)	Cd (ppm)	Co (ppm)	Cr (ppm)	Mo (ppm)	Ni (ppm)	Pb (ppm)	Sb (ppm)	Se (ppm)	Sn (ppm)	Zn (ppm)
Detection Limit	0.01	0.5	0.01	0.001	0.001	0.01	0.01	0.04	0.005	0.005	0.003	0.01	0.1
Mean	42.8	215.2	1.2	0.3	14.8	31.9	1.7	35.1	52.4	2.4	0.4	2.5	91.9
Median	16.0	196.5	1.0	0.1	12.9	22.4	0.6	20.7	29.8	0.8	0.1	1.3	64.2
Std. Deviation	95.6	123	0.7	0.4	8.0	33.7	3.8	40.9	58.8	4.0	1.0	4.3	132.7
Range	607.5	708	3.2	2.1	40.2	227.5	19.9	233.2	246.0	16.0	6.5	29.9	966.5
Minimum	2.5	54.8	0.2	0.02	1.1	1.5	0.1	1.8	10	0.1	0	0.4	13.5
Maximum	610	763	3.4	2.2	41.3	229	20	235	256	16.2	6.5	30.2	980
MAC[a]	20	n.d.	10	5	50	200	10	60	300	10	n.d.	n.d.	300
TAV[b]	30	600	300	20	100	450	20	20	300	50	10	50	1500
Average Soil[b]	6.83	460	1.34	0.41	11.3	59.5	1.1	29	27	0.67	0.44	2.5	70
Percentiles													
10th	3.5	85.7	0.6	0.03	4.9	11.2	0.2	6.4	14.4	0.3	0.02	0.5	29.4
50th	16.0	196.5	1.0	0.1	12.9	22.4	0.6	20.7	29.8	0.8	0.1	1.3	64.2
90th	127.9	327	2.3	0.6	25.6	66.5	2.8	78.6	146	9.2	0.8	5.3	125.3

(a) Maximum allowable concentration (MAC) values can be found commonly in the literature, compiled from Kabata-Pendias and Sadurski (2004). (b) Trigger action values (TAV) proposed in some European countries and average soil content Kabata-Pendias (2011).

4.3 Soil Contamination Indices of İzmir City Center

Contamination factor (CF), geo accumulation index (Igeo), and pollution load index (PLI) indices have been calculated from the samples of İzmir city center and reference values for pollution assessment are chosen as average soil values in the world (Kabata-Pendias, 2011).

Boxplots of calculated values of these indices are used for a clear representation of data where the top of the box represents the 3rd quartile (75% percentile) and bottom of the box represents 1st quartile (25% percentile), the middle line of the box is the 2nd Quartile (50%), the median (Tukey, 1977) and upper whisker show 4th quartile, above the whisker there are outlier values.

4.3.1.1 Contamination Factors of the Samples of İzmir City Center

Contamination factors of As, Ba, Be, Cd, Co, Cr, Mo, Ni, Pb, Sb, Se, Sn and Zn are calculated for sediment and soil layers of İzmir city center, and results are shown (Figure 4.1, 4.2 and 4.3) as boxplots. Contamination factor boxplots show some elements like As and Co have significant grade contamination to high-grade contamination in most of their percentiles.

As values above its 50th percentile show significant grade contamination for all layers, and the bottom layer above the 75th percentile shows high-grade contamination.

Co values from its 25th percentile to the upper whisker show significant grade contamination for all layers, and all layers show similar statistics.

Ni, Pb, Sb, and Zn show moderate to significant grade contamination in most percentiles.

Ni values show moderate grade contamination from the 50th percentile in the upper layer and 60th percentile in the intermediate and bottom layer, and above the 95th percentile show significant contamination.

Pb values from median values (50th percentile) show moderate contamination for all layers except the bottom layer, where the upper whisker ends in significant contamination.

Sb values show moderate grade contamination from the 50th percentile to the 80th percentile and significant grade contamination above the 80th to upper whisker.

Zn values between the median (the 50th percentile) to upper whisker show moderate contamination.

Be, Ba, Cd, Cr, Mo, Se, and Sn show low-grade contamination to moderate-grade contamination for some outliers or above the 80th percentile for some elements.

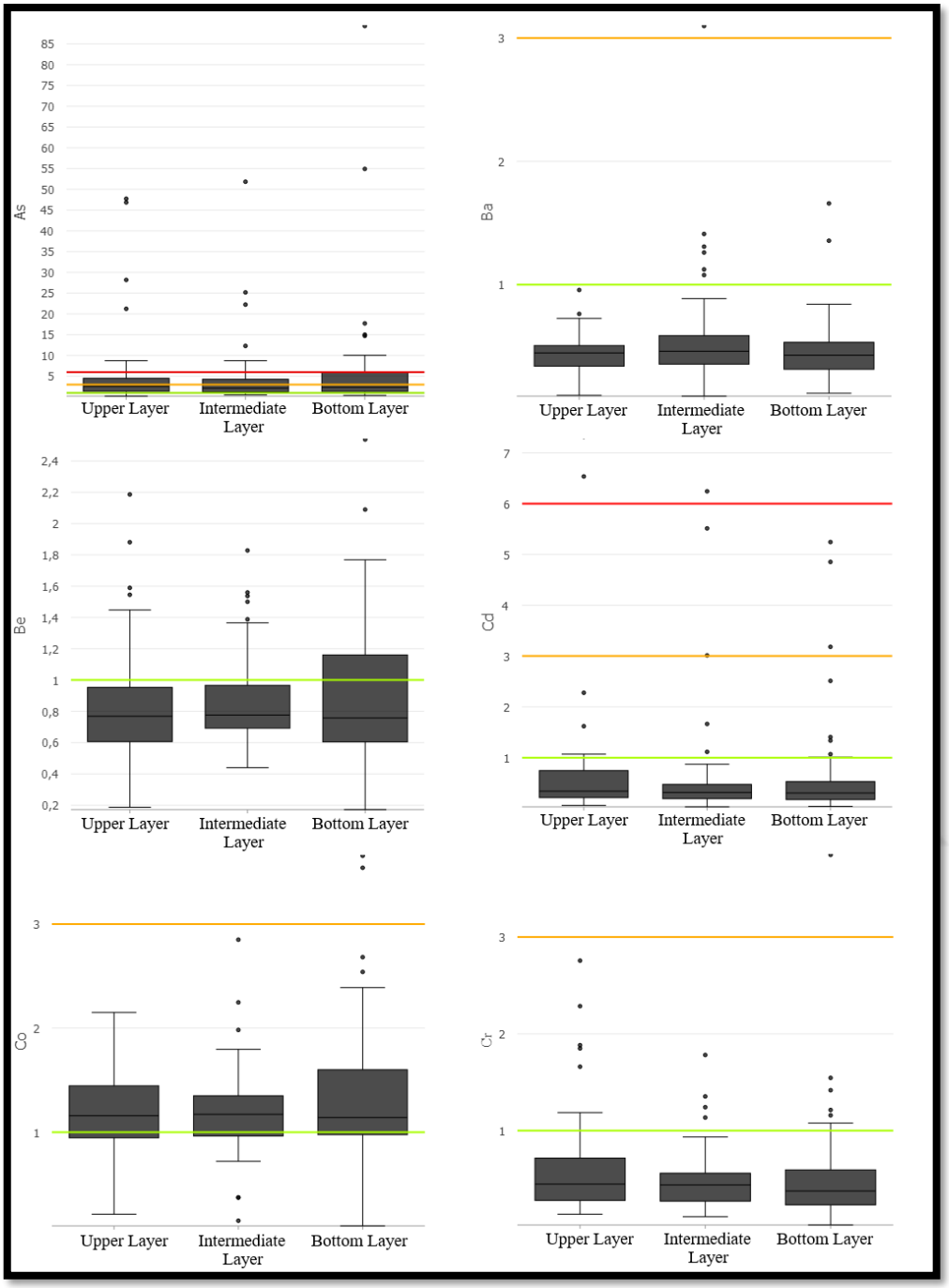

Figure 4.1 Contamination Factor (CF) of As, Ba, Be, Cd, Co, Cr of the soil and sediments from 54 sites of İzmir city center, regarding soil and sediment depths; upper layer (0-10 cm), intermediate layer (10-30 cm), bottom layer (30-50 cm). The added line indicates CF levels (Green=1, Orange=3, Red=6), below 1 low contamination, between 1 and 3 moderate contamination and above 6 high grade contamination is indicated.

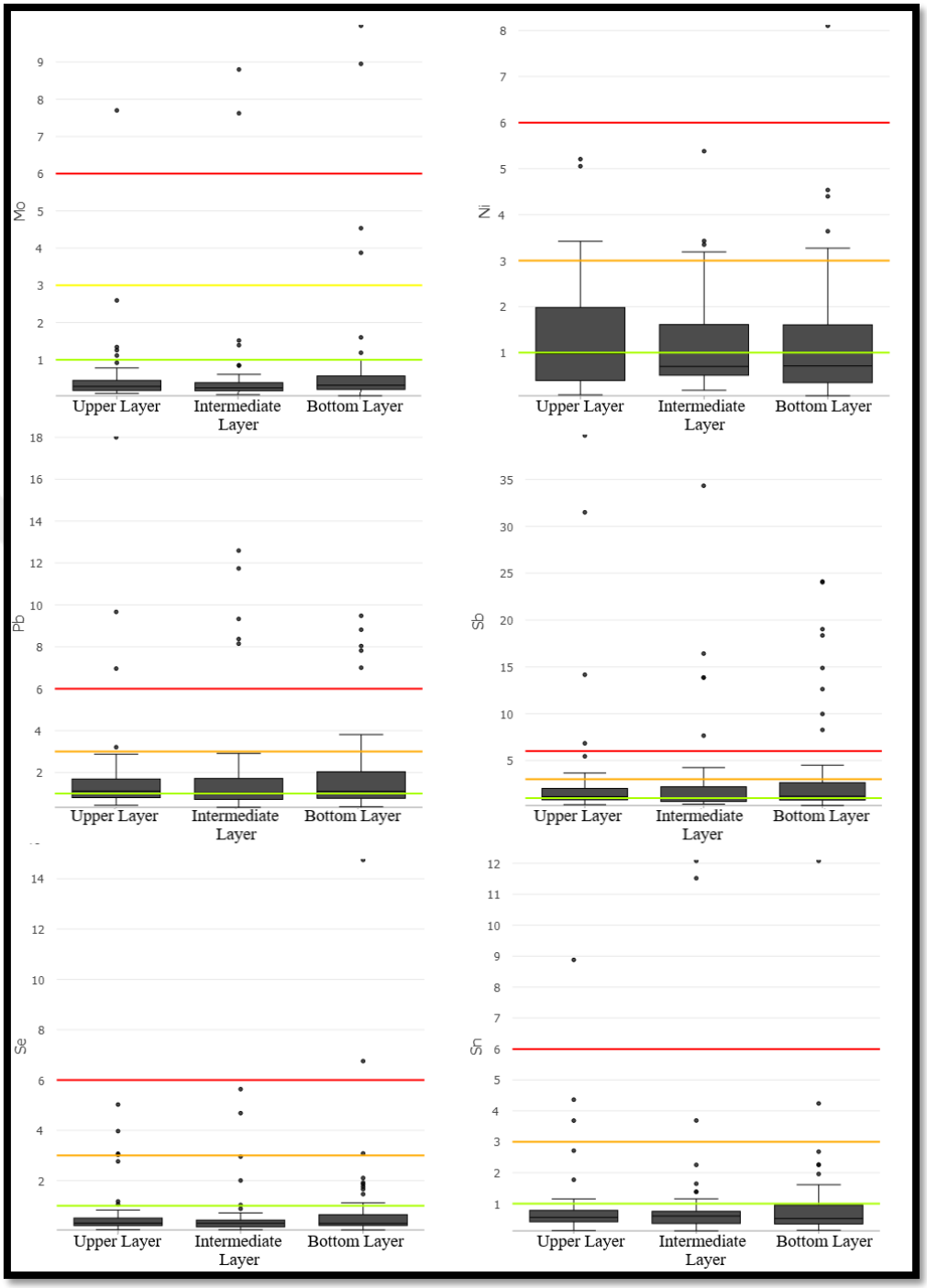

Figure 4.2 Contamination Factor (CF) of Mo, Ni, Pb, Sb, Se, Sn of the soil and sediments from 54 sites of İzmir city center, regarding soil and sediment depths; upper layer (0-10 cm), intermediate layer (10-30 cm), bottom layer (30-50 cm). The added lines indicate CF levels (Green=1, Orange=3, Red=6), below 1 low contamination, between 1 and 3 moderate contamination and above 6 high grade contamination is indicated.

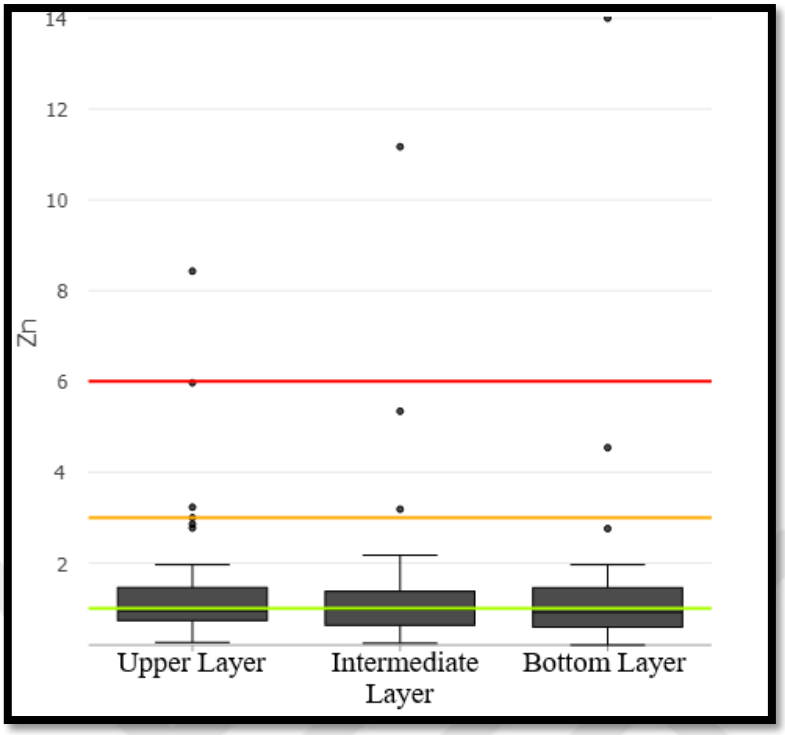

Figure 4.3 Contamination Factor (CF) of Zn of the soil and sediments from 54 sites of İzmir city center, regarding soil and sediment depths; upper layer (0-10 cm), intermediate layer (10-30 cm), bottom layer (30-50 cm). The added lines indicate CF levels (Green=1, Orange=3, Red=6), below 1 low contamination, between 1 and 3 moderate contamination and above 6 high grade contamination is indicated.

4.3.1.2 Geo-accumulation Index of Samples of İzmir City Center

Geo-accumulation index of As, Ba, Be, Cd, Co, Cr, Mo, Ni, Pb, Sb, Se, Sn and Zn are calculated for sediment and soil layers of İzmir city center, and results are shown (Figure 4.4, 4.5 and 4.6) as boxplots. These graphs show lower pollution grades than contamination factor results.

As is the most polluted element, and even As shows in its 80th-90th percentiles very low to low pollution and from its 90th to 100th percentile shows moderate pollution except for bottom layer where it shows high pollution and its upper whisker is in very high pollution range.

Sb is the next polluted element, above the 75th-80th percentile, it shows very low to low pollution, and only the upper whiskers of the component are in the moderately polluted range. Other elements: Ba, Be, Cd, Co, Cr, Mo, Ni, Pb, Se, Sn, and Zn shows no pollution to very low pollution/low pollution.

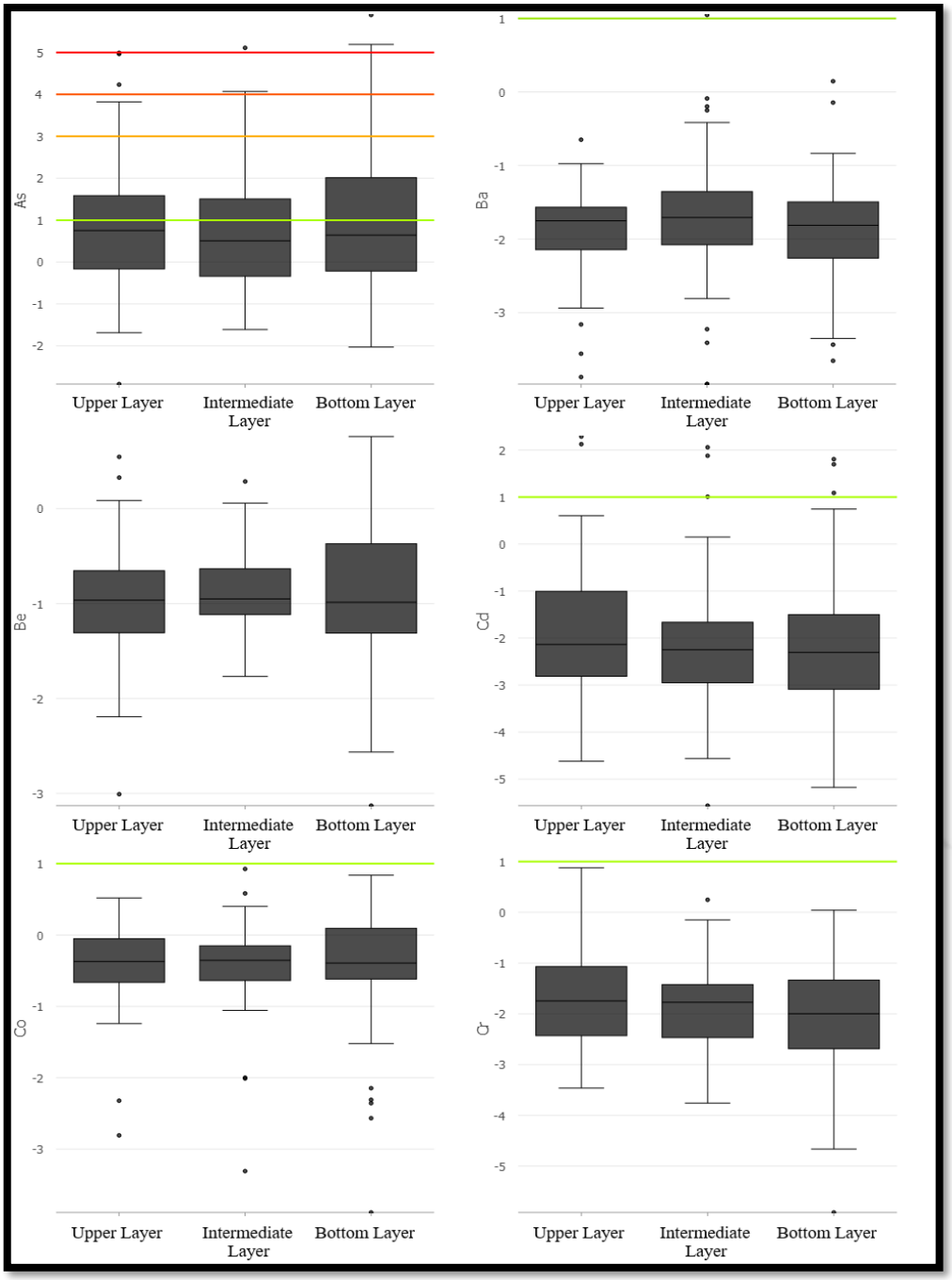

Figure 4.4 Geo-accumulation Index (I_{geo}) of As, Ba, Be, Cd, Co, Cr of the soil and sediments from 54 sites of İzmir city center, regarding soil and sediment depths; upper layer (0-10 cm), intermediate layer (10-30 cm), bottom layer (30-50 cm). The added lines indicate I_{geo} levels (Green=1, Orange=3, Dark Orange=4, Red=5), below 1 low pollution, between 1 and 3 moderate pollution, between 4 and 5 high pollution, and 5 very high pollution is indicated.

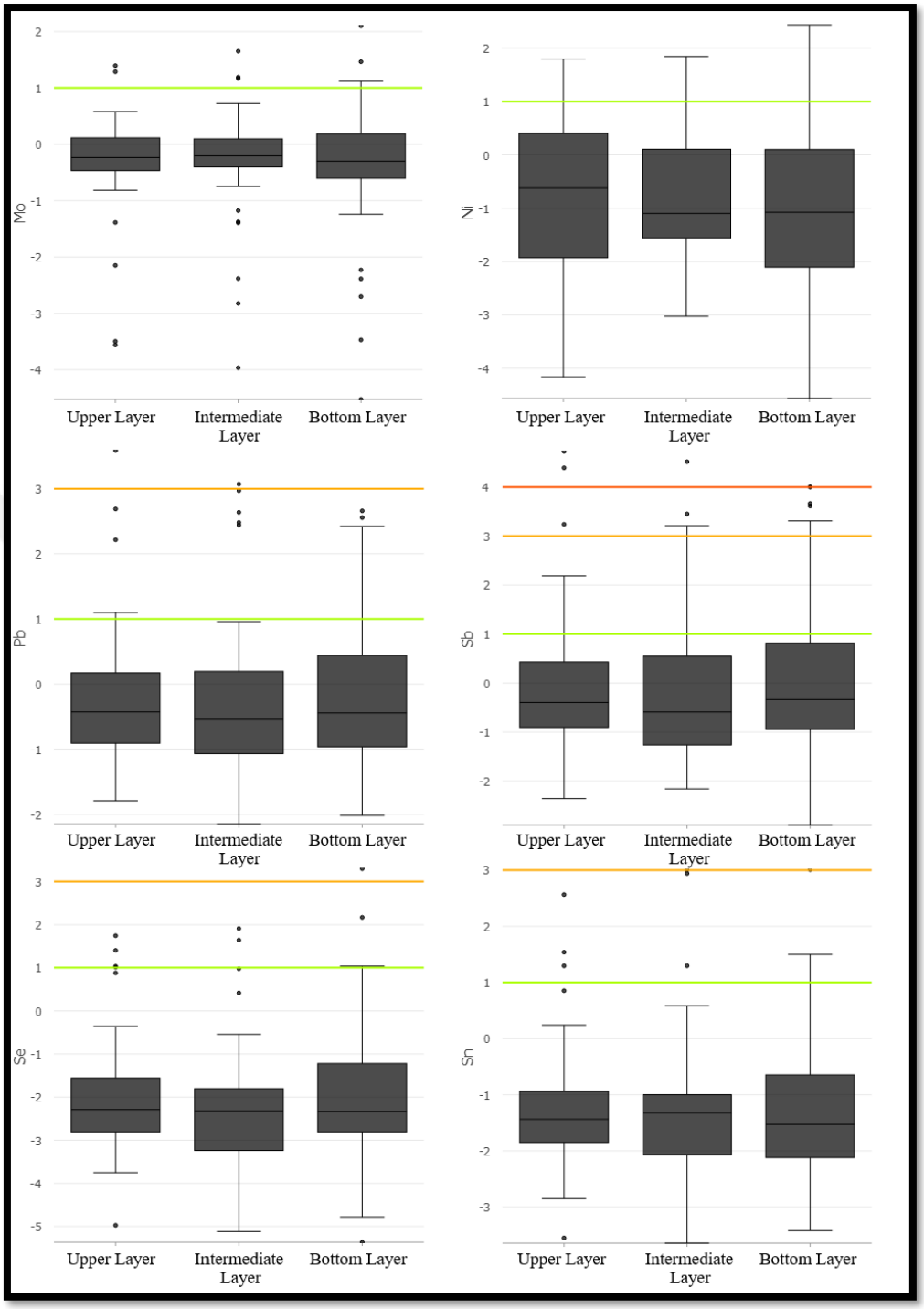

Figure 4.5 Geo-accumulation Index (I_{geo}) of Mo, Ni, Pb, Sb, Se, Sn of the soil and sediments from 54 sites of İzmir city center, regarding soil and sediment depths; upper layer (0-10 cm), intermediate layer (10-30 cm), bottom layer (30-50 cm). The added lines indicate I_{geo} levels (Green=1, Orange=3, Dark Orange=4, Red=5), below 1 low pollution, between 1 and 3 moderate pollution, between 4 and 5 high pollution, and 5 very high pollution is indicated.

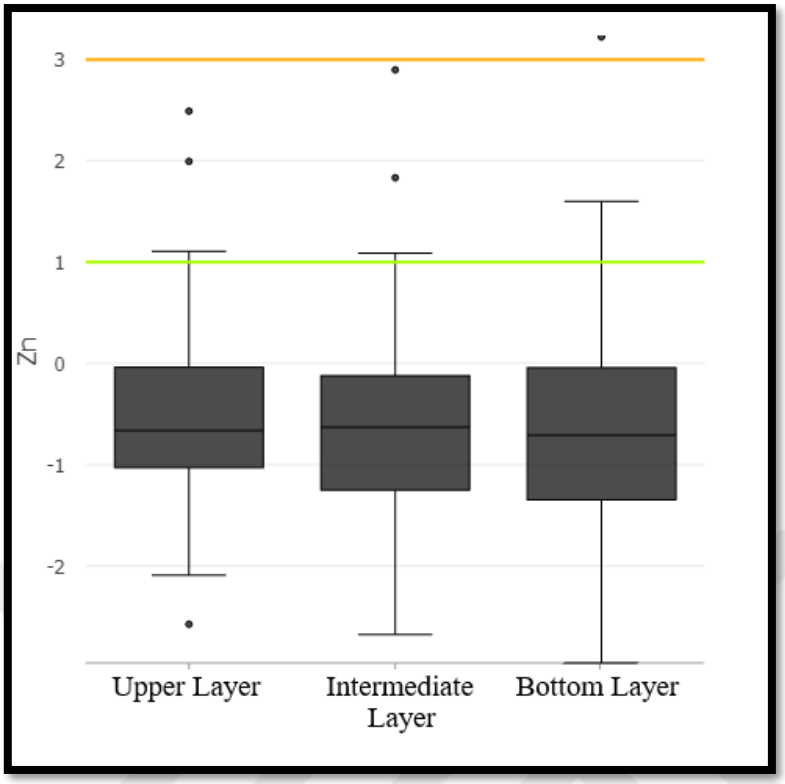

Figure 4.6 Geo-accumulation Index (I_{geo}) of Zn of the soil and sediments from 54 sites of İzmir city center, regarding soil and sediment depths; upper layer (0-10 cm), intermediate layer (10-30 cm), bottom layer (30-50 cm). The added lines indicate I_{geo} levels (Green=1, Orange=3, Dark Orange=4, Red=5), below 1 low pollution, between 1 and 3 moderate pollution, between 4 and 5 high pollution, and 5 very high pollution is indicated.

4.3.1.3 Pollution Load Index of Samples of İzmir City Center

As mentioned before pollution load index can be calculated with the formula provided previously. Thirteen different elements for the calculation in İzmir city center is used: namely, As, Ba, Be, Cd, Co, Pb, Mo, Ni, Sb, Se, Sn, Zn. Distribution of PLI for different soil/sediment levels show that most of the samples are between the range of 0.5 to 0.95 which is classified as non-contaminated (Tomlinson et al., 1980).

Above 80th percentile of PLI shows pollution for some samples and outliers (Figure 4.7).

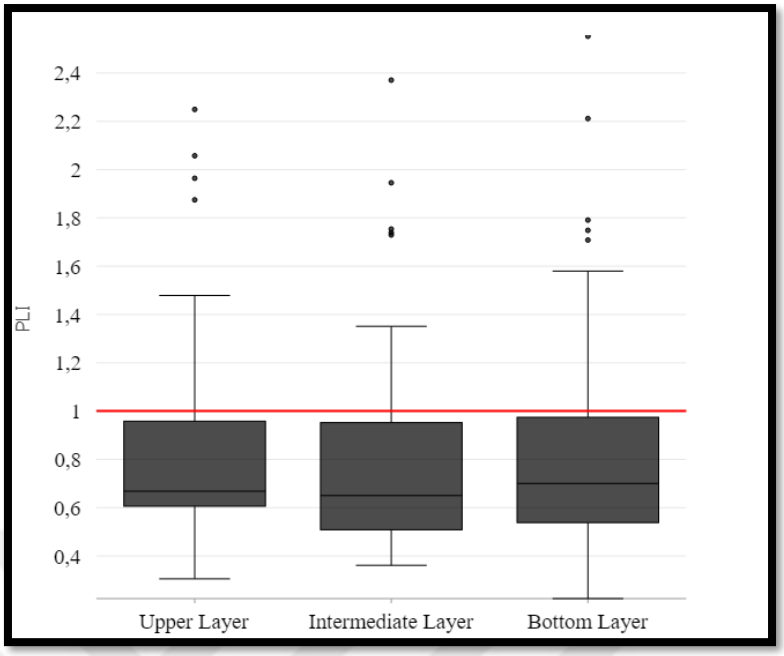

Figure 4.7 PLI Distribution of Samples in İzmir city center.

4.4 Geochemical Distribution Maps

Distribution maps of different elements in İzmir city center are presented herein and elements are chosen depending on descriptive statistics, soil contamination indices; contamination factor, geo-accumulation index, pollution load index and relative differences between rock results and soil/sediment results.

As a result, potentially toxic elements As, Co, Cr, Ni, Pb and Sb distribution maps are produced.

4.4.1 Arsenic Distribution Maps

Arsenic distribution maps are produced for different layers of soil/sediment samples. As values are above averages of soil, rock and crustal values (6.83 and 1.8 ppm) in most of the İzmir city center samples (Figure 4.8, 4.9 and 4.10).

Distribution maps show that only northern part has lower As values, whereas, northwestern, eastern, southern parts of İzmir city center have above trigger action value of 30 ppm. Moreover, from the upper layer to the bottom layer, distributions are similar.

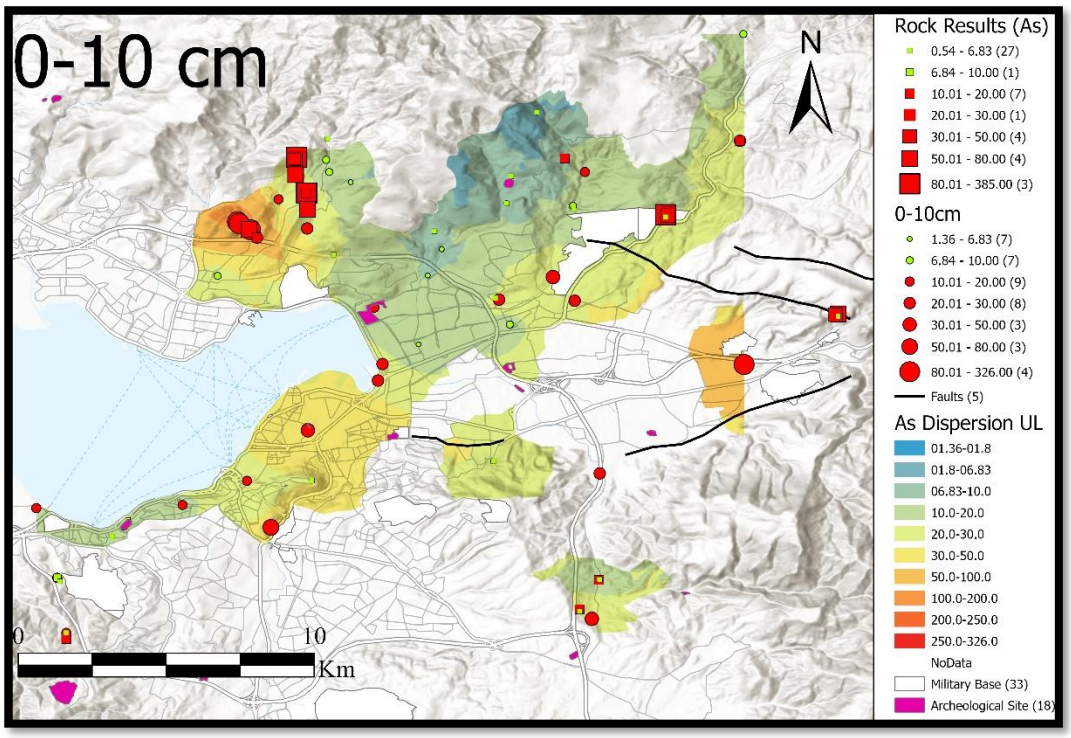

Figure 4.8 Geochemical distribution of arsenic in upper layer in İzmir city center.

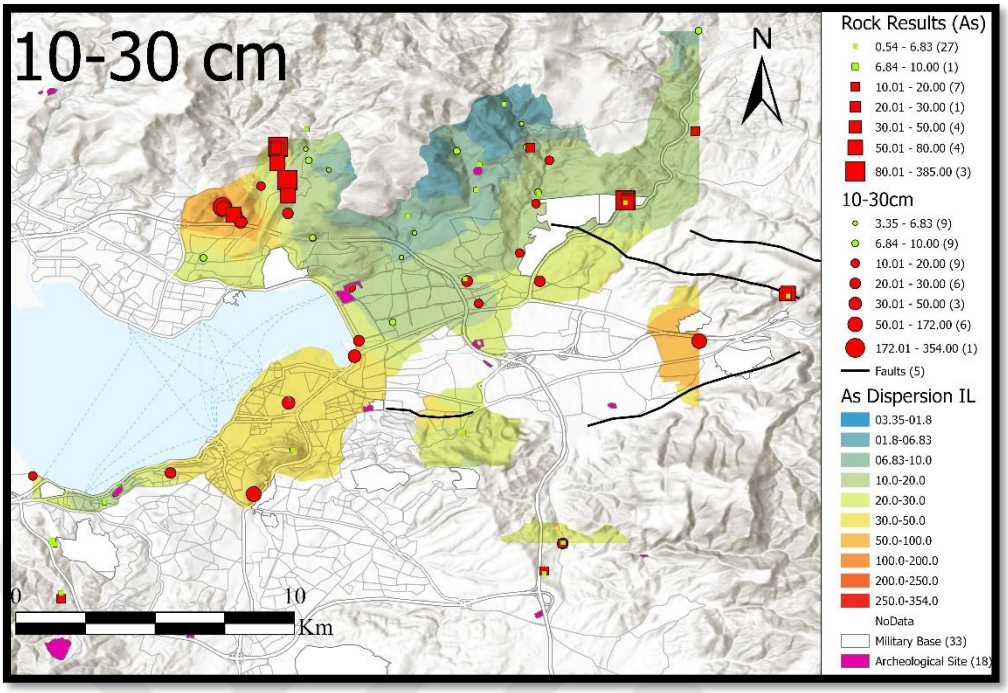

Figure 4.9 Geochemical distribution of arsenic in intermediate layer in İzmir city center.

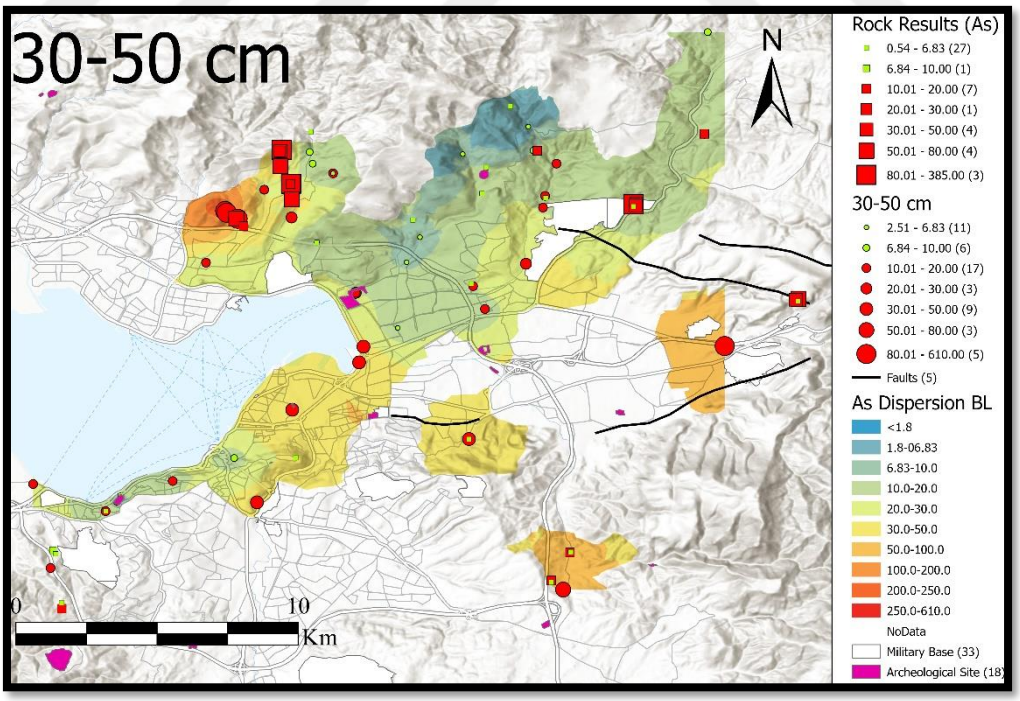

Figure 4.10 Geochemical distribution of arsenic in bottom layer in İzmir city center.

4.4.2 Cobalt Distribution Maps

Cobalt distribution maps, produced for different layers of soil/sediment sample data, shows that Co is below average soil value and crustal values (11.3 and 10 ppm) in most of the sample locations and rock samples in the dispersion maps (Figure 4.11, 4.12 and 4.13) only northern and southern parts have higher Co values and but other parts of İzmir city center have below trigger action value of 50 ppm. Moreover, from upper layer to bottom layer distributions are similar.

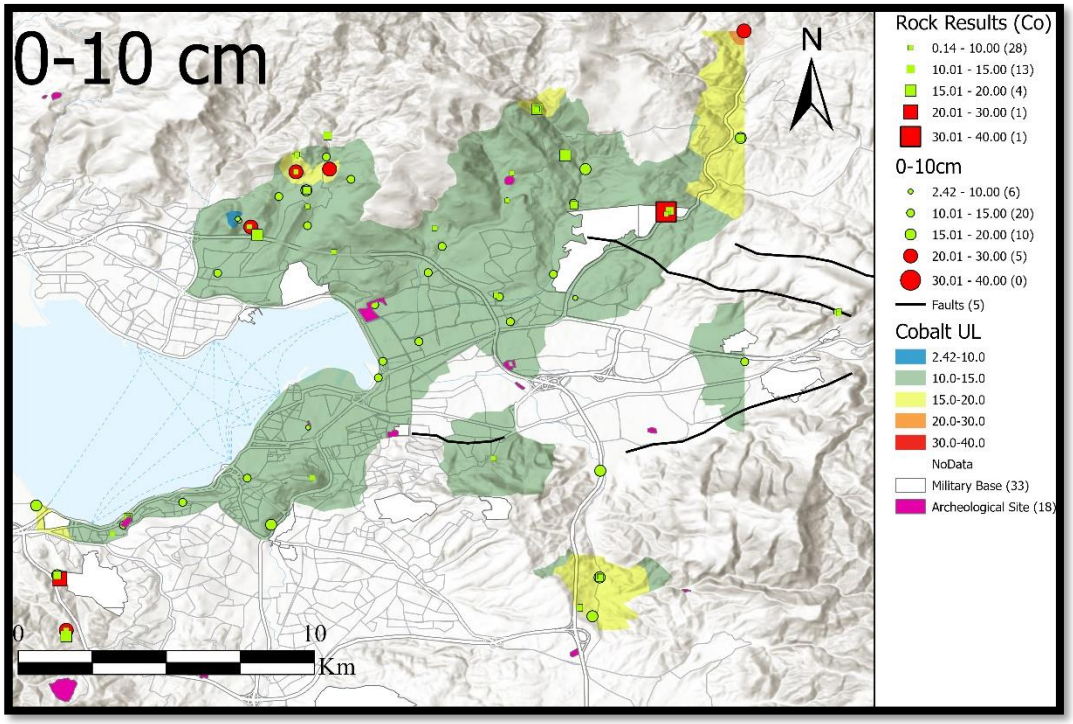

Figure 4.11 Geochemical distribution of cobalt in upper layer in İzmir city center.

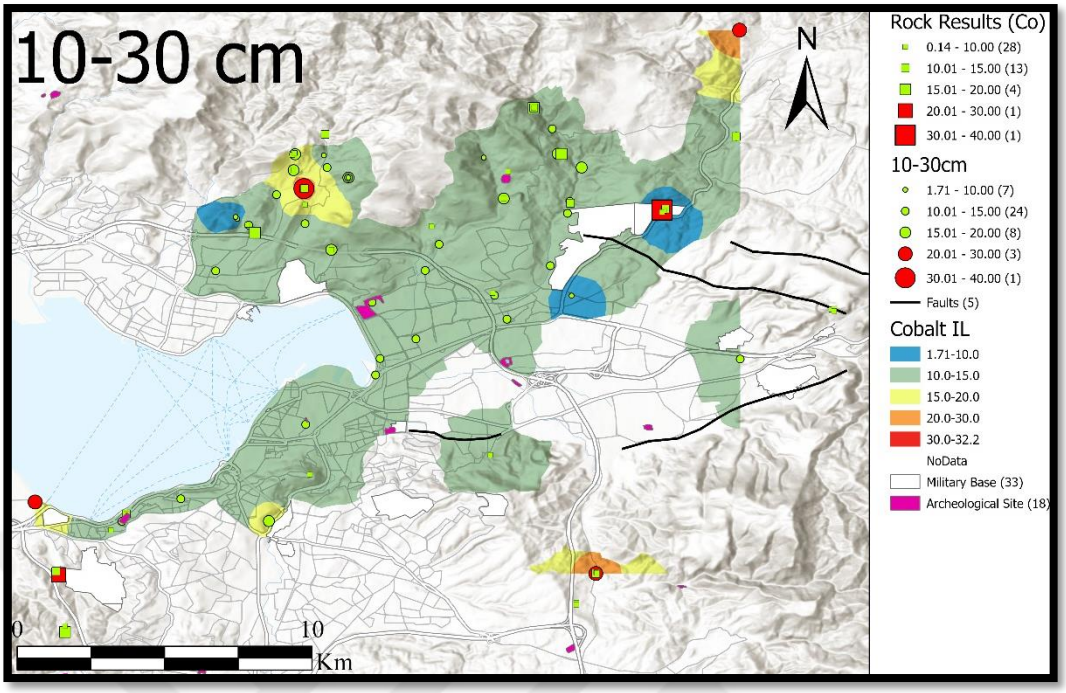

Figure 4.12 Geochemical distribution of cobalt in intermediate layer in İzmir city center.

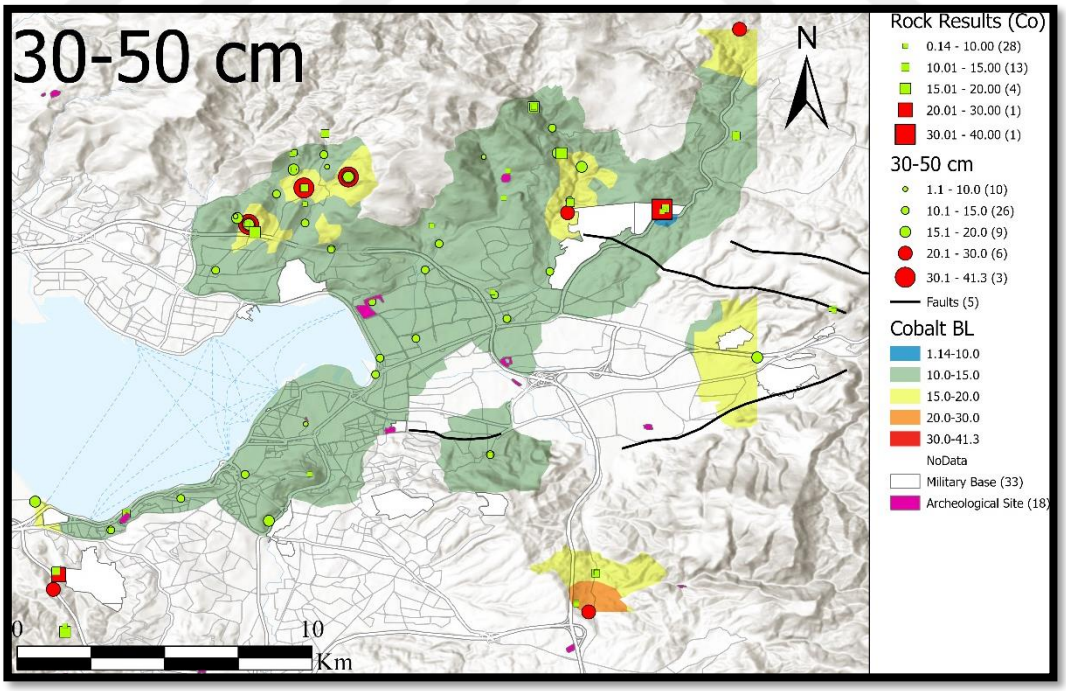

Figure 4.13 Geochemical distribution of cobalt in bottom layer in İzmir city center.

4.4.3 Chromium Distribution Maps

Chromium distribution maps, produced for different layers of soil/sediment sample data, shows that Cr is below average soil value and crustal values (59.5 and 100 ppm) in most of the sample locations and rock samples in the dispersion maps (Figure 4.14, 4.15 and 4.16), northeastern, southwestern and southern parts have higher soil average Cr values.

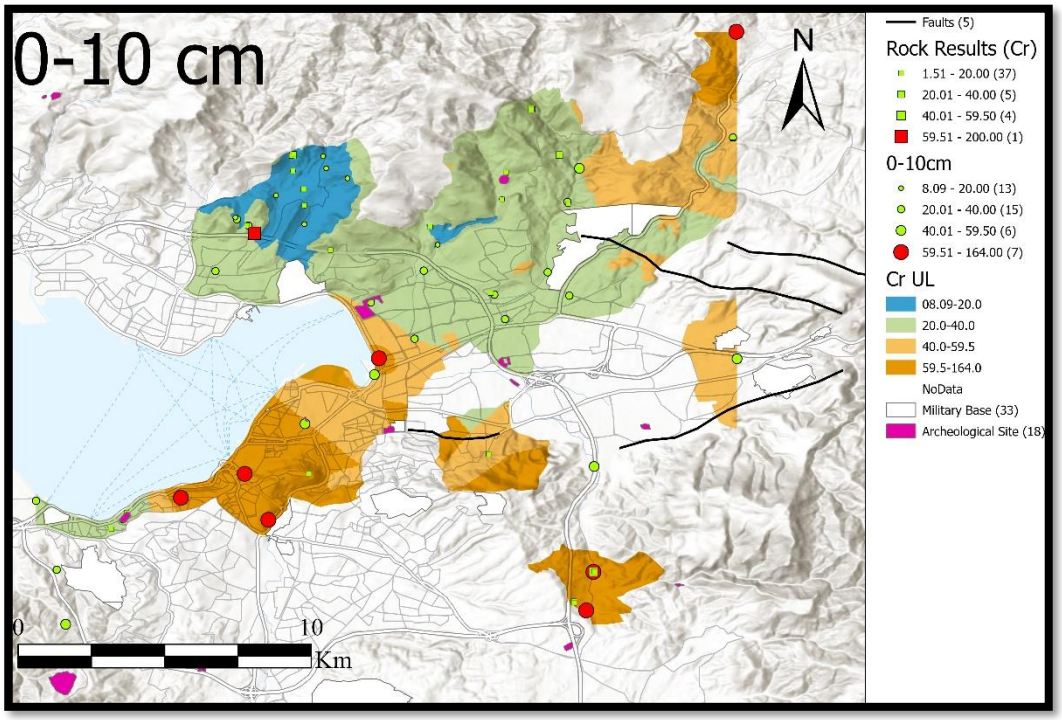

Figure 4.14 Geochemical distribution of chromium in upper layer in İzmir city center.

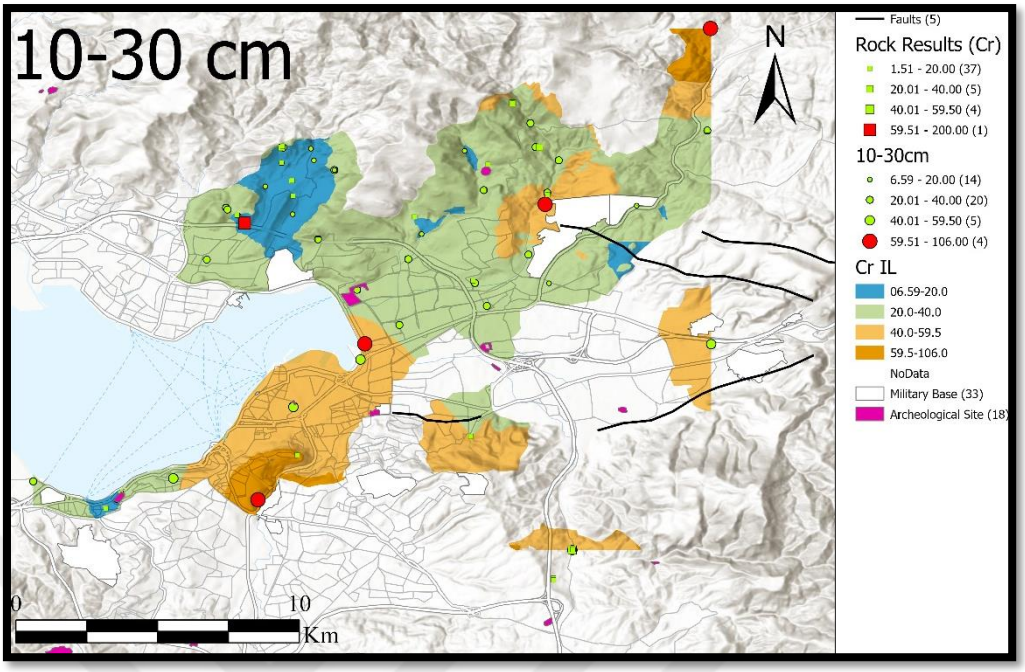

Figure 4.15 Geochemical distribution of chromium in intermediate layer in İzmir city center.

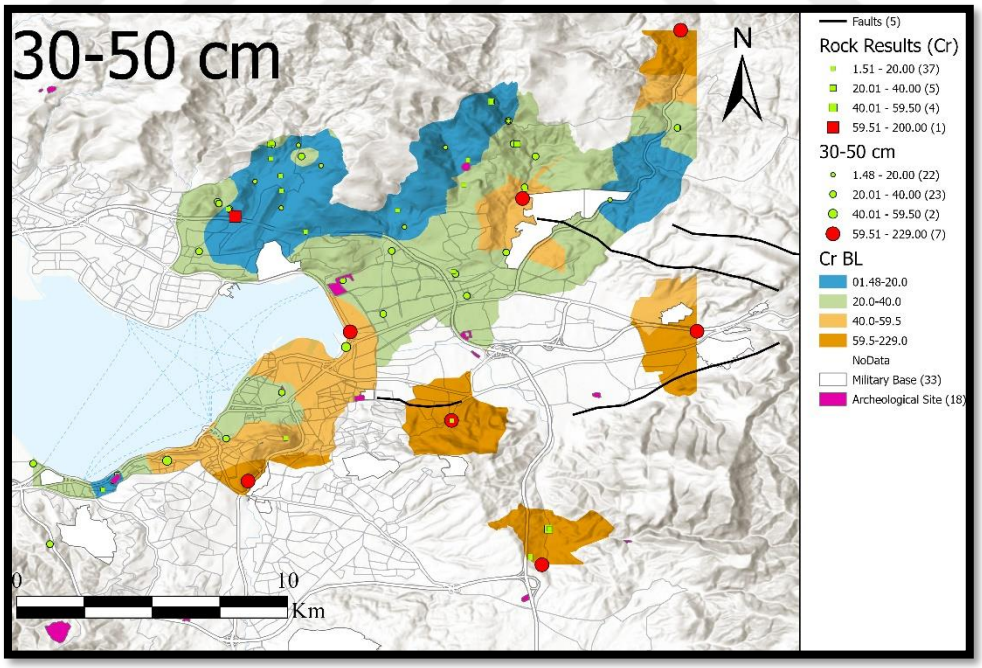

Figure 4.16 Geochemical distribution of chromium in bottom layer in İzmir city center.

4.4.4 Nickel Distribution Maps

Nickel distribution maps, produced for different layers of soil/sediment sample data, shows that Ni is above average soil value and crustal values (29 and 20 ppm) in most of the sample locations and rock samples in the dispersion maps (Figure 4.17, 4.18 and 4.19) only northern part has lower Ni values and eastern, southern parts of İzmir city center have above trigger action value of 40 ppm. Moreover, from upper layer to bottom layer distributions are similar.

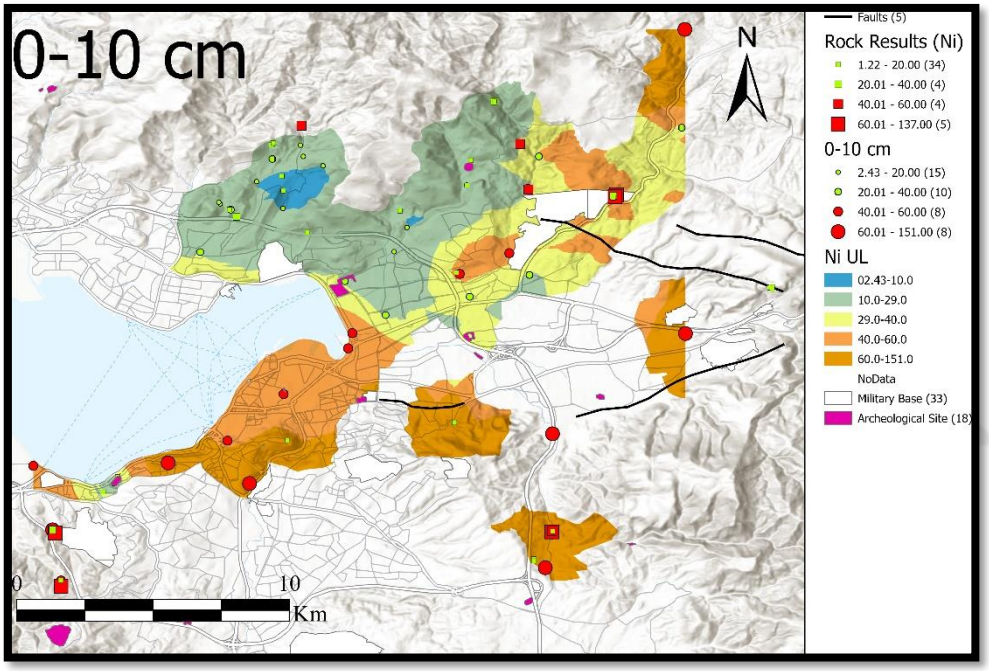

Figure 4.17 Geochemical distribution of nickel in upper layer in İzmir city center.

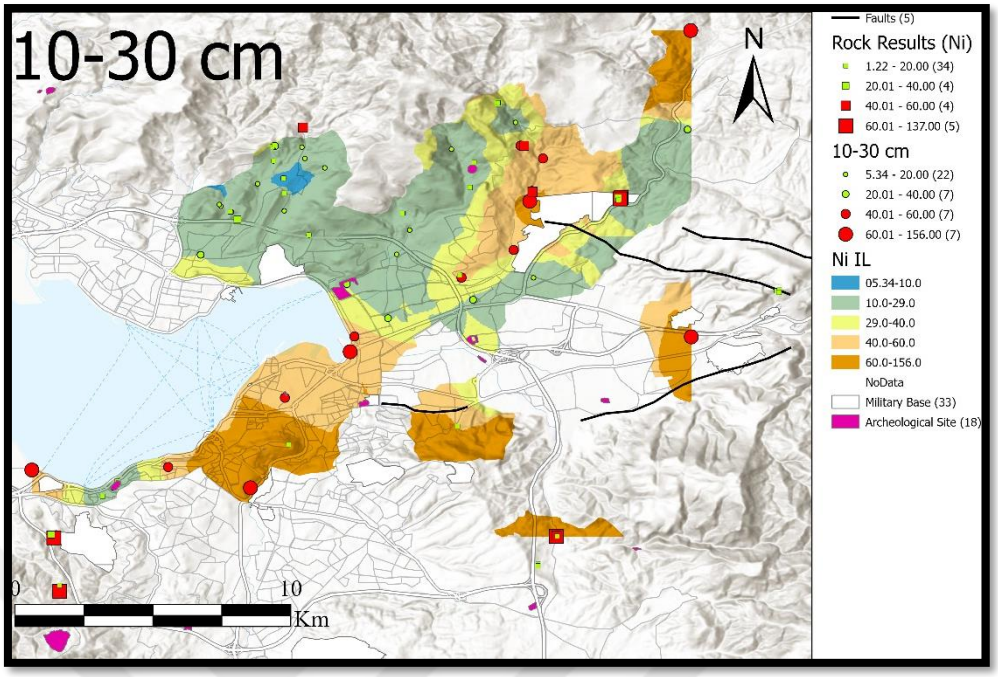

Figure 4.18 Geochemical distribution of nickel in intermediate layer in İzmir city center.

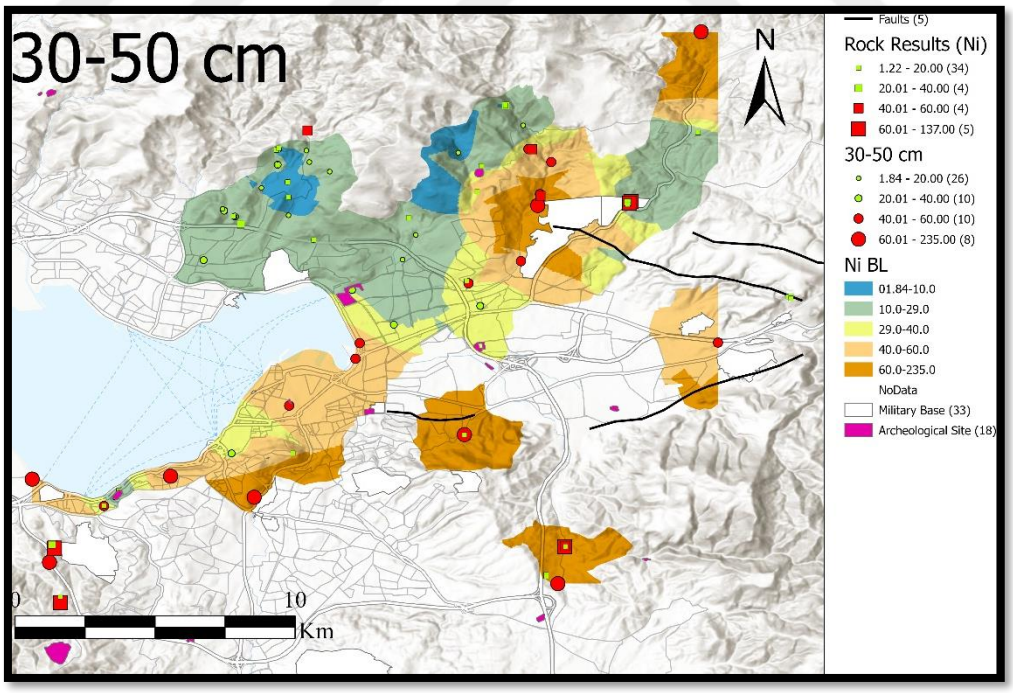

Figure 4.19 Geochemical distribution of nickel in bottom layer in İzmir city center.

4.4.5 Lead Distribution Maps

Lead distribution maps, produced for different layers of soil/sediment sample data, shows that Pb is below average soil value and crustal values (27 and 15 ppm) in most of the sample locations and rock samples in the dispersion maps (Figure 4.20, 4.21 and 4.22), however around İzmir Bay, Pb values are higher, but all of the area shows a value which is below trigger action value of 300 ppm. Moreover, from upper layer to bottom layer distributions are similar.

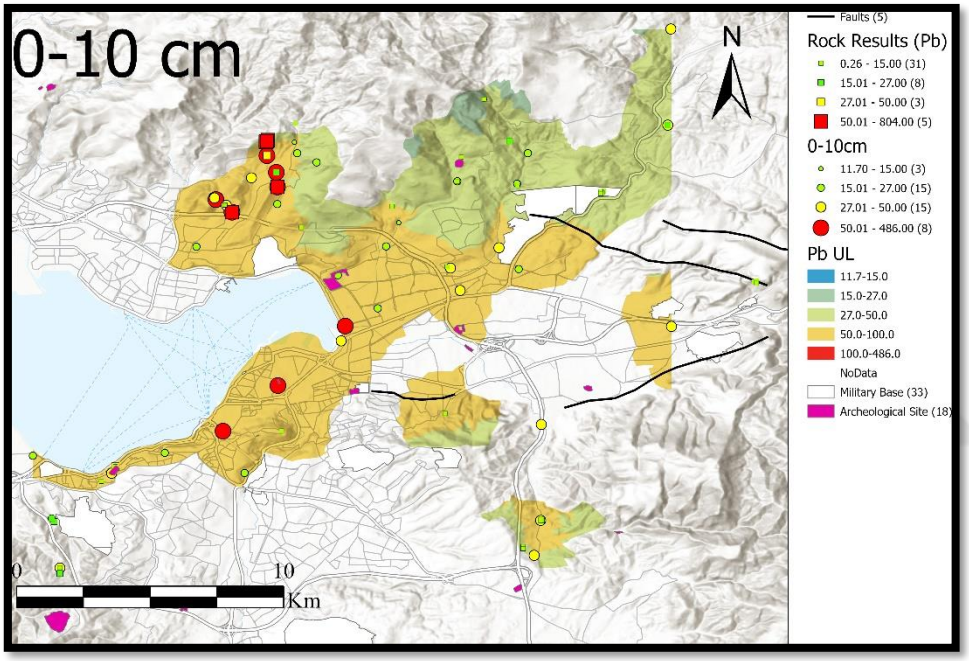

Figure 4.20 Geochemical distribution of lead in intermediate layer in İzmir city center.

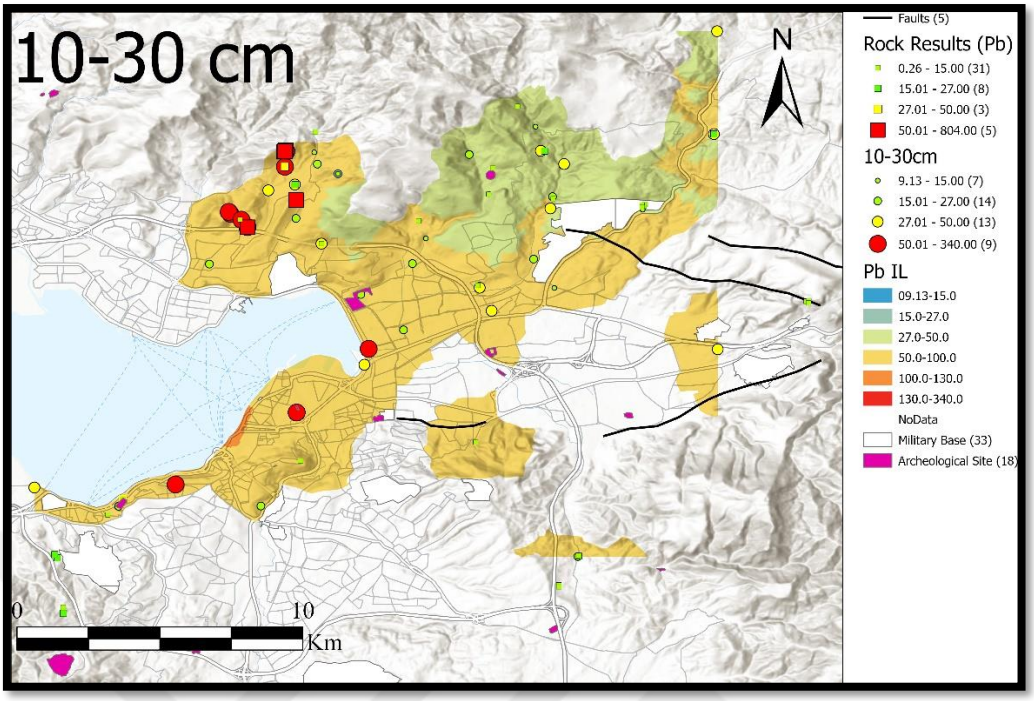

Figure 4.21 Geochemical distribution of lead in intermediate layer in İzmir city center.

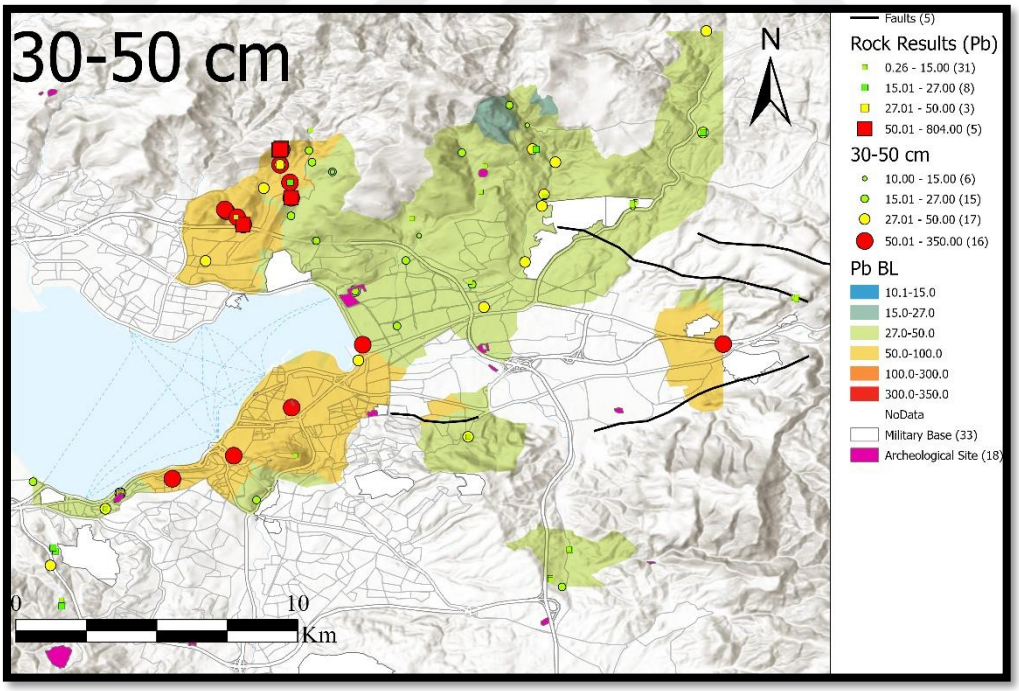

Figure 4.22 Geochemical distribution of lead in bottom layer in İzmir city center.

4.4.6 Antimony Distribution Maps

Antimony distribution maps, produced for different layers of soil/sediment sample data, shows that Sb is below average soil value and crustal values (0.67 and 0.2 ppm) in most of the sample locations and rock samples in the dispersion maps (Figure 4.23, 4.24 and 4.25), however around northwestern part of İzmir city center, Sb values are exceeding average and trigger action values. Moreover, from upper layer to bottom layer distributions are similar.

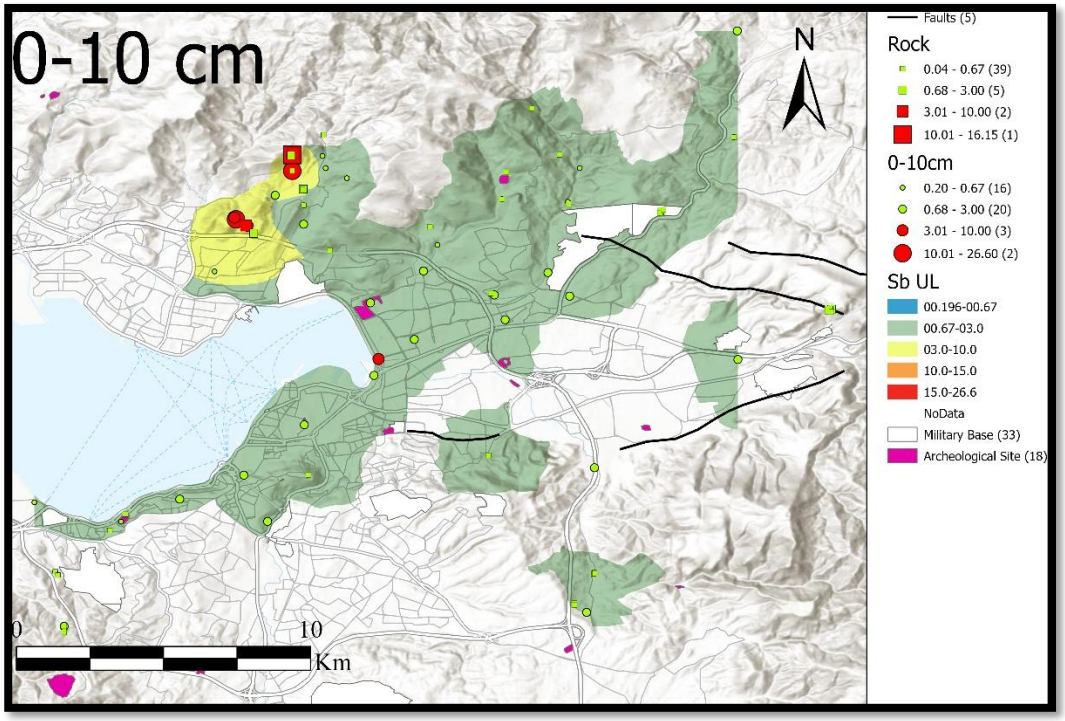

Figure 4.23 Geochemical distribution of antimony in upper layer in İzmir city center.

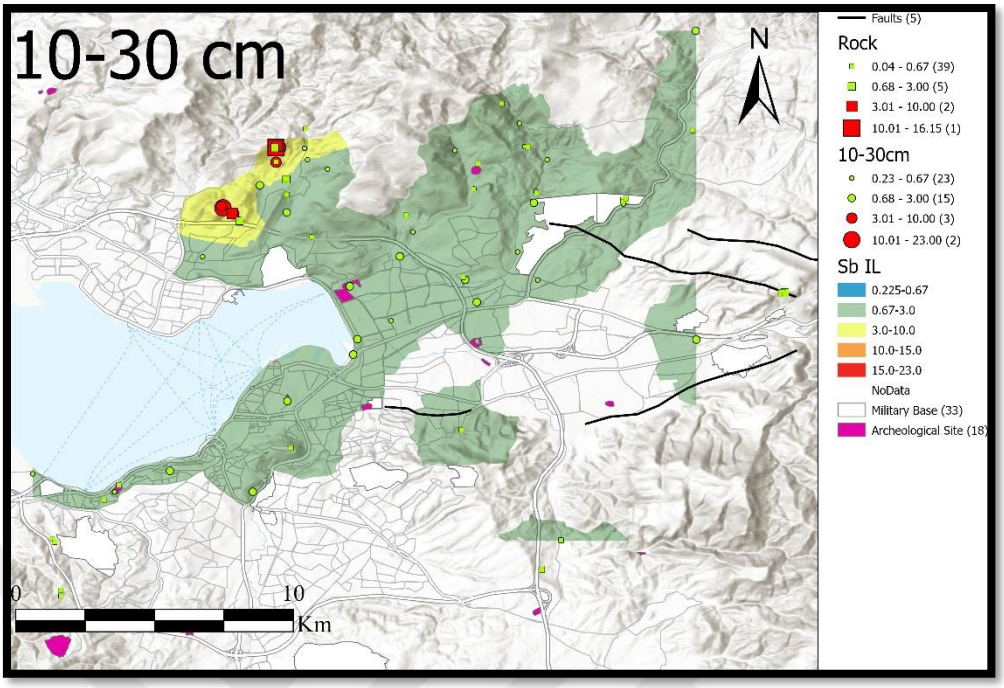

Figure 4.24 Geochemical distribution of antimony in intermediate layer in İzmir city center.

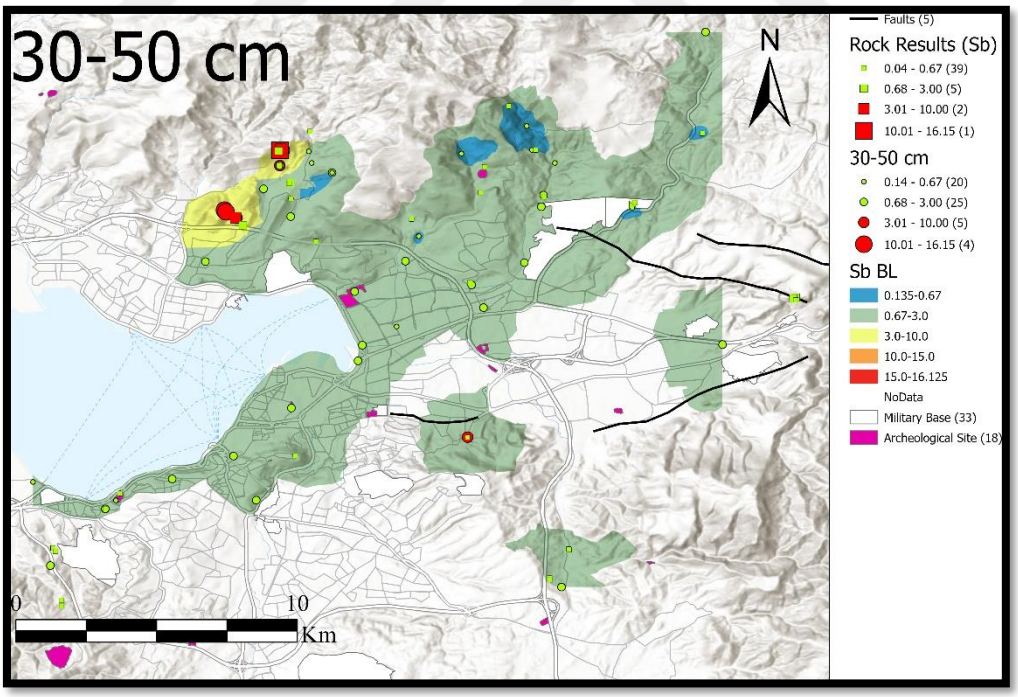

Figure 4.25 Geochemical distribution of antimony in bottom layer in İzmir city center.

CHAPTER 5

GEOMEDICAL RISK ASSESSMENT OF İZMİR CİTY CENTER

Toxic elements have certain safety limits, since they are hazardous for living organisms, and humans are one of the primary subjects. Geochemical processes in the environment can play a variety of important roles in controlling how humans are exposed to potential toxicants in a wide range of geogenic or anthropogenic materials.

Examples of important geochemical processes include mineral dissolution to release toxicants, mineral precipitation to sequester toxicants, pH changes in ground or surface waters, sorption/desorption of waterborne toxicants onto solids, complexation of aqueous metals by ligands, volatilization of organic compounds oxidation or reduction, and photolytic reactions (Finkelman et al., 2018).

Once taken up by the body, geogenic or anthropogenic materials and their contained toxicants can react chemically with the body's fluids, and these chemical interactions can play key roles in toxicity.

Different risk assessment calculations can be used to find out elemental risks in soil and sediments, such as, total carcinogenic and total non-carcinogenic hazard index (HI) risk assessments of elements on human health.

Elements such as antimony (Sb), arsenic (As), barium (Ba), beryllium (Be), cadmium (Cd), cobalt (Co), chromium (Cr), molybdenum (Mo), nickel (Ni), lead (Pb), selenium (Se), tin (Sn), zinc (Zn) are used in risk calculations of İzmir city center.

The risk assessments of İzmir province are visualized by creating distribution maps produced in the ArcGIS Pro using better result giving interpolation methods.

5.1 Geomedical Risk Assessment of İzmir City Center

Carcinogenic and non-carcinogenic risk calculations were made for three different groups, women, men, and children, by using a total of 140 soil and sediment samples taken from the area covering the borders of Bornova, Bayraklı and Konak districts within the province of Izmir. In the 2016 census, the distribution percentages of the children population between 0 and 10 years old (total number of 142650) in these three districts are 13.9% in Bayraklı, 12.8% in Bornova and 11.4% in Konak (İzmir Metropolitan Municipality- Geographic Information Systems, 2023). Due to the distribution of the children population at these rates, the risk maps created are important regarding children health.

5.1.1 Noncarcinogenic Risk Assessment for İzmir City Center

Noncarcinogenic risk calculations were made by considering the physical characteristics and coefficients of women, men, and children. The average male weight was 77 kg, and female weight was 67 kg, and the average child weight was 18 kg for children between 0-10 years of age (TURKSTAT, 2023), considering the average weights for different ages recommended by paediatricians.

The total HI (sum of hazard coefficients) values can be observed in the box plots (Figures 5.1, 5.2 and 5.3) prepared for each soil and sediment layer. All values show a parallel distribution for each layer (except for the children group bottom layer's upper whisker ends at 5 but ends at 4 for upper and intermediate layers).

When dermal and inhalation risks are considered, all individual groups show no risk except some outlier values since upper whiskers are below the threshold value of 1. In the case of ingestion, no risk is observed for men and women in general except for outliers, but for children; ingestion values exceed the threshold value of 1 from 23rd percentiles for all layers, which means for ingestion, children are at risk of noncarcinogenic effects of different elements.

Hazard index values (the sum of all noncarcinogenic risks) show that (Figures 4.1d, 4.2d and 4.3d), women and men show no risk. However, children calculations show a noncarcinogenic risk from the 25th percentile, which means 75% of samples have a noncarcinogenic risk for children.

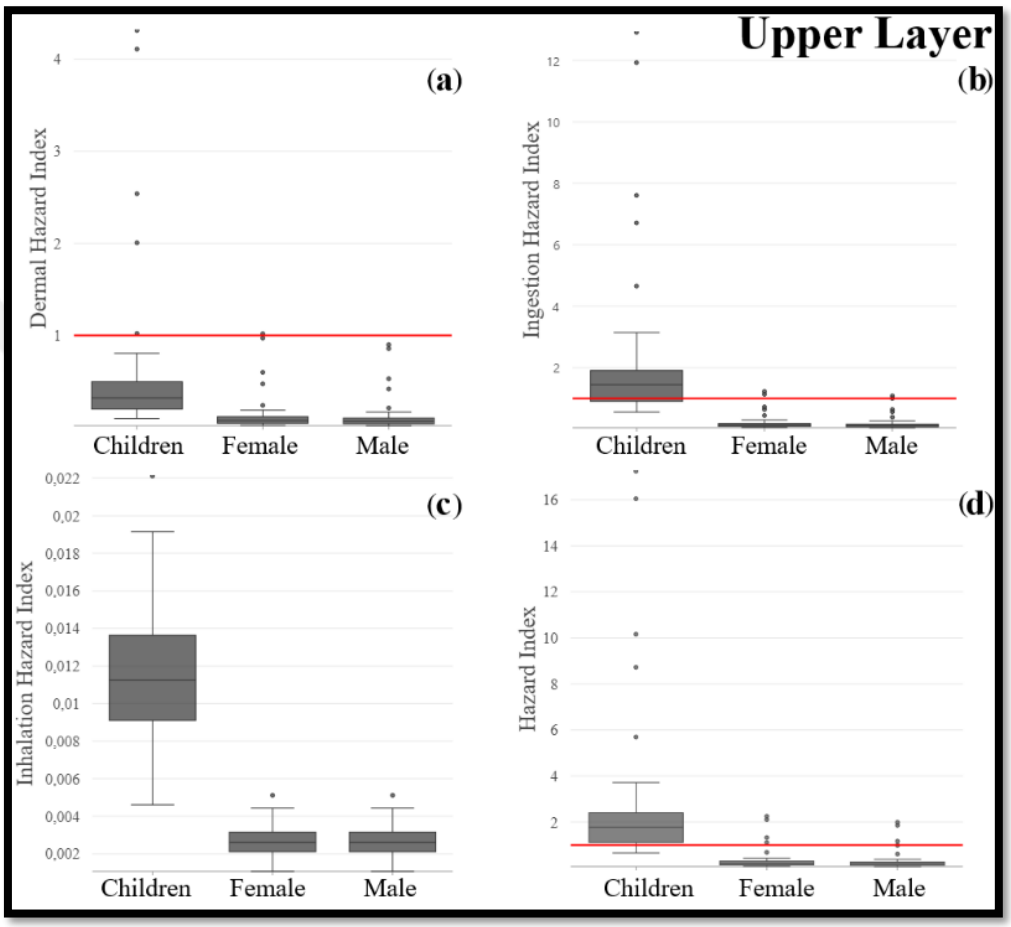

Figure 5.1 Hazard index box plots of the soil and sediments from İzmir city center's upper layer (0-10 cm), (a) dermal hazard index, (b) inhalation hazard index, (c) inhalation hazard index, (d) sum of hazard indexes, above 1 (red line) indicates noncarcinogenic health risk.

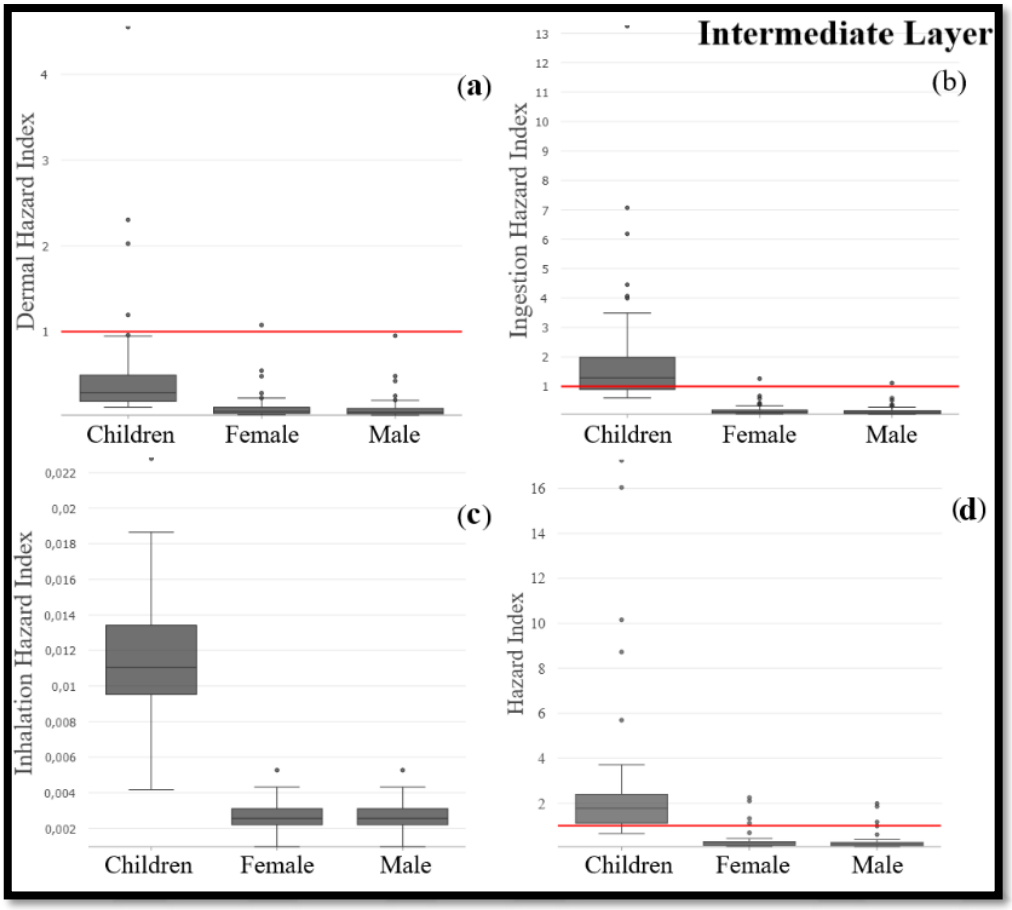

Figure 5.2 Hazard index box plots of the soil and sediments from İzmir city center's intermediate layer (10-30 cm), (a) dermal hazard index, (b) inhalation hazard index, (c) inhalation hazard index, (d) sum of hazard indexes, above 1 (red line) indicates noncarcinogenic health risk.

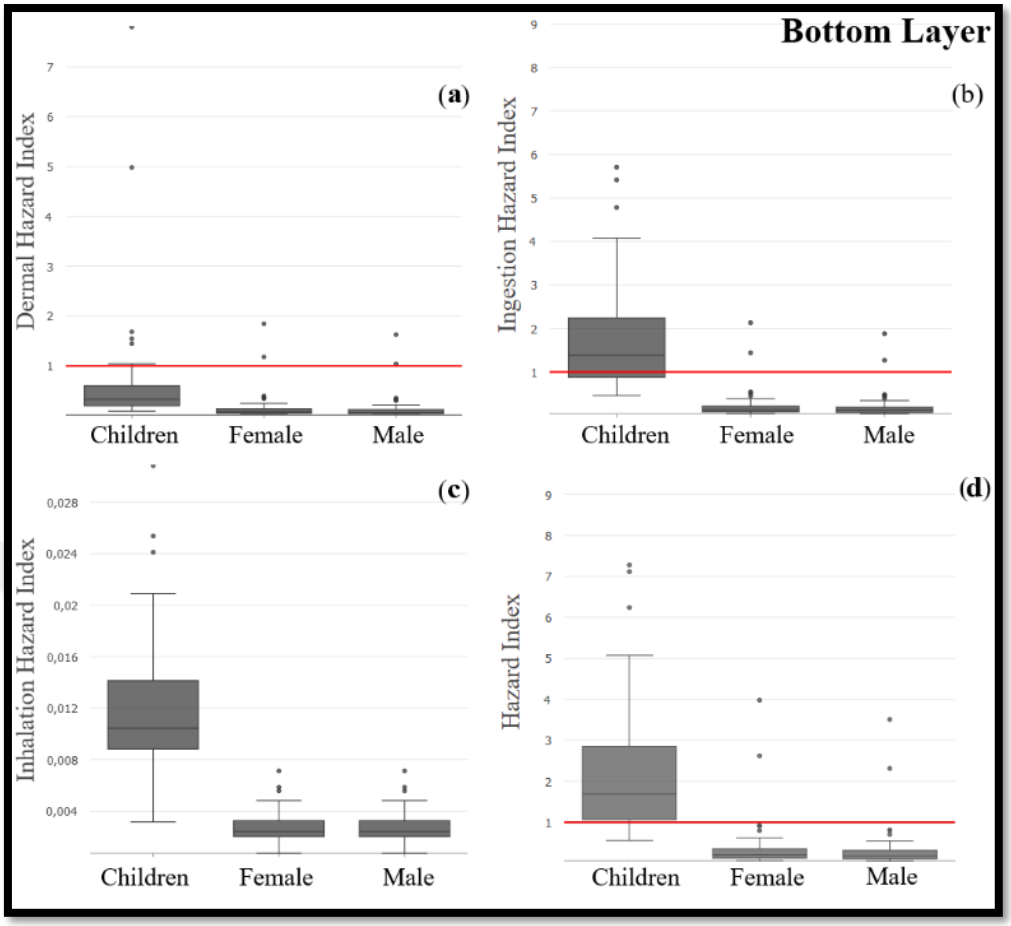

Figure 5.3 Hazard index box plots of the soil and sediments from center's bottom layer (30-50 cm), (a) dermal hazard index, (b) inhalation hazard index, (c) inhalation hazard index, (d) sum of hazard indexes, above 1 (red line) indicates noncarcinogenic health risk.

When, each element's percentages in hazard coefficients for ingestion, dermal and inhalation routes (Figures 5.4) are considered, it can be observed that the greatest risk is caused by Arsenic, followed by Cobalt, Lead, Antimony and Nickel, respectively.

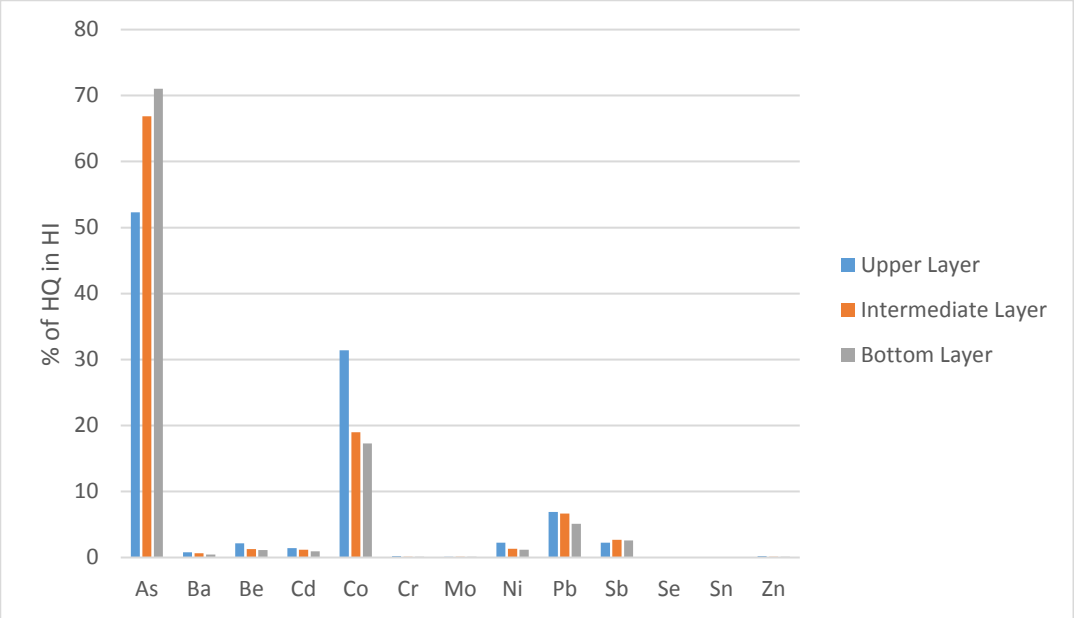

Figure 5.4 Elemental contributions for hazard quotients for different soil/sediment levels.

5.1.1.1 Hazard Index Distribution Maps

Hazard index values based on the toxic elements found in soil and sediment are evaluated according to the risky elements that can be exposed by dermatological, inhalation and ingestion. The risk distribution around the region can be determined by geostatistical interpolation methods from the sample locations.

Distribution maps are created for every individual group. Since there seems to be no risk for women and men, hazard index distribution maps of these individuals are only

created for women because of their average body weight; more risk distribution is expected.

As expected, problematic areas are very small and only can be found in the northwestern part of Bayraklı and eastern part of Bornova (Figure 5.5, 5.6 and 5.7).

Based on the noncarcinogenic risk distribution maps for children, the regions can be ranked from the riskiest to the least risky in each soil and sediment layer. The riskiest region is located in the north of İzmir Bay (Bayraklı region). The eastern part of Bornova district also poses a similar level of risk although it is considered lower than Bayraklı since the sampling frequency is lower. After these regions, high risk is observed in Bornova and Konak district centers. These findings are based on Figures 5.8, 5.9, and 5.10.

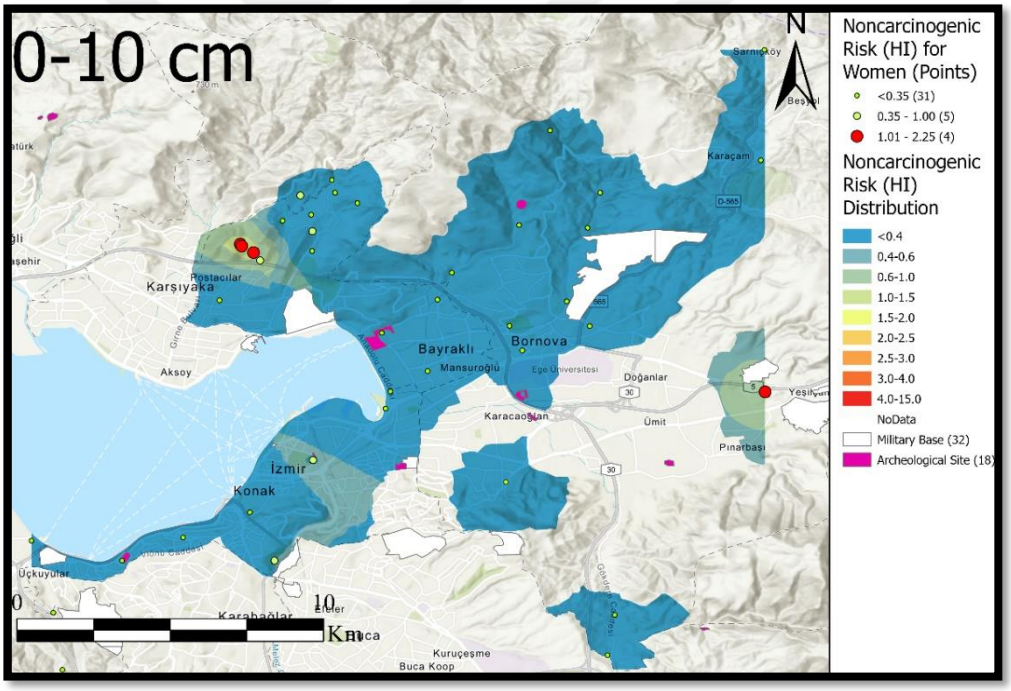

Figure 5.5 Hazard Index Distribution map of upper layer for women in soil and sediments of İzmir City Center.

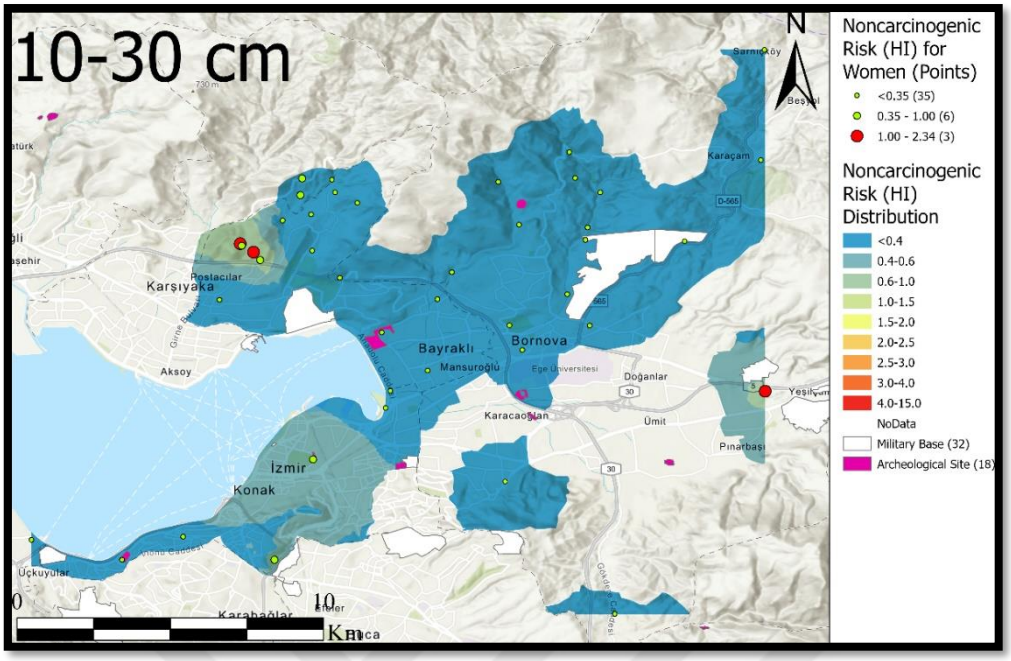

Figure 5.6 Hazard Index Distribution map of intermediate layer for women in soil and sediments of İzmir City Center.

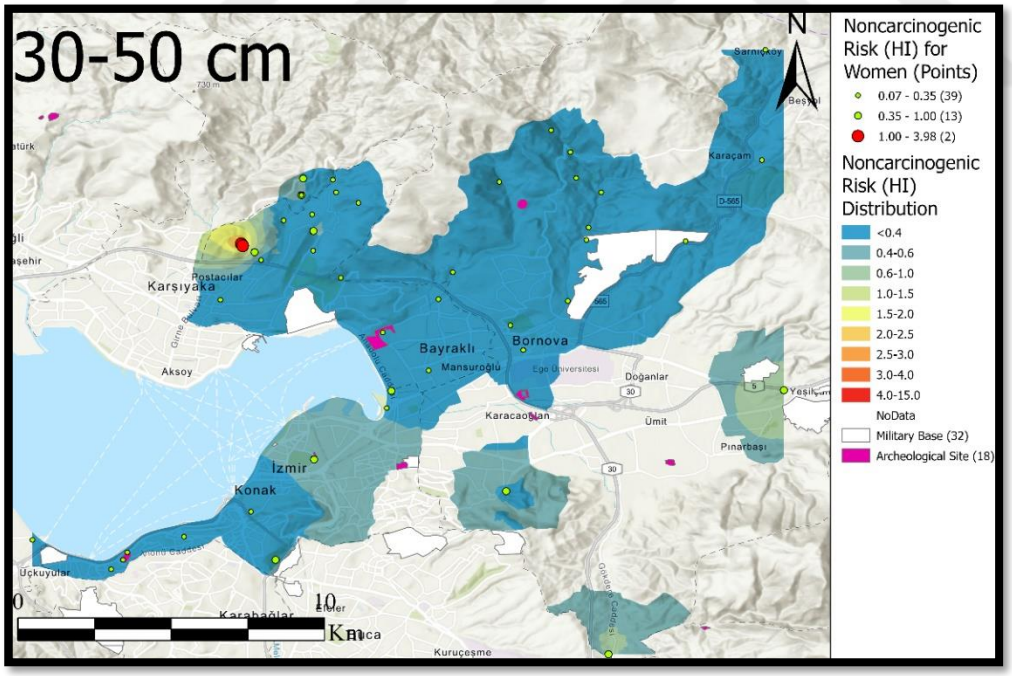

Figure 5.7 Hazard Index Distribution map of bottom layer for women in soil and sediments of İzmir City Center.

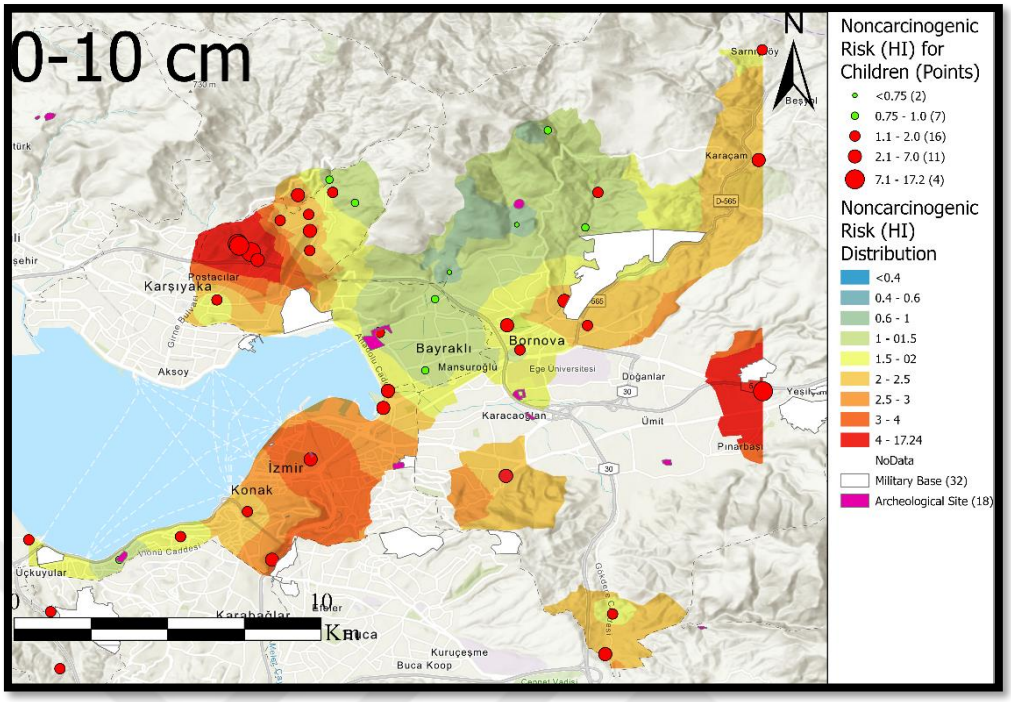

Figure 5.8 Hazard Index Distribution map of upper layer of soil and sediments in İzmir City Center.

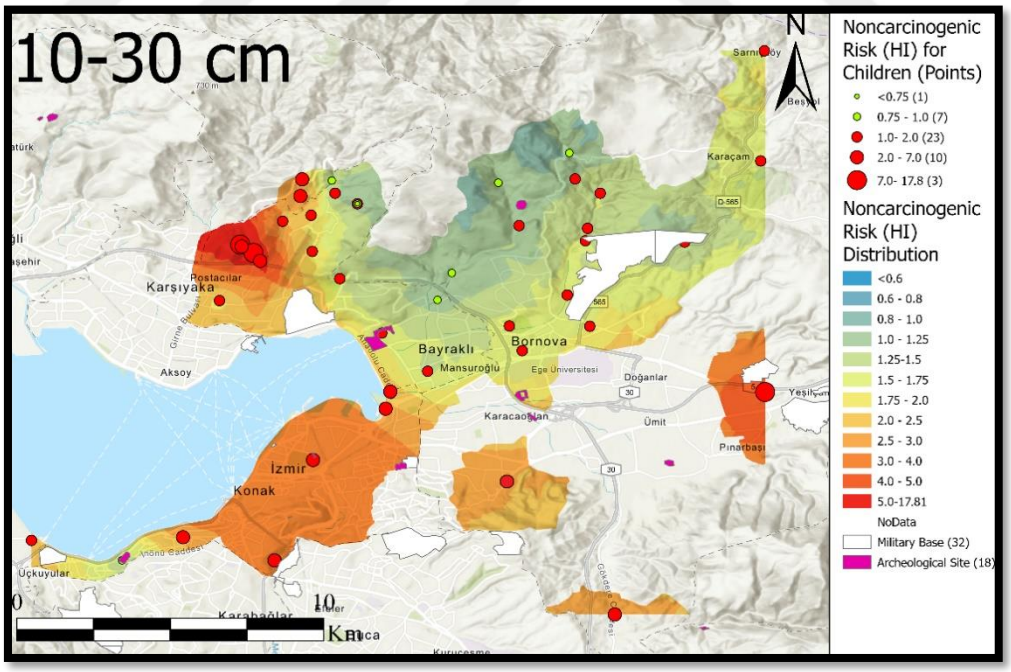

Figure 5.9 Hazard Index Distribution map of intermediate layer (10-30 cm) of soil and sediments in İzmir City Center.

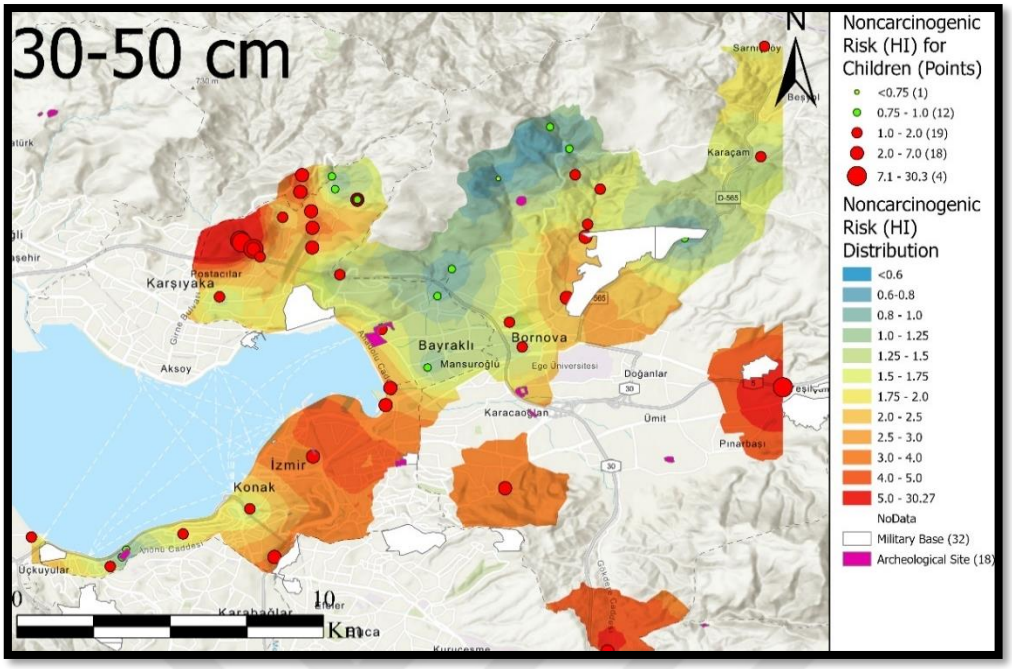

Figure 5.10 Hazard Index Distribution map of bottom layer (30-50 cm) of soil and sediments in İzmir City Center.

5.1.2 Carcinogenic Risk Assessment for İzmir City Center

Carcinogenic risk calculations are done similarly to noncarcinogenic risk calculations, in both calculations CDI values are the same, which is calculated for the average male (77 kg in weight) and female (67 kg in weight), and the average child weight (18 kg in weight).

The total carcinogenic risk for different sample areas' box plots (Figure 5.11, 5.12 and 5.13) show that no individual group are at risk in the case of inhalation risk. In the case of dermal and ingestion risk (apart from the bottom layer's dermal where the upper whisker exceeds 10^{-4} (risk threshold), women and men are in an acceptable risk range.

However, the total carcinogenic risk for women and men in all layers, women exceed the threshold value at the 75th percentile, and men exceed the threshold value at the 80th percentile (Figure 5.11d, 5.12d and 5.13d). On the other hand, the dermal risk

of children starts at the 30th percentile (exceeding the threshold), for all soil/sediment layers (Figure 5.11a, 5.12a and 5.13a); also, ingestion risk where the threshold value exceeded nearly the 20th percentile (Figure 5.11b, 5.12b and 5.13b).

Total carcinogenic risk for children is more dramatic; lower whiskers are nearly or directly at the threshold, except for the upper layer (15th percentile exceeds a threshold) (Figure 5.11d, 5.12d and 5.13d).

When each element's percentages in hazard coefficients for ingestion, dermal and inhalation routes (Figures 5.14) are considered, it can be observed that the most significant risk is caused by As, Be, Ni, Pb and Cd, respectively.

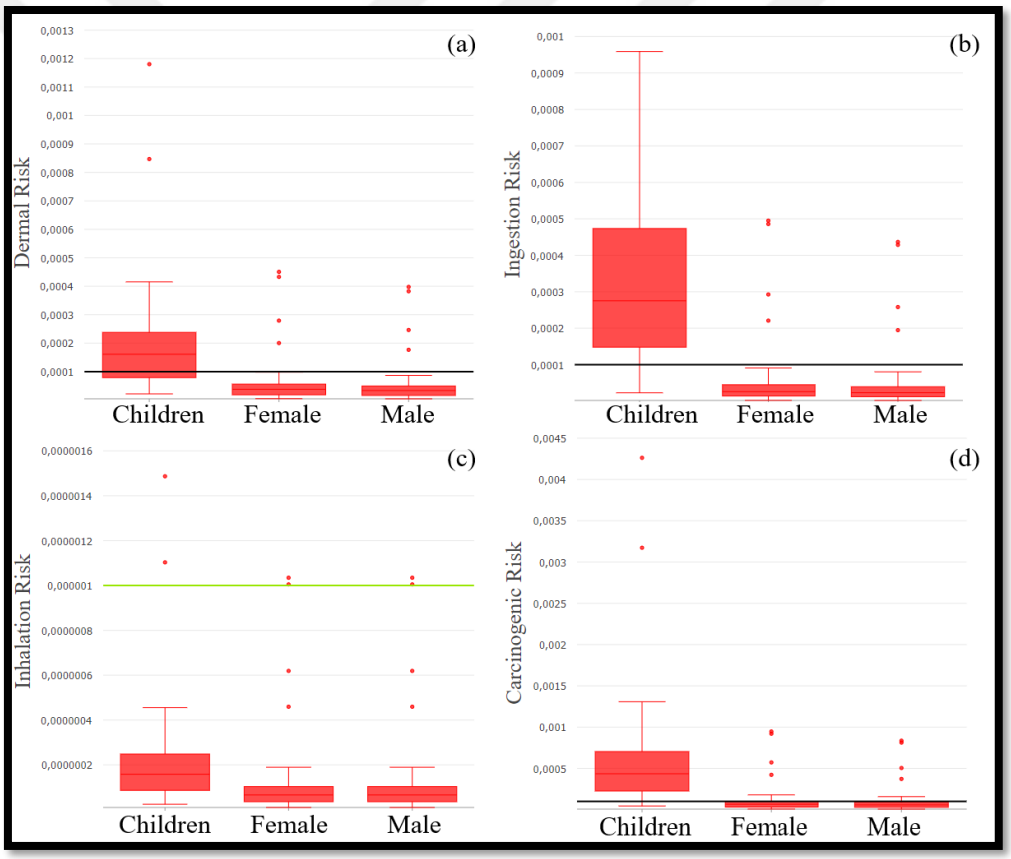

Figure 5.11 Total carcinogenic risk for individual box plots of the soil and sediments of İzmir city center's upper layer (0-10 cm), (a) dermal carcinogenic risk, (b) inhalation carcinogenic risk, (c) inhalation carcinogenic risk, (d) sum of carcinogenic risks, above 0.0001 (black line) indicates carcinogenic health risk.

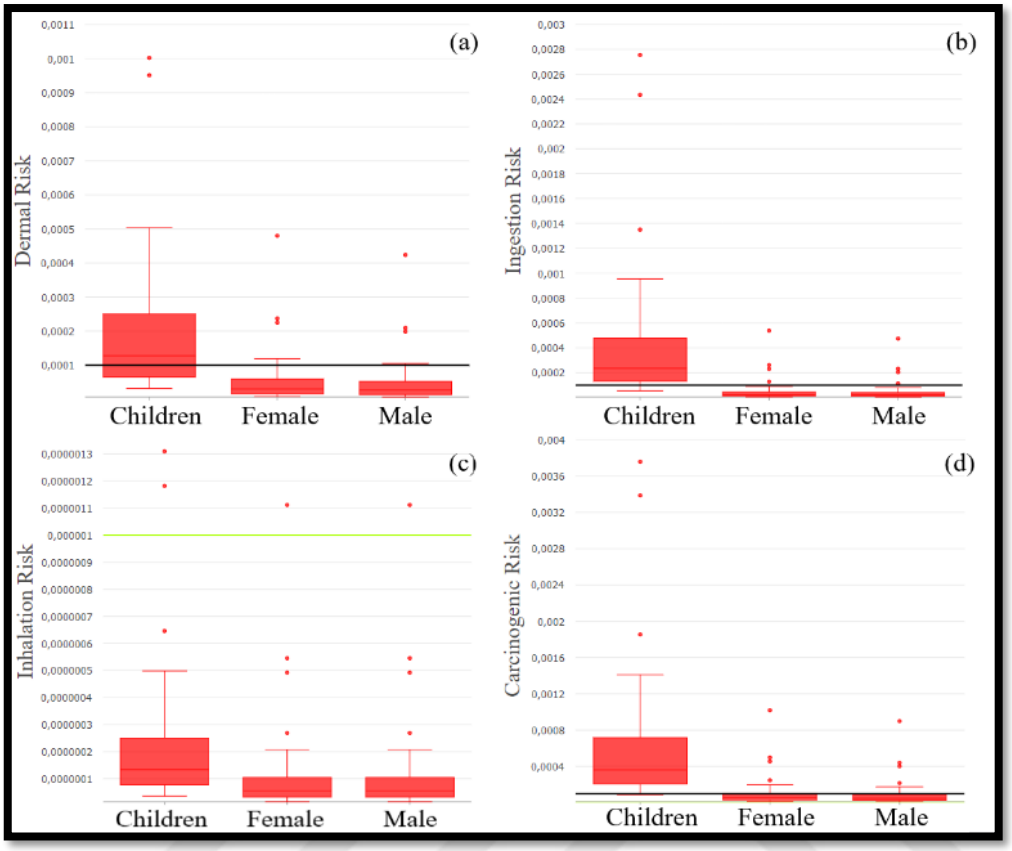

Figure 5.12 Total carcinogenic risk for individual box plots of the soil and sediments of İzmir city center's intermediate layer (10-30 cm), (a) dermal carcinogenic risk, (b) inhalation carcinogenic risk, (c) inhalation carcinogenic risk, (d) sum of carcinogenic risks, above 0.0001 (black line) indicates carcinogenic health risk.

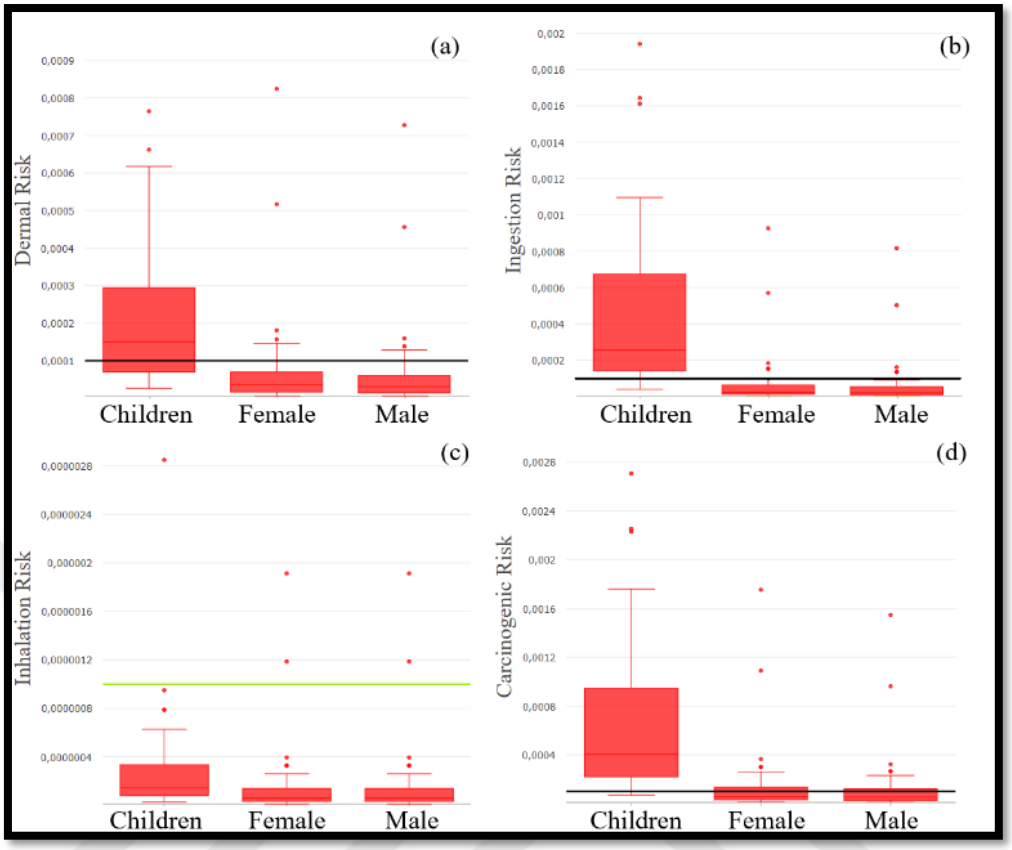

Figure 5.13 Total carcinogenic risk for individual box plots of the soil and sediments of İzmir city center's bottom layer (30-50 cm), (a) dermal carcinogenic risk, (b) inhalation carcinogenic risk, (c) inhalation carcinogenic risk, (d) sum of carcinogenic risks, above 0.0001 (black line) indicates carcinogenic health risk.

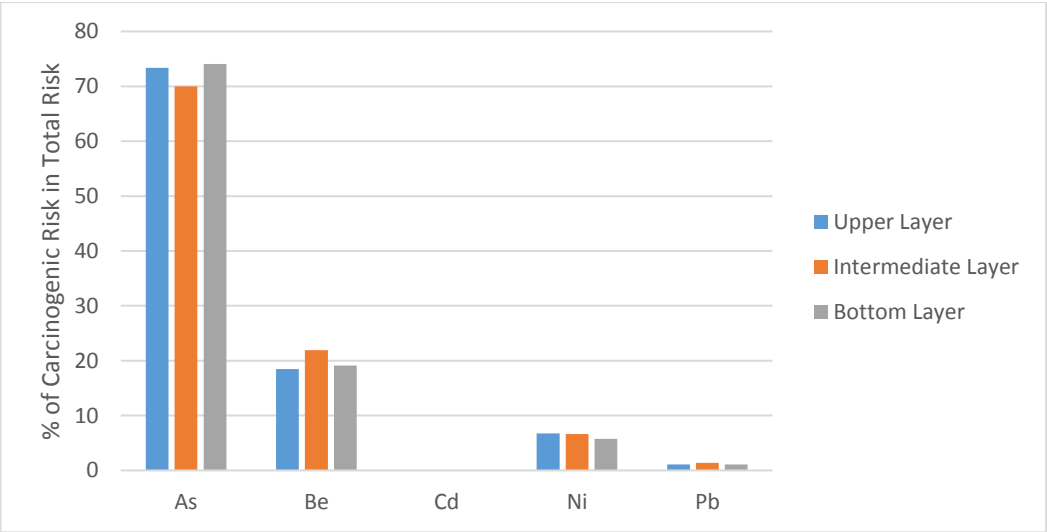

Figure 5.14 Elemental contributions for carcinogenic risk for different soil/sediment levels.

5.1.2.1 Carcinogenic Risk Distribution Maps

Carcinogenic risk distribution is based on the toxic elements As, Be, Cd, Ni, and Pb found in soil and sediment and can be exposed in different ways; dermal, inhalation and ingestion. The risk distribution around the region can be interpolated and drawn with geostatistical interpolation methods from the sample locations.

As per the noncarcinogenic risk distribution maps, separate distribution maps have been created for each group (Figure 5.15-5.23). The maps for women and men (Figure 5.15-5.20) show similar risk distribution patterns ranging from the riskiest regions to the least risky ones, as follows: the north of the İzmir Bay has a significant increase in the risk distribution in all layers within the borders of Bayraklı district compared to other regions. A similar risk level can be observed in the eastern part of Bornova district. However, since the sampling frequency is lower than that of Bayraklı, the risk distribution of this region is considered lower than that of Bayraklı for the time being. After these regions, high risk is observed in Konak district center. On the other hand, for children (Figure 5.21, 5.22, and 5.23), all areas have a similar risk distribution with other individuals, and the risk levels are drastically higher than those for men and women.

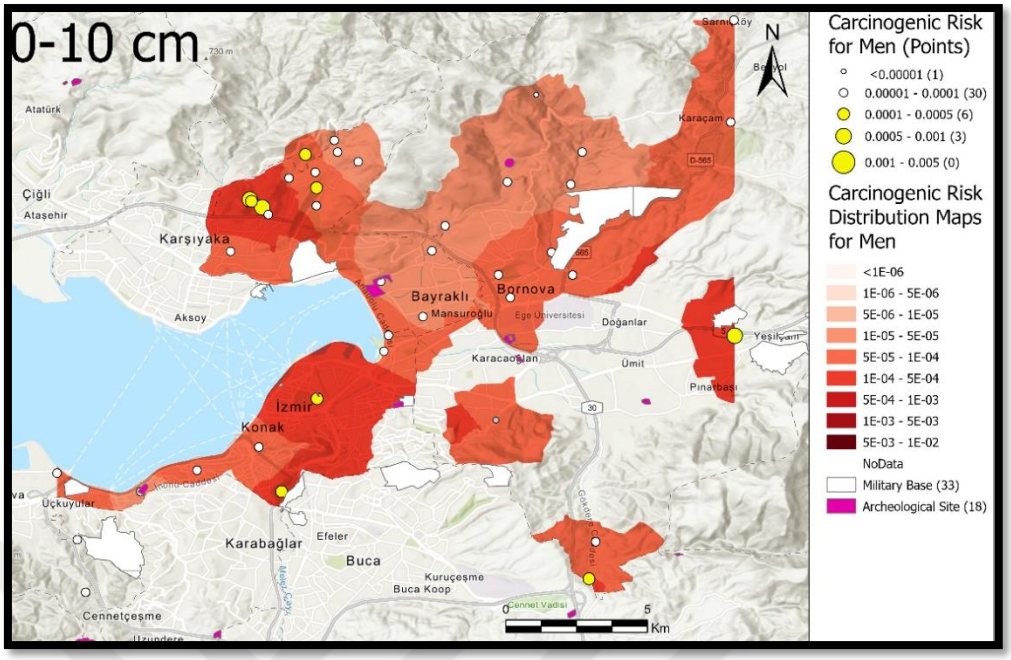

Figure 5.15 Carcinogenic risk distribution for men at upper layer.

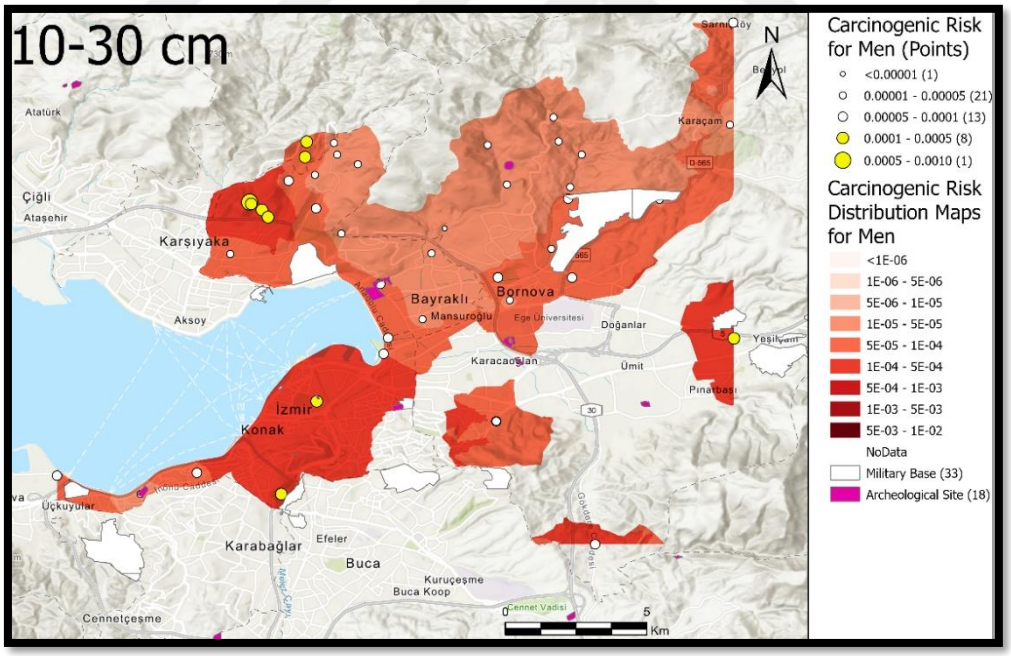

Figure 5.16 Carcinogenic risk distribution for men at intermediate layer.

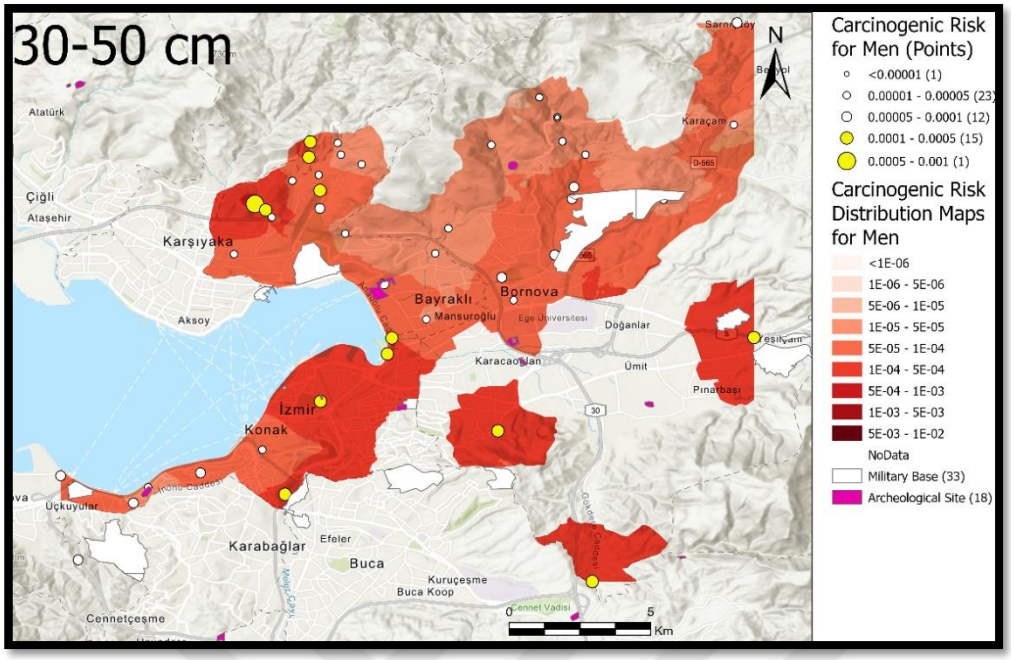

Figure 5.17 Carcinogenic risk distribution for men at bottom layer.

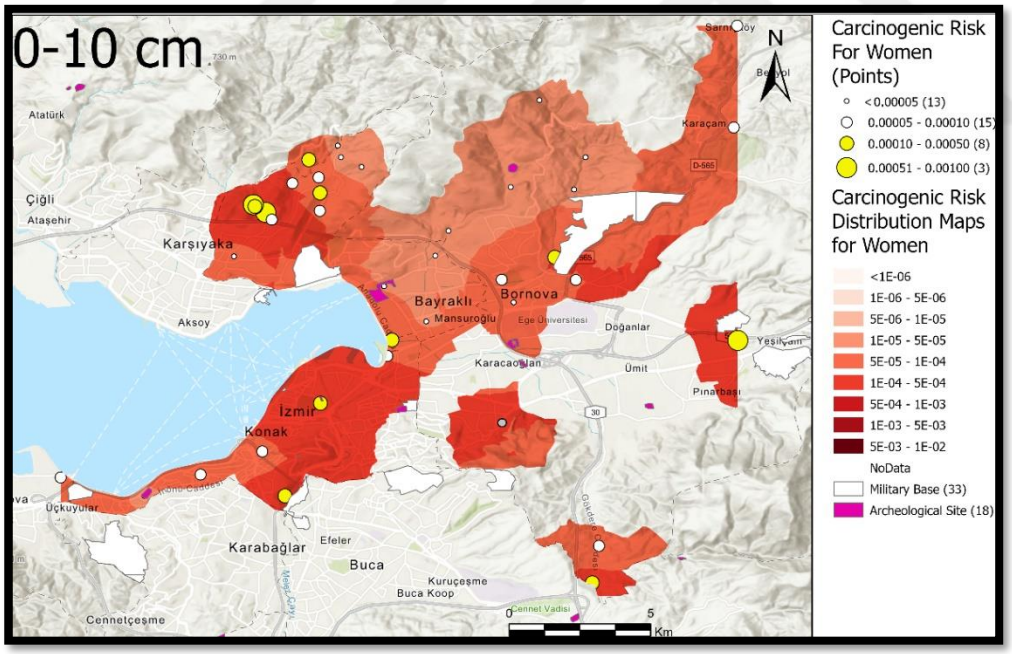

Figure 5.18 Carcinogenic risk distribution for women at upper layer.

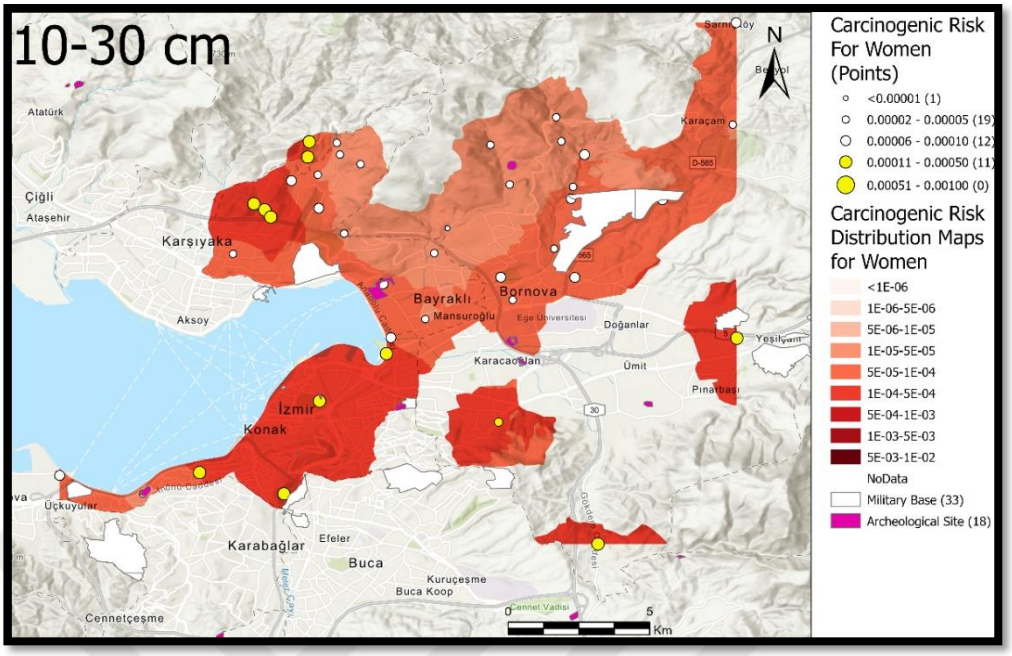

Figure 5.19 Carcinogenic risk distribution for women at intermediate layer.

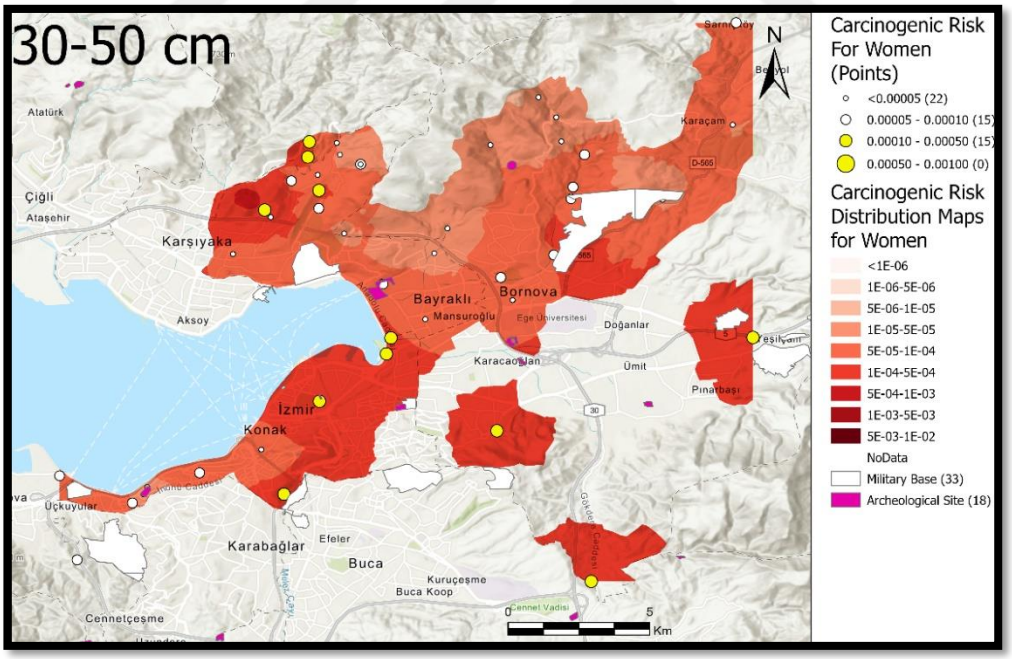

Figure 5.20 Carcinogenic risk distribution for women at bottom layer.

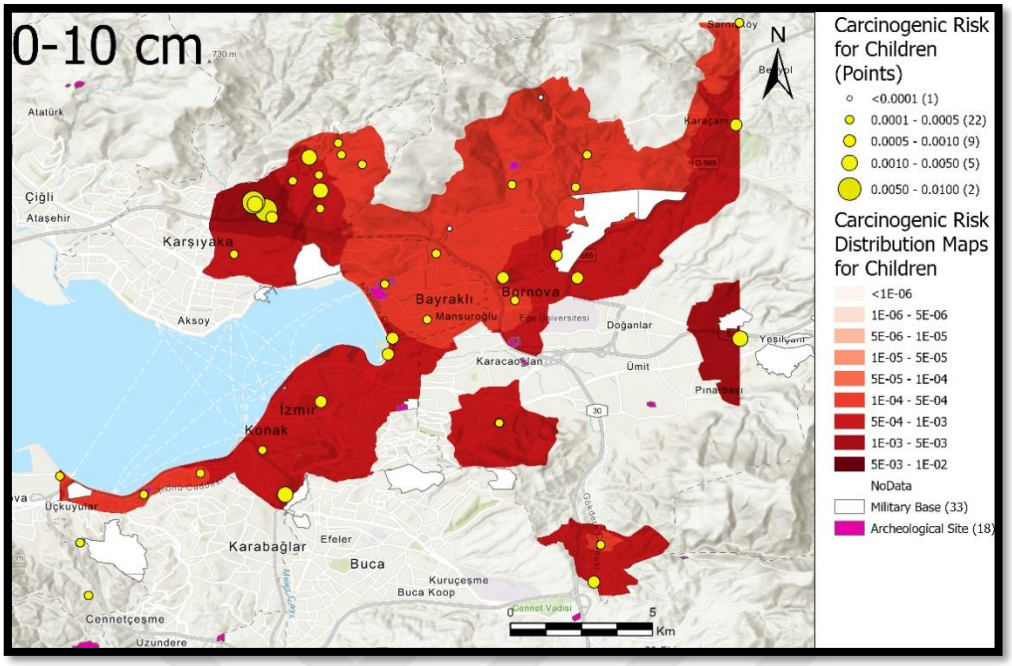

Figure 5.21 Carcinogenic risk distribution for children at upper layer.

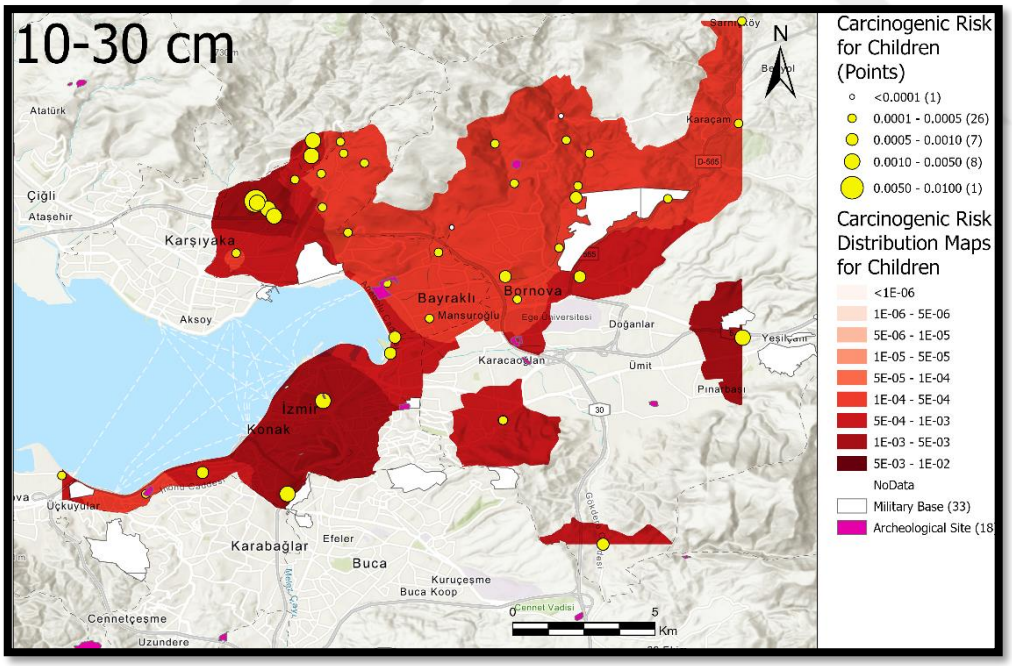

Figure 5.22 Carcinogenic risk distribution for children at intermediate layer.

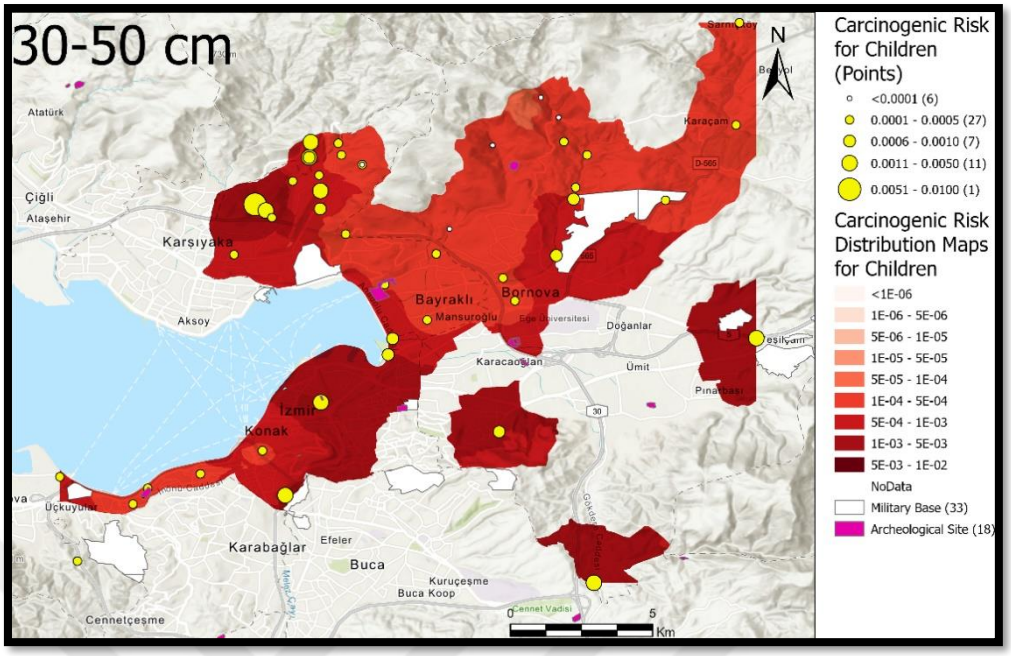

Figure 5.23 Carcinogenic risk distribution for men at bottom layer.

CHAPTER 6

DISCUSSION

6.1 Sources of Toxic Elements

When carcinogenic and noncarcinogenic risk (contaminated soil), possible health problems to indiviuals of İzmir city center, are taken into account, risky regions of İzmir, can be listed as follows: the north of the İzmir Bay, where there is a significant increase in the risk distribution at all layers within the borders of Bayraklı district compared to other regions are at more risk. A similar risk level can be observed in the eastern part of Bornova district, but since the frequency of sampling is less than Bayraklı, the risk distribution of this region can be considered lower than the Bayraklı region mentioned for the time being. After these regions, high risk is observed in Bornova and Konak district centers. Rock sample results and soil/sediment results show that the amount of potentially toxic elements show similar distributions. Therefore, to discuss the source of contamination volcanism and tectonism and comparison with other studies which were taken place in in İzmir city center are considered. As a result, the source might be stated as geogenic because of geological properties of İzmir.

6.1.1 Volcanism and Tectonism

In the case of the northwestern part of Bayraklı region, the source of these elements can be caused by Yamanlar volcanics and young tectonism. Mineral provinces (gold and antimony) at Altıntepe (Arapdağ), Çilektepe (Pilavtepe) are part of Yamanlar volcanics and have arsenic, antimony, mercury, lead, zinc minerals (Dora, 1970;

Sönmez and Gonca, 1999) (Figure 6.2). As enrichment can be observed in both rock samples and soil/sediment samples around these mineral provinces.

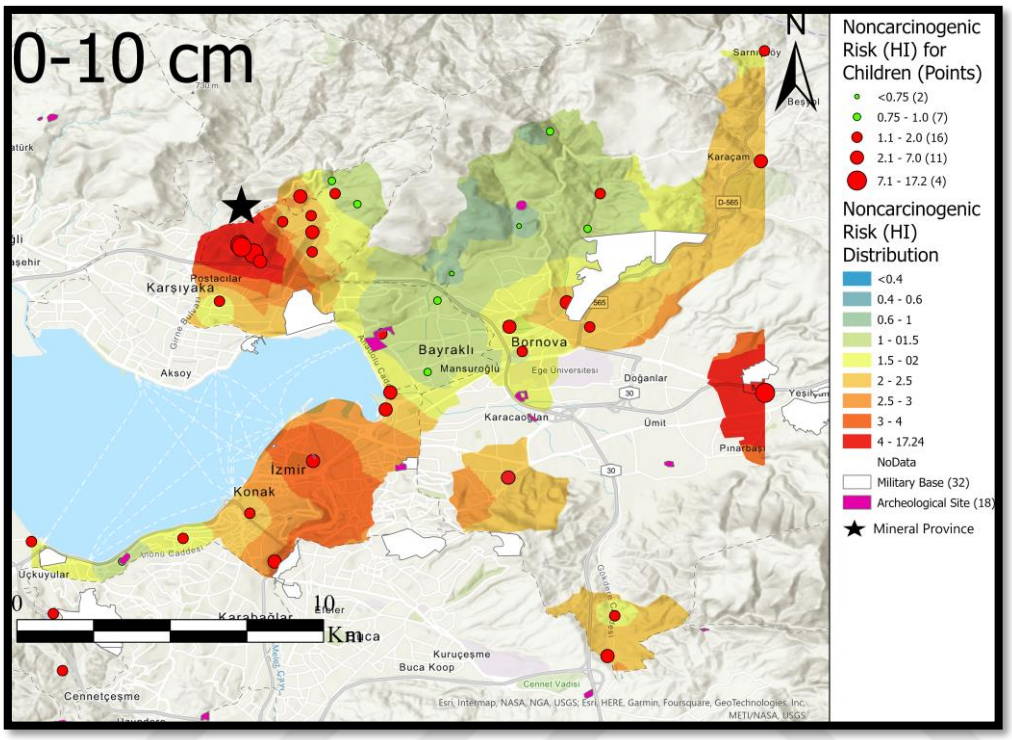

Figure 6.1 Noncarcinogenic distribution map of children at upper layer, Altıntepe and Çilektepe gold provinces marked as black star.

In the southern part of İzmir (near Konak), As distribution is not as high as northern part (Bayraklı region), this might be caused by differences in Yamanlar volcanics. At the southern part of İzmir city center Yamanlar volcanics are also observed but there is no known metallic mineral province in the area but carcinogenic and noncarcinogenic risks can be observed, so it can be said that main reason of high risk in northern part is caused by gold provinces and by characteristics of Yamanlar volcanics. Regional doming is proposed with an E-W in Early to Middle Miocene period (Kaya, 1999).

Phases of compressional and extensional tectonics along related faults and joints from Late Cretaceous to Late Pleistocene in western Turkey and calcalkaline

volcanic centers formed on NE-SW trending faults between latest Oligocene to Early Miocene and active faults around the area shows same trends (Kaya, 1999).

Some rock samples that are taken from Limestone quarries (Figure 6.3 and 6.4) inside of Bornova Mélange have high amount of metallic content and rocks are recrystallized (aragonite minerals can be observed) along fault planes and limestone samples are red in colour. Soil samples along the area and in fault zones are red in colour (Figure 6.5).

Contamination of soil and sediments causing high risk for children and risk in some regions for adults (men and women) within the İzmir city center could possibly be due to two reasons; 1) soil and sediments derived from active fault zones, 2) faulted volcanic provinces.

Figure 6.2 Limestone quarry located at eastern part of İzmir and Bornova (38.46291674759309, 27.31025118444313).

Figure 6.3 Recrystalized aragonite mineralization in limestone blocks from the quarry located in easter part of İzmir and Bornova (38.4629167, 27.3102511) with values of As=79.5, Cd=0.14, Co=2.18, Ni=8.06, Sb=2.08, Zn=29.5 ppm.

Figure 6.4 Soil sample from fault zone (38.448830, 27.286847) around the eastern part of İzmir and Bornova which shows elemental values of As=121, Cd=0.548, Co=19.1, Cr=68, Ni=60 Pb=64.9, Sb=2.75, Zn=12.75 ppm.

6.1.2 İzmir Bay Studies

Heavy metal contamination in Izmir Bay has been studied by different authors (Aksu et al., 1998; Kucuksezgin, 2001; Kontas, 2008; Özkan, 2012; Atalar et al., 2013), and in these studies, they have used soil contamination indices such as contamination factor and geo accumulation factors to sediment cores that are taken from Izmir Bay. They suggested that anthropogenic effects cause the enrichment of some elements because the average values of elements and soil contamination indices in Izmir Bay are not similar to the Mediterranean Sea. For example, Atalar et al. (2013) showed that samples C1, C2, and C3 (Figure 6.6) have different results from average values of sedimentary rocks (Turekian and Wedepohl 1961); however, except for Pb and Zn (Figure 6.7) with increasing depth of core, all elements show similar distributions, As even shows an increase with depth in the outer bay of İzmir. Yümün et al. (2016) have done carbon dating (14C) for sediment cores near Bayraklı, which is near to C3 location at 18.5-meter depth; they found 7690 ± 30 BP and near Karşıyaka, near to C2 location, at a depth of 20 meters they found 4150 ± 30 BP, by considering these ages the rate of sediments to create 2-meter depth should be at least 415 BP if we do simple arithmetic from these ages. Thus, core results at a 2-meter depth from Atalar et al. (2013) should be before the industrial revolution, where the anthropogenic effect weakens. Moreover, when rock and soil/sediment averages of İzmir city center are considered in their study, Cr values are smaller than sediment core values which can be related to the Cr distribution in the area. Cr has higher values (50-72 in soil, 51 in rock) in the southern part of İzmir. Although average Cr values are lower than sediment cores, near-sea samples show similar values. They can be the source of Cr in sediments. As and Pb values are more than sediment cores and Ni values except inner bay is lower than sediment cores. Zn results show that for soil/sediment averages, sediment cores have a lower amount of Zn, but for rock samples, sediment cores are more enriched.

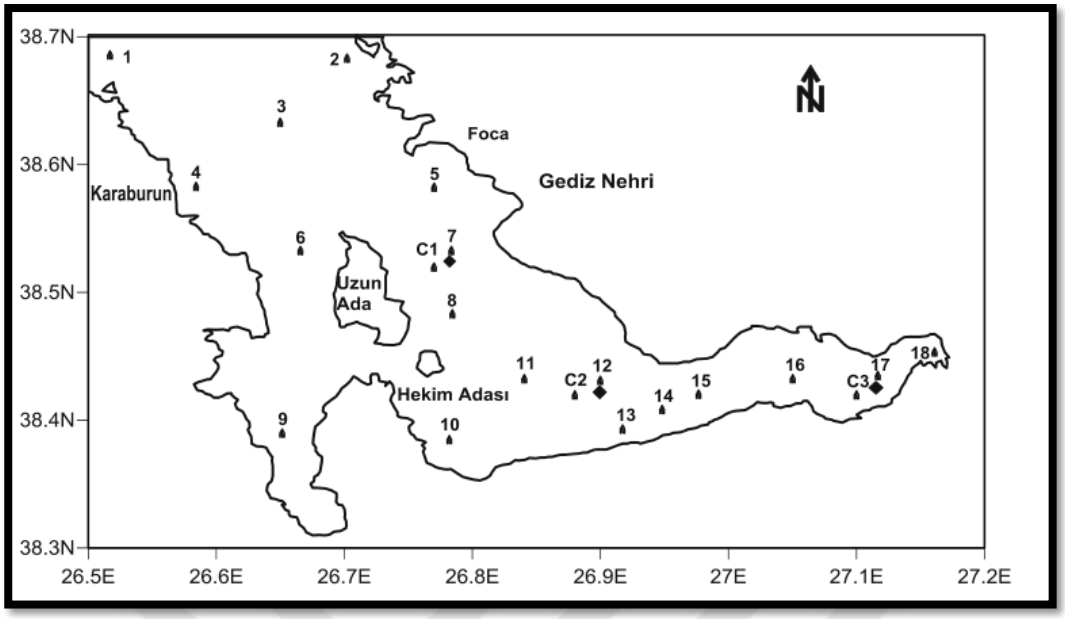

Figure 6.5 Sediment core sampling location in İzmir Bay. Retrieved from Atalar et al. (2013).

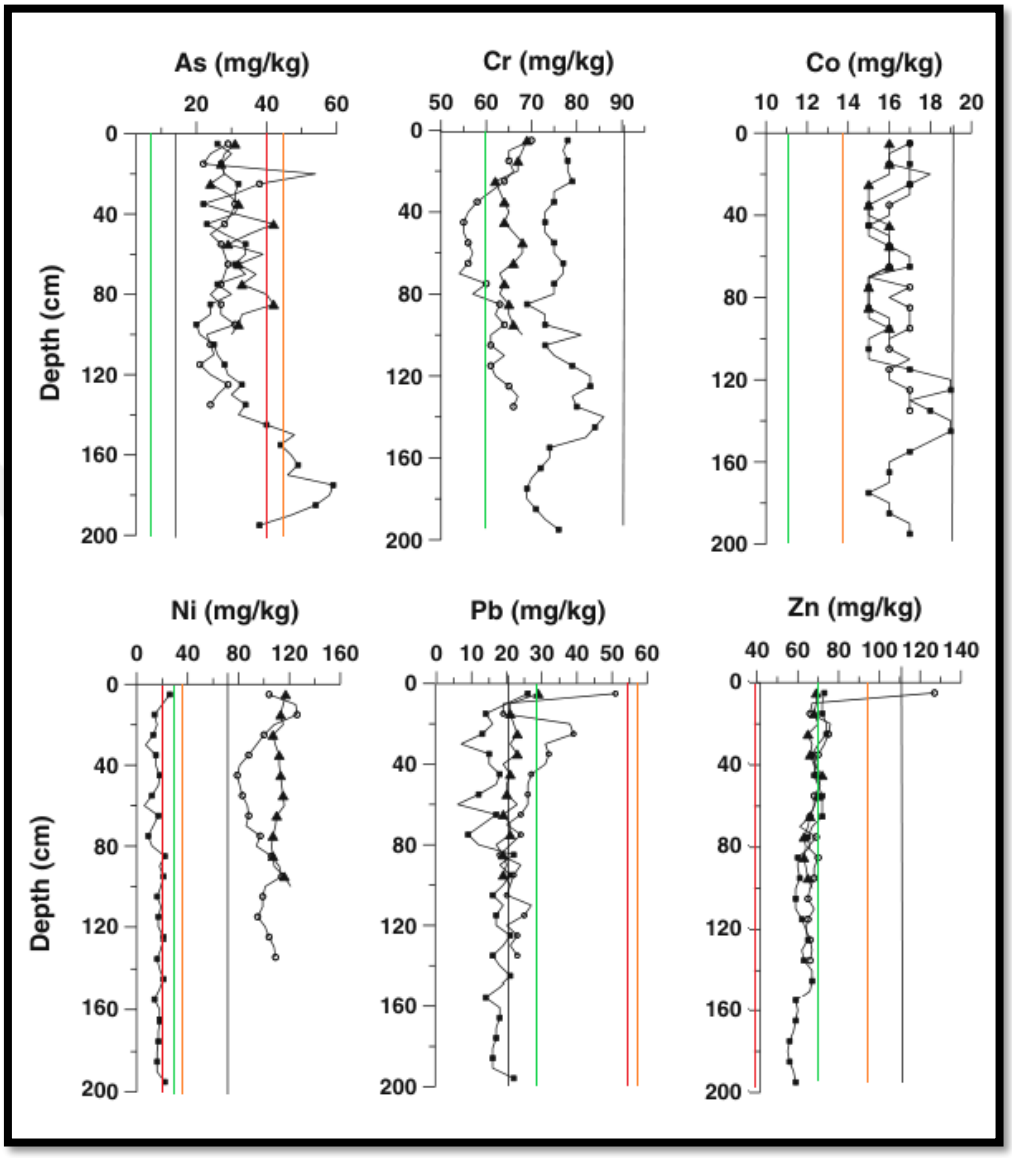

Figure 6.6 Depth profiles of the concentration of As, Cr, Co, Ni, Pb, Zn (C1: Black square, C2: Black triangle, C3: circle) of Izmir Bay's sediment cores. The black line represents the distribution of the elements at sedimentary rocks (Turekian and Wedepohl 1961), and green line is average soil content (Kabata-Pendias, 2011). Retrieved and modified from Atalar et al. (2013), red line represents rock averages from İzmir city center, orange line represents soil and sediment averages from İzmir city center.

6.2 Risk Assessment of İzmir City Center

Geomedical risk assessment of İzmir city center is regional scaled and comprises 3 districts of İzmir city and studied for different individual groups: children, men, and women. Risk assessment calculations are done and represented for average individuals who lived in certain areas for a certain time and average bodyweights of children, men, and women are used.

People who are below average bodyweight are more susceptible for carcinogenic and noncarcinogenic risks. Moreover, people who lived more than 20 years (adults) or 6 years (children) in risky areas are also more susceptible for risks.

The key pathway of exposure to toxic elements is accidental ingestion through everyday activities such as gardening and from dust (Cave et al., 2011).

Living environment (houses) and work environment (workplaces) of individuals should be considered as well since on average, house dust includes 30–70% soil material, indicating that contaminated soil can lead to contaminated house dust (Oomen and Lijzen 2004).

Mineralogical constraints on the bioaccessibility of arsenic and other potentially toxic elements are one of the most important aspects of further studies. According to Davis et al. (1996) bioaccessibility of arsenic content in soil are constrained by.

- "Encapsulation in insoluble matrices, for instance, enargite in quartz. "
- "Formation of insoluble alteration or precipitation rinds, for instance, authigenic iron hydroxide and silicate rinds precipitating on arsenic phosphate grains."
- "Formation of iron oxide and arsenic oxide and arsenic phosphate cements that reduce the arsenic–bearing surface area available for dissolution."

CHAPTER 7

CONCLUSION AND RECOMMENDATIONS

The geochemical and geomedical properties of İzmir city center were studied and the following conclusions can be made:

- Northern, Eastern and Southern parts of İzmir city center (İzmir inner bay) are at carcinogenic and noncarcinogenic risk for different individual groups; in case of carcinogenic risk, children are at high risk, and women and men are at risk, but for noncarcinogenic risk, children are at high risk for specific areas, women and men have minor risk.
- Statistical and geostatistical summaries show that both carcinogenic and noncarcinogenic risks are caused mainly by arsenic dispersion in İzmir city center; for noncarcinogenic risk, Arsenic is followed by Cobalt, Lead, Antimony and Nickel, respectively, and for carcinogenic risk Beryllium, Nickel, and Lead follow it.
- Although soil contamination indices show less pollution, risk assessment calculations show more problematic results. The reason for this is soil contamination indices use only a reference value which is an average value of elements in soil most of the time, which may not mean elements at near average values can cause health problems. However, risk assessment calculations which are constructed by considering average values of elements (RfD), slope factors (CSF) and chronic daily intake (CDI) for individual groups may give better results for the time being because exposure types, exposure time, body weight is considered.
- The source of potentially toxic elements which contaminate soil looks geogenic in origin because of the distribution of elements in different layers are similar and high value giving soil/sediment samples are close to high

value giving rock samples, and when results are checked with heavy metal contamination studies, using sediment cores, in İzmir bay show similar distribution with depth and comparable results to this study except for some peaks at the top of cores for Lead and Zinc, which is probably due to anthropogenic effects in sediments of İzmir bay.

- Active tectonism in the area and Miocene volcanics may be the source for contamination of soils/sediments and risk levels, and mineralogical data will be needed to pinpoint toxicity levels of soils/sediments. Moreover, for better interpretations, additional sampling and lowering grid dimensions is needed, for this purpose, additional sampling was conducted (78 more samples sent to laboratories) in July of 2023.
- Specific areas in İzmir city, such as the Northwestern part of Bayraklı, should be avoided in future city planning; for example, Doğançay graveyard is very close to Altıntepe and Çilektepe gold provinces, and the graveyard is still expanding in the area where hydrothermal alterations are observed. New buildings are constructed in the area; this expansion may become problematic in future; if building expansion cannot be stopped, at least children's parks should be built accordingly. Moreover, in the Eastern part of İzmir, lots of stone quarries are still in production where fault zones have recrystallized carbonates with high metallic content, and airborne particles are polluting the air; furthermore, produced rock chips are used in road making or landscaping in İzmir city which can cause contamination to grow.
- Carcinogenic and noncarcinogenic risky areas should be investigated with smaller scaled grids such as 250 m^2 grid squares. Results are showing that main risky areas are close to other districts such as, Buca, Balçova, Karşıyaka and Çiğli. Thus, these districts should also be studied.
- Pathway of exposure, particle sizes, elemental charges and bioaccessibility, which refers to the fraction of a substance that is released from soil and becomes available for absorption in the human body, should also be considered.

- Pica disorder (eating non-food items, such as soil) in children and pregnant women should be investigated since some areas in İzmir city center show high risk and contamination of certain elements.

REFERENCES

Aendo, P., Netvichian, R., Thiendedsakul, P., Khaodhiar, S., & Tulayakul, P. (2022). Carcinogenic Risk of Pb, Cd, Ni, and Cr and Critical Ecological Risk of Cd and Cu in Soil and Groundwater around the Municipal Solid Waste Open Dump in Central Thailand. Journal of Environmental and Public Health.

ATSDR. (2003). Toxicological profile for Selenium: Atlanta, Ga., U.S. Department of Health and Human Services, Public Health Service, Agency for Toxic Substances and Disease Registry.

ATSDR. (2004). Toxicological Profile for Cobalt: Atlanta, Ga., U.S. Department of Health and Human Services, Public Health Service, Agency for Toxic Substances and Disease Registry.

ATSDR. (2005). Toxicological profile for Nickel and Compounds: Atlanta, Ga., U.S. Department of Health and Human Services, Public Health Service, Agency for Toxic Substances and Disease Registry.

ATSDR. (2005). Toxicological profile for Zinc: Atlanta, Ga., U.S. Department of Health and Human Services, Public Health Service, Agency for Toxic Substances and Disease Registry.

ATSDR. (2007). Toxicological profile for barium and barium compounds: Atlanta, Ga., U.S. Department of Health and Human Services, Public Health Service, Agency for Toxic Substances and Disease Registry.

ATSDR. (2007). Toxicological profile for Tin and Tin compounds: Atlanta, Ga., U.S. Department of Health and Human Services, Public Health Service, Agency for Toxic Substances and Disease Registry.

ATSDR. (2012). Toxicological Profile for Cadmium: Atlanta, Ga., U.S. Department of Health and Human Services, Public Health Service, Agency for Toxic Substances and Disease Registry.

ATSDR. (2012) Toxicological Profile for Chromium: Atlanta, Ga., U.S. Department of Health and Human Services, Public Health Service, Agency for Toxic Substances and Disease Registry.

ATSDR. (2019). Toxicological profile for Antimony and Compounds: Atlanta, Ga., U.S. Department of Health and Human Services, Public Health Service. Agency for Toxic Substances and Disease Registry

ATSDR. (2020). Toxicological profile for Molybdenum: Atlanta, Ga., U.S. Department of Health and Human Services, Public Health Service, Agency for Toxic Substances and Disease Registry.

ATSDR. (2020). Toxicological profile for Lead: Atlanta, Ga., U.S. Department of Health and Human Services, Public Health Service, Agency for Toxic Substances and Disease Registry.

ATSDR. (2022). Toxicological Profile for Beryllium: Atlanta, Ga., U.S. Department of Health and Human Services, Public Health Service, Agency for Toxic Substances and Disease Registry.

Akartuna M., İzmir–Torbalı–Seferihisar–Urla Bölgesinin Jeolojik Etüdü, Istanbul Üniversitesi Fen Fakültesi Monografileri (1962).

Akdeniz, N., Konak, N., Ozturk, Z., and M. H. Cakir, "Izmir-Manisa Arasinin Jeolojisi (Geology of Izmir Manisa Area)," Report of Gen. Direc. of Min. Res. and Expl., No. 7929, 1–164 (1986) (in Turkish).

Aksu, A. E., Yaşar, D., Canada, N., Yaşar, D., & Uslu, O. (1998). Assessment of Marine Pollution in ˙ Izmir Bay: Heavy Metal and Organic Compound Concentrations in Surficial Sediments. Turkish Journal of Engineering and Environmental Sciences.

Atalar M, Kucuksezgin F, Duman M, Gonul LT. (2013). Heavy metal concentrations in surficial and core sediments from Izmir Bay: an assessment of contamination and comparison against sediment quality benchmarks. Bull Environ Contam Toxicol.

Balamurugan, P., Kumar, P. S., Shankar, K., Shankar, K., Shankar, K., Shankar, K., Nagavinothini, R., Nagavinothini, R., Nagavinothini, R., & Vijayasurya, K. (2020). Non-Carcinogenic Risk Assessment of Groundwater in Southern Part of Salem District in Tamilnadu, India. Journal of The Chilean Chemical Society.

Barceloux, D.G. (1999). Molybdenum. J Toxicol Clin Toxicol 37(2):231-237.

Barth, Delbert S., and Mason, Benjamin J. (1984). Soil sampling quality assurance user's guide. United States.

Baselt, R.C, Cravey R.H. (1995). Disposition of Toxic Drugs and Chemicals in Man. 4th Edn. Chicago,IL: Year Book Medical Publishers; 1995. pp. 105-107.

Borsi, S., Ferrara, G., Innocenti, F. & Mazzuoli, R. (1972). Geochronology and petrology of recent volcanics in the eastern Aegean Sea (west Anatolia and Lesbos Island). Bulletin of Volcanology 36, 473–496.

Bølviken, B., Bergström, A., Björklund, A., Kontio,M., Lehmuspelto, P., Lindholm, T., Magnusson, J.,Ottesen, R.T., Steenfelt, A. & Volden, T. (1986) .Geochemical Atlas of Northern Fennoscandia. Nordkallott project, Nordic Collaboration Supported by the Nordic Council of Ministers, 19pp.

Bølviken, B., Bogen, B., Demetriades, A., De Vos, W., Ebbing, J., Hindel, R., Ottesen, R.T., Salminen, R., Schermann, O. & Swennen, R. (1993). Final

Report of the Working Group on Regional Geochemical Mapping 1986-93. Geochemical Mapping of Western Europe towards the Year 2000. Forum of European Geological Surveys (FOREGS). Geological Survey of Norway, Trondheim, NGUReport93.092,18pp.,6.

BGS. (1992). Regional geochemistry of the Lake District and adjacent areas. British Geological Survey, Keyworth, Nottingham, 98 pp.

BGS. (2000). Regional geochemistry of Wales and west-central England: stream sediment and soil. British Geological Survey, Keyworth, Nottingham.

Brinkmann, R. (1966). "Geotektonische Gliederung von Westanatolien", Neues Jahrbuch für Geologie und Palaontologie-Monatshefte 10, 603-618

Bozkurt, E., Park, R.G & Winchester, J.A. (1993). Evidence against the core/cover interpretation of the southern sector of the Menderes Massif, west Turkey. Terra Nova, 5, 445-451.

Buxton, S., Garman, E., Heim, K. E., Lyons-Darden, T., Schlekat, C. E., Taylor, M. D., & Oller, A. R. (2019). Concise Review of Nickel Human Health Toxicology and Ecotoxicology. Inorganics, 7(7), 89. MDPI AG. Retrieved from http://dx.doi.org/10.3390/inorganics7070089

CALEPA. (2005). Human Exposure Based Screening Numbers Developed to Aid Estimation of Cleanup Costs for Contaminated Soil, Sacramento. California Environmental Protection Agency

Carter, R. L. (1980). IARC Monographs on the Evaluation of the Carcinogenic Risk of Chemicals to Humans. Journal of Clinical Pathology.

Cave, M., Wragg, J., Denys, S., Jondreville, C., Cyril, F., (2011). Oral Bioavailability. 10.1007/978-90-481-9757-6_7.

Cornfield, J., & Cornfield, J. (1977). Carcinogenic risk assessment. Science. https://doi.org/10.1126/science.910152

Choi, B.-W., Jung, J.-H., Choi, W.-J., Jeon, C.-J., & Shon, B.-H. (2006). The Distribution Characteristics of Ambient Heavy Metals based on the Pollution Source and their Carcinogenic Risk Assessment in Ulsan, Korea. Korean Journal of Environmental Health Sciences.

Çağlayan M.A., Öztürk, E.M., Öztürk, Z., Sav, H., and Akat, U. (1980). Menderes masifi güneyine ait bulgular ve yapısal yorum. Bull. Geol. Eng. 10: 9-17.

Darnley, A.G., Bjorklund, A., Bolviken, B. N. Gustavsson, P.V. Koval, J.A. Plant, A. Steenfelt, M. Tauchid and X. Xie. (1995). A Global Geochemical Database for Environmental and Resource Management. Recommendations for International Geochemical Mapping. Final Report of IGCP Project 259. Earth Sciences 19, UNESCO, Paris

Das, K., Reddy, R., Bagoji, I., Das, S., Bagali, S., Mullur, L., Khodnapur, J. & Biradar, M. (2019). Primary concept of nickel toxicity – an overview. Journal of Basic and Clinical Physiology and Pharmacology, 30(2), 141-152. https://doi.org/10.1515/jbcpp-2017-0171

Davis JE, Fields JP. 1958. Experimental production of polycythemia in humans by administration of cobalt chloride. Proc Soc Exp Biol Med 99:493-495.

Davies, Brian & Bowman, Charlotte & Davies, Theophilus & Selinus, O.s. (2013). Medical Geology: Perspectives and Prospects.

Demetriades, A., Smith, D. B., & Wang, X. (2018). General concepts of geochemical mapping at global, regional, and local scales for mineral exploration and environmental purposes. Geochimica Brasiliensis, 32(2), 136.

De Vos, W., Tarvainen, T. (Chief Editors), Salminen,R., Reeder, S., De Vivo. B., Demetriades, A., Pirc,S., Batista, M.J., Marsina, K., Ottesen, R.T.,O'Connor, P.J., Bidovec, M., Lima, A., Siewers, U., Smith, B., Taylor, H., Shaw, R., Salpeteur, I.,Gregorauskiene, V., Halamic, J., Slaninka, I., Lax,K., Gravesen, P., Birke, M., Breward, N., Ander,E.L., Jordan, G., Duris, M., Klein, P., Locutura, J.,Bel-lan, A., Pasieczna, A., Lis, J., Mazreku, A.,Gilucis, A., Heitzmann, P., Klaver, G. & Petersell, V. (2006). Geochemical Atlas of Europe. Part 2 –Interpretation of geochemical maps, Additional Tables, Figures, Maps and related publications. Geological Survey of Finland, Espoo, Finland, 692pp. http://weppi.gtk.fi/publ/foregsatlas/.

Delgado-Iniesta, M. J., Sanleandro, P. M., Campo-Bescós, M. A., Bautista, F., Romero, M., Sanleandro, P. M., & Navarro, A. S. (2022). Estimation of Ecological and Human Health Risks Posed by Heavy Metals in Street Dust of Madrid City (Spain). International Journal of Environmental Research and Public Health. https://doi.org/10.3390/ijerph19095263

Dora, Ö. (1970). Arapdağ (Karşıyaka) kuvars-altın filonlarının mineralojik etüdü; Madencilik dergisi (in Turkish), cilt IX. Sayı 4, 25–41 (Mineralogic study of Arapdağ (Karşıyaka) quartz-gold veins. Mining Journal, IX, 4, 25-41).

Dönmez, M., Tükecan, A., Akçay, A.E., Hakyemez. Y. and Sevin, D. (1998). İzmir ve kuzeyinin jeolojisi. Tersiyer volkanizmasının petrografik ve kimyasal özellikleri; MTA Rep.: 10181 (unpublished) Ankara.

Ercan, E., Satır, M., Sevin, D., Türkecan, A. (1996). Some new radiometric ages from Tertiary and Quaternary volcanic rocks from West Anatolia (in Turkish). Bull. Mineral Res. Explor. Inst. Turk. 119, 103–112.

Ercan, T., Dinçel, A., Metin, S., Türkecan, A., Günay, E. (1978). Uşak Yöresindeki Neojen Havzalarının Jeolojisi. Türkiye Jeoloji Kurumu Bülteni, 21, 97- 106.

Erdoğan, B. (1990). İzmir-Ankara Zonu'nun İzmir ile Seferihisar arasındaki bölgede stratigrafik özellikleri ve tektonik evrimi, TPJD Bülteni, 2, 1-20. [24] Lüttig

G., Steffens P., Explanatory notes for the paleogeographic Atlas of Turkey from the Oligocene to the Pleistocene, Bundesanstalt für Geowissenschaften und Rohstoffe, Hannover, 1976, pp. 1–42.

Eşder, T. & Şimşek, Ş. (1975). Geology of İzmir (Seferihisar) geothermal area western Anatolia of Turkey determination of reservoirs by means of gradient driling. In: Proceedings of 2nd UN. Symposium, San Francisco, 349–361.

EuroGeoSurveys Geochemistry Working Group. (2008). EuroGeoSurveysGeochemical mapping of Geochimica Brasiliensis 32(2): 136 - 179, 2018 174 agricultural and grazing land soil of Europe (GEMAS) - Field manual. Open file report 2008.038, Geological Survey of Norway, Trondheim, 46 pp.

Fergusson J.E. (1990). The heavy elements: chemistry, environmental impact, and health effects. Pergamon Press, New York

Ferreira-Baptista, L., & Miguel, E. de. (2005). Geochemistry and risk assessment of street dust in Luanda, Angola: A tropical urban environment. Atmospheric Environment. https://doi.org/10.1016/j.atmosenv.2005.03.026.

Finkelman, R., Catherine, H., Skinner, W., Plumlee, G., Bunnell, J., (2001). Medical Geology. 46.

Fritz, W. (1983). WHO-IARC Monographs on the evaluation of the carcinogenic risk of chemicals to humans. Vol. 28: The: Rubber Industry. 486 Seiten. International Agency for Research on Cancer, Lyon 1982. Preis: 70, – sfrs. Nahrung-Food. https://doi.org/10.1002/food.19830270315.

Genç, S.C., Altunkaynak, Ş., Karacık, Z. & Yılmaz, Y. (2001). The Çubukludağ Graben, Karaburun Peninsula: it’s tectonic significance in the Neogene geological evolution of the western Anatolia. Geodinamica Acta 14, 45–55.

Goyer R.A. (2001). Toxic effects of metals. In: Klaassen CD (ed) Cassarett and Doull’s toxicology: the basic science of poisons. McGraw-Hill, New York, NY, pp 811–867

Graciansky, P. (1965). Menderes masifinin güney kıyısı boyunca (Türkiye'nin SW sı) görülen metamorfizma hakkında açıklamalar. Al.T.A. Derg., no. 64, Ankara.

Hakanson L. (1980) An ecological risk index for aquatic pollution control: A sediment ecological approach. Water Res. 1980; 14:975–1001. doi: 10.1016/0043-1354(80)90143-8.

IGS. (1978). Regional geochemical atlas: Shetland. Institute of Geological Sciences, London.

IRSST. (2012). Evaluation of beryllium toxicity according to chemical form and particle size.

İzmir Büyükşehir Belediyesi - Coğrafi Bilgi Sistemleri. (2023). Retrieved from https://cbs.izmir.bel.tr/cbs_portal/IkiBoyutlu on 31.07.2023.

Johnson, C.C. (2005). 2005 G-Base field procedures manual. British Geological Survey, Internal Report IR/05/097, 130 pp.

Kabata-Pendias A., Pendias, H. (2001) Trace Elements in Soils and Plants; CRC Press, Boca Raton, FL.

Kabata-Pendias, A., Sadurski. W., 2004-Trace elements and compounds in soil, In: Merian E, Anke M, Ihnat M, Stoepppler M (eds) Elementsand their compounds in the environment, Wiley-VCH, Weinheim, 2nd ed., pp: 79–99.

Kabata-Pendias, Alina. (2011). Trace elements in soils and plants: Fourth edition.

Kaya O. (1981). Miocene reference section for the coastal parts of west Anatolia, Newslet. Stratig. 164–191.

Kaya, O. (1999). Batı Anadolu kırık dizgeleri; petrol ve jeotermal potansiyel yönünden değerlendirme; Baksem'99 1. Batı Anadolu Hammadde Kaynakları Semp. 8-14 Mart1999, İzmir. Bildiriler kitapçığı 1-11

Konuk, T. (1977). Bornova filişinin yaşı hakkında: Ege Üniv. Fen Fak. Bull., Sen B, 1/1, 65-74.

Kontas, A. (2008). Trace metals (Cu, Mn, Ni, Zn, Fe) Contamination in Marine Sediment and Zooplankton Samples from Izmir Bay. (Aegean Sea, Turkey). Water Air and Soil Pollution. https://doi.org/10.1007/s11270-007-9547-1

Kucuksezgin, F. (2001). Distribution of heavy metals in the surficial sediments of Izmir Bay (Turkey). Toxicological & Environmental Chemistry. https://doi.org/10.1080/02772240109359010

Kunesh C.J. (1978). Barium. In: Grayson M, Eckroth D, eds. Kirk-Othmer encyclopedia of chemical technology. Vol. 3, 3rd ed. New York, NY: John Wiley and Sons, 457-463.

Lahermo, P., Ilmasti, M., Juntunen, R. & Taka, M. (1990). The Geochemical Atlas of Finland, Part 1: The hydrogeochemical mapping of Finnish groundwater. Geological Survey of Finland, Espoo,66 pp.

Lahermo, P., Väänänen, P., Tarvainen, T. & Salminen, R. (1996). Geochemical atlas of Finland. Part 3: Environmental geochemistry–stream waters and sediments. Geological Survey of Finland, Espoo,149 pp.

Latham R. (1958). The travels of Marco Polo. Penguin, London

Lech, M.E., Caritat, P. de, McPherson, A.A. (2007). National Geochemical Survey of Australia: Field Manual. Geoscience Australia Record 2007/08, 53pp.http://www.ga.gov.au/metadata-gateway/metadata/record/gcat_65234.

Lüttig G., Steffens P. (1976). Explanatory notes for the paleogeographic Atlas of Turkey from the Oligocene to the Pleistocene, Bundesanstalt für Geowissenschaften und Rohstoffe, Hannover, pp. 1–42.

Makris, J., Papoulia, J., Papanikolaou, D., Fasoulaka, Ch. (2022). Crustal structure beneath the Cyclades Metamorphic Core Complex, Aegean Sea, Greece. Tectonophysics. 842. 229585. 10.1016/j.tecto.2022.229585.

Masri, S., LeBrón, A. M. W., Logue, M. D., Valencia, E., Ruiz, A., Reyes, A., & Wu, J. (2021). Risk assessment of soil heavy metal contamination at the census tract level in the city of Santa Ana, CA: implications for health and environmental justice. Environmental Science: Processes & Impacts. https://doi.org/10.1039/d1em00007a.

Miner S. (1969). Air pollution aspects of barium and its compounds. Bethesda, MD: Litton Systems, Inc Contract No. Ph-22-68-25, 69.

Muller, G., (1969). Index of geoaccumulation in sediments of the Rhine River. Geojournal, 2: 108- 118.

NAS (National Academy of Sciences). 2000. Selenium. In: Dietary reference intakes for vitamin C, vitamin E, selenium, and carotenoids. Washington, DC: National Academy of Sciences, National Academy Press, 284-324.

Nriagu J.O. (1998). Tales told in lead. Science 281:1622–1623

Okay, A.İ. & Siyako, M. (1993). The new position of the İzmir-Ankara Neo-Tethyan Suture between İzmir and Balıkesir. Tectonics and Hydrocarbon Potential of Anatolia and surrounding regions Ozan Sungurlu Symposium Proceedings, pp. 333-355.

Okay, A. İ. (2001). Stratigraphic and metamorphic inversions in the central Menderes Massif: a new structural model. International Journal of Earth Science 89, 709‑727.

Oomen AG, Lijzen JPA (2004) Relevancy of human exposure via house dust to the contaminants lead and asbestos. RIVM Report 711701037/2004. RIVM, Bilthoven, the Netherlands.

Ozkan, E. Y. (2012). A New Assessment of Heavy Metal Contaminations in an Eutrophicated Bay (Inner Izmir Bay, Turkey). Turkish Journal of Fisheries and Aquatic Sciences. https://doi.org/10.4194/1303-2712-v12_1_16

Özgenç, İ. (1978). Relative age relationships between two extrusion phases of Cumaovası acidic volcanics (İzmir)]. Geological Society of Turkey Bulletin21, 31–34.

Pan, L., Fang, G., Wang, Y., Wang, L., Su, B., Li, D., & Xiang, B. (2018). Potentially Toxic Element Pollution Levels and Risk Assessment of Soils and Sediments in the Upstream River, Miyun Reservoir, China. International journal of

environmental research and public health, 15(11), 2364. https://doi.org/10.3390/ijerph15112364

Parejas, E. (1940). Le flysch cretace des environs de Smyrne. Pub. Inst. Geol. Univ. İstanbul.

Reimann, C. (2005). Sub-continental scale geochemical mapping: sampling, quality control and data analysis issues. Geochemistry, Exploration, Environment, Analysis, 5, 311-323.

Reimann, C., & de Caritat, P. (2005). Distinguishing between natural and anthropogenic sources for elements in the environment: regional geochemical surveys versus enrichment factors. Science of The Total Environment. https://doi.org/10.1016/j.scitotenv.2004.06.011.

Rinklebe, J. & Antoniadis, V. & Rosche, O. & Altermann, M. (2019). Health risk assessment of potentially toxic elements in soils along the Central Elbe River, Germany. Environment International. 126. 76-88. 10.1016/j.envint.2019.02.011.

Finkelman, R.B. Orem, G. S. Plumlee, O. Selinus, (2018). Chapter 17 - Applications of Geochemistry to Medical Geology, Editor(s): Benedetto De Vivo, Harvey E. Belkin, Annamaria Lima, Environmental Geochemistry (Second Edition), Elsevier, Pages 435-465.

Saleh, H. N., Panahande, M., Yousefi, M., Asghari, F. B., Conti, G. O., Talaee, E., Mohammadi, A., & Mohammadi, A. A. (2019). Carcinogenic and Non-carcinogenic Risk Assessment of Heavy Metals in Groundwater Wells in Neyshabur Plain, Iran. Biological Trace Element Research. https://doi.org/10.1007/s12011-018-1516-6

Salminen, R., Tarvainen, T., Demetriades, A., Duris, M., Fordyce, F.M., Gregorauskiene, V., Kahelin, H., Kivisilla, J., Klaver, G., Klein, H., Larson, J.O., Lis, J., Locutura, J., Marsina, K., Mjartanova, H., Mouvet, C., O'Connor, P., Odor, L., Ottonello, G., Paukola, T., Plant, J.A., Reimann, C., Schermann, O., Siewers, U., Steenfelt, A., Van der Sluys, J. & Williams, L. (1998). FOREGS Geochemical Mapping Field Manual. Geological Survey of Finland, Espoo, Guide 47, 36 pp., 1 Appendix http://arkisto.gtk.fi/op/op47/op47.pdf.

Salminen, R., Chekushin, V., Tenhola, M., Bogatyrev,I., Glavatskikh, S.P., Fedotova, E., Gregorauskiene,V., Kashulina, G., Niskavaara, H., Polischuok, A.,Rissanen, K., Selenok, L., Tomilina, O. &Zhdanova, L. (2004). Geochemical Atlas of theEastern Barents Region. Elsevier, Amsterdam, 548pp.

Salminen, R. (Chief Editor), Batista, M.J., Bidovec,M., Demetriades, A., De Vivo, B., De Vos, W.,Duris, M., Gilucis, A., Gregorauskiene, V.,Halamic, J., Heitzmann, P., Lima, A., Jordan, G.,Klaver, G., Klein, P., Lis, J., Locutura,

J., Marsina,K., Mazreku, A., O'Connor, P.J., Olsson, S.Å.,Ottesen, R.T., Petersell, V., Plant, J.A., Reeder, S.,Salpeteur, I., Sandström, H., Siewers, U., Steenfelt,A. & Tarvainen, T. (2005). FOREGS GeochemicalAtlas of Europe, Part 1: Background Information, Methodology and Maps. Geological Survey of Finland, Espoo,526pp.

Salminen, R. (2005). Geochemical Atlas of Europe. Geological Survey of Finland.

Sönmez, S., İ. & Gonca, Ş. (1999). Geology, Petrography and Precious Metal Mineralizations of Altıntepe and Çilektepe Sectors of Karşıyaka Ore Occurences, İzmir, Turkey. Bulletin of The Mineral Research and Exploration. 121. 33-49.

Seghedi, Ioan & Helvacı, Cahit & Pecskay, Zoltan. (2015). Composite volcanoes in the south-eastern part of İzmir-Balıkesir Transfer Zone, Western Anatolia, Turkey. Journal of Volcanology and Geothermal Research. 291. 10.1016/j.jvolgeores.2014.12.019.

Schuiling, R. D. (1962). Türkiye'nin Güneybatisindaki Menderes Migmatit Kompleksinin Petrolojisi, Yaşi Ve Yapisi Hakkinda. Bulletin of the Mineral Research and Exploration, 58 (58), 71-84.

Smith, D.B., Cannon, W.F., Woodruff, L.G., Garrett,R.G., Klassen, Rodney, Kilburn, J.E., Horton, J.D.,King, H.D., Goldhaber, M.B. & Morrison, J.M. (2005). Major- and trace-element concentrations in soils from two continental-scale transects of the United States and Canada: U.S. Geological SurveyOpen-FileReport2005-1253.

Sözbilir, H., Sarı, B., Uzel, B., Sümer, Ö. ve Akkiraz, S. (2010). Tectonic implications of transtensional supradetachment basin development in on extension paralel transfer zone: the Kocaçay basin, western Anatolia, Basin Research.

Strickland, H.E. (1840). On the Geology of the Neighbourhood of Smyrna. Transactions of the Geological society of London. doi:10.3906/yer-0910-11.

Sutherland, R. A. (2000). Bed sediment-associated trace metals in an urban stream, Oahu, Hawaii. Environmental Earth Sciences. https://doi.org/10.1007/s002540050473.

Şengör, A.M.C & Yilmaz, Y. (1981). Tethyan evolution of Turkey: A plate tectonic approach. Tectonophysics.

Şengör, A.M.C., & Yılmaz, Y., and Sungurlu, O. (1984). Tectonics of the Mediterranean Cimmerides: nature and evolution of the western termination of Palaeotethys. In: J.E. Dixon and A.H.F. Robertson (Eds.), The Geological Evolution of the Eastern Mediterranean. Spec. Publ. Geol. Soc. London, 17: 77- 112.

Tchounwou, P. B., Yedjou, C. G., Patlolla, A. K., & Sutton, D. J. (2012). Heavy metal toxicity and the environment. Experientia. Supplementum. https://doi.org/10.1007/978-3-7643-8340-4_6

Teppo, L. (1998). Health effects of cadmium exposure - a review of the literature and a risk estimate. Scandinavian Journal of Work, Environment & Health. https://doi.org/10.5271/sjweh.270

Tian, Y., Zha, X., Gao, X., & Yu, C. (2022). Geochemical characteristics and source apportionment of toxic elements in the Tethys–Himalaya tectonic domain, Tibet, China. Science of The Total Environment. https://doi.org/10.1016/j.scitotenv.2022.154863

Tomatis, L. (1976). The IARC program on the evaluation of the carcinogenic risk of chemicals to man. Annals of the New York Academy of Sciences. https://doi.org/10.1111/j.1749-6632.1976.tb23139.x

Tomlinson D.L., Wilson J.G., Harris C.R., Jeffrey D.W. (1980). Problems in the assessment of heavy-metal levels in estuaries and the formation of a pollution index. Helgoländer Meeresuntersuchungen. 1980; 33:566–575. doi: 10.1007/BF0241478.

TURKSTAT. (2023). Türkiye Health Survey, 2022. Retrieved from https://data.tuik.gov.tr/Bulten/Index?dil=2&p=Turkiye-Health-Survey-2022-49747.

Tukey, J. W. (1977). Exploratory data analysis, Addison-Wesley, 1st ed.

USEPA. (1989). Risk assessment guidance for Superfund. Volume I: Human health evaluation manual (Part A). Interim Final. Office of Emergency and Remedial Response. EPA/540/1-89/002.0. U.S. Environmental Protection Agency

USEPA. (2000). Data Quality Objectives Process for Hazardous Waste Site Investigations. Office of Environmental Information, Washington, DC. EPA/600/R-00/007. January. U.S. Environmental Protection Agency

USEPA. (2011). National Contingency Plan §300.430, pp. 76–87. U. S. Environmental Protection Agency.

Uzel, B. and Sözbilir, H. (2008). A first record of strike-slip basin in western Anatolia and its tectonic implication: the Cumaovası basin as an example, Turkish Journal of Earth Sciences, 17, 559-591.

Uzel, B., Sözbilir, H., Özkaymak, C., (2012). Neotectonic evolution of an actively growing superimposed basin in western Anatolia: The inner bay of İzmir, Turkey. Turkish Journal of Earth Sciences 22 (4), 439–471.

Uzel, B., Sozbilir, H., Özkaymak, C., Kaymakci, N., Langereis, C. (2013). Structural evidence for strike-slip deformation in the İzmir-Balıkesir transfer zone and consequences for late Cenozoic evolution of western Anatolia (Turkey).

Vermeulen., F. (1996) Minutes of the IGCP 360 Analytical Committee Meeting March 1996. British Geological Survey, Keyworth.

Yedjou GC, Moore P, Tchounwou P.B. (2006) Dose and time dependent response of human leukemia (HL-60) cells to arsenic trioxide. Int J Environ Res Public Health 3:136–140.

Wang, H., Wang, J., Liu, R., Yu, W., & Shen, Z. (2015). Spatial variation, environmental risk and biological hazard assessment of heavy metals in surface sediments of the Yangtze River estuary. Marine Pollution Bulletin. https://doi.org/10.1016/j.marpolbul.2015.01.026.

Wei, B., & Yang, L. (2010). A review of heavy metal contaminations in urban soils, urban road dusts and agricultural soils from China. Microchemical Journal. https://doi.org/10.1016/j.microc.2009.09.014.

WHO/FAO/IAEA. World Health Organization. Switzerland: Geneva; 1996. Trace Elements in Human Nutrition and Health.

WHO. 1996. Zinc, Trace elements in human nutrition and health. World Health Organization,72-104.

WHO. (1998). Evaluation of certain food additives and contaminants. World Health Organization.

WHO. (2000). Air quality guidelines for Europe, 2nd ed. World Health Organization. Regional Office for Europe. World Health Organization.

Yalcin, M. G., Coskun, B., Nyamsari, D. G., & Yalcin, F. (2019). Geomedical, ecological risk, and statistical assessment of hazardous elements in shore sediments of the Iskenderun Gulf, Eastern Mediterranean, Turkey. Environmental Earth Sciences. https://doi.org/10.1007/s12665-019-8435-5.

Yousefi, H., Lak, E., Mohammadi, M. J., & Shahriyari, H. A. (2021). Carcinogenic Risk Assessment among Children and Adult due to Exposure to Toxic Air Pollutants. Environmental Science and Pollution Research. https://doi.org/10.1007/s11356-021-17300-0.

Yongming, H., Peixuan, D., Junji, C., & Posmentier, E. S. (2006). Multivariate analysis of heavy metal contamination in urban dusts of Xi'an, Central China. Science of The Total Environment. https://doi.org/10.1016/j.scitotenv.2005.02.026

Yümün, Z. Ü., Meriç, E., Avşar, N., Nazik, A., Barut, İ. F., Yokeş, B., Sagular, E. K., Yildiz, A., Eryilmaz, M., Kam, E., Başsarı, A., Başsari, A., Sonuvar, B., Dinçer, F., Baykal, K., & Kaya, S. (2016). Meiofauna, microflora and geochemical properties of the late quaternary (Holocene) core sediments in the Gulf of Izmir (Eastern Aegean Sea, Turkey). Journal of African Earth Sciences. https://doi.org/10.1016/j.jafrearsci.2016.09.015

Zheng, X., Zhao, W., Zhao, W., Yan, X., Yan, X., Shu, T., Xiong, Q., Xiong, Q., & Chen, F. (2015). Pollution Characteristics and Health Risk Assessment of Airborne Heavy Metals Collected from Beijing Bus Stations. International Journal of Environmental Research and Public Health. https://doi.org/10.3390/ijerph120809658